# NGU

Norges geologiske undersøkelse

1858

Nr. 363

Bulletin 60

Universitetsforlaget 1981

Trondheim - Oslo - Bergen - Tromsø

# NGU
# Norges geologiske undersøkelse

Geological Survey of Norway

*Norges geologiske undersøkelse* (Geological Survey of Norway), Leiv Eirikssons vei 39, Trondheim. Telephone: national (075) 15860, international + 47 75 15860. Postal address: Box 3006, N-7001 Trondheim, Norway.

Administrative Director: Dr. philos. *Knut S. Heier*

Geological division: Director Dr. philos. *Peter Padget*

Geophysical division: Director *Inge Aalstad*

Chemical division: Director *Bjørn Bølviken*

The publications of *Norges geologiske undersøkelse* are issued as consecutively numbered volumes, and are subdivided into two series, Bulletin and Skrifter.

*Bulletins* comprise scientific contributions to the earth sciences of regional Norwegian, general, or specialist interest.

*Skrifter* comprise papers and reports of specialist or public interest of regional, technical, economic, environmental, and other aspects of applied earth sciences, issued in Norwegian, and with an Abstract in English.

EDITOR
Førstestatsgeolog Dr. *David Roberts*, Norges geologiske undersøkelse, P.O.Box 3006, N-7001 Trondheim, Norway.

PUBLISHER
*Universitetsforlaget*, P.O.Box 2959, Tøyen, Oslo 6, Norway.

DISTRIBUTION OFFICES
*Norway*: Universitetsforlaget, P.O.Box 2977, Tøyen, Oslo 6. *United Kingdom*: Global Book Resources Ltd., 109 Great Russell Street, London WC 1 B, 3ND.
*United States and Canada*: Columbia University Press, 136 South Broadway, Irvington on Hudson, New York 10533.

EARLIER PUBLICATIONS AND MAPS
The most recent list of NGU publications and maps, 'Publikasjoner og kart 1891 — 1977', appeared in 1977. Copies can be obtained from the Publisher.

The most recent maps available from NGU are listed inside the back cover.

MANUSCRIPTS
Instructions to contributors to the NGU Series can be found in NGU Nr. 273, pp. 1-5. Offprints of these instructions can be obtained from the editor. Contributors are urged to prepare their manuscripts in accordance with these instructions.

# The Structure of the Magerøy Nappe, Finnmark, North Norway

TORGEIR BJØRGE ANDERSEN

Andersen, T. B. 1981: The structure av the Magerøy Nappe, Finnmark, North Norway. *Norges geol. Unders. 363*, 1–23.

The Magerøy Nappe was emplaced during the Scandinavian phase of the Caledonian orogeny, of Middle/Upper Silurian age. Two main episodes of deformation ($D_1$ and $D_2$) with attendant Barrovian-type regional metamorphism are recorded in the metasediments of Upper Ordovician/Lower Silurian age forming the Magerøy Supergroup (minimum thickness 5.5 km). The $D_1$ deformation produced overturned to recumbent regional folds which due to opposite vergence form a mushroom-like culmination in central Magerøy. $D_1$ folds east of the structural divergence zone are tight, recumbent folds with eastward vergence, while those to the west are overturned asymmetrical folds verging to the west. Textural and structural observations indicate that $D_1$ consisted of two deformational events ($D_{1a}$ and $D_{1b}$) of which the later coincides with the final movements along the basal thrust of the nappe. The metamorphism reached its peak in the period between $D_1$ and $D_2$, and was accompanied by acid and mafic/ultramafic intrusions (417 ± 11 m.y., Finnvik Granite). $D_2$, which occurred under retrograde metamorphism, produced a large synformal structure, essentially coaxial with the $F_1$ folds, but with a subvertical axial surface. In the structural depression along the axial trace of this fold the highest structural levels of the Magerøy Nappe mushroom-structure, and an erosional klippe of a higher nappe, the Skarsvåg Nappe, are preserved. The $F_2$ folding of Magerøy is correlated with the late, large-scale buckling of the Finnmarkian phase nappes of the mainland in West Finnmark.

*T. B. Andersen, Geologisk Institutt Avd. A, University of Bergen, 5014 Bergen, Norway*

## Introduction

Studies during the last two decades in west Finnmark and northeast Troms, northern Norway, have shown that the orthotectonic Caledonides of the region comprise two major nappe sequences. These were deformed and metamorphosed through two, major, time-separated, orogenic events, which are known as the *Finnmarkian phase* (late Cambrian/early Ordovician) and the *Scandinavian phase* (middle/late Silurian) (Ramsay & Sturt 1976, Sturt et al. 1978, Sturt et al. in prep.). In the evolution of the Caledonides of northern Norway the Magerøy Nappe occupies a key position, being the only known nappe in the Finnmark sequence which records a post-Finnmarkian evolution and the tectonothermal characteristics of the Scandinavian phase. The emphasis in the present paper is placed on a description of the structural pattern of the nappe.

## Geological setting and history of research

The island of Magerøy (lat. 71°N) contains three main tectono-stratigraphic units. Most of the eastern and central parts of the island (Fig. 1) are occupied by the Magerøy Nappe, underlain to the west by the Gjesvær Migmatite Complex (Ramsay & Sturt 1976) assigned to the Kalak Nappe Complex (Roberts 1974) of Finnmarkian age. In the Skarsvåg area of N.E. Magerøy a small erosional remnant of a higher nappe, the Skarsvåg Nappe, is present. This nappe represents the highest unit in the tectono-stratigraphy of Finnmark (Kjærsrud, in prep.). The junction between the Magerøy Nappe and the Gjesvær migmatites is a major thrust plane, the Magerøy Thrust (Ramsay & Sturt 1976). The Magerøy Nappe and the higher Skarsvåg Nappe have been preserved from erosion by downfaulting of the northern block on the Magerøysundet fault (Fig. 1). This fault separates Magerøy from the Porsanger Peninsula where rocks assigned to the Kalak Nappe Complex occur. The displacement along the fault is of unknown magntitude, but in addition to a dip-slip component there was probably a considerable component of dextral strike-slip.

The discovery of a Lower Silurian fauna in eastern Magerøy (Henningsmoen 1961) posed a number of questions concerning the age and geological evolution of the Magerøy assemblage, which previously had been correlated with the autochthonous Eocambrian rocks of east Finnmark (Holtedahl 1944). This correlation was based on the lithological similarity between the so-called 'Duksfjord tillite' and the tillites of east Finnmark. The fossil discoveries prompted Føyn (1967) to re-examine the eastern and central parts of the island, where additional finds of fossils in the Sardnes area (Fig. 1) led him to conclude that the 'Duksfjord tillite' represented a Silurian intraformational conglomerate. This conclusion has since been supported by additional fossil-finds (D. M. Ramsay, pers. comm. in Curry (1975)).

In the late sixties and early seventies Curry (1975) carried out a more detailed study of eastern Magerøy. She established a preliminary lithostratigraphy, and on the basis of this demonstrated that the metasediments were folded in large-scale overturned to recumbent folds ($D_1$), resulting in extensive areas of inversion. She also recognized a second, less pervasive fold phase ($D_2$), and showed that the regional metamorphism was a Barrovian zonal sequence. Curry was chiefly concerned, however, with the mafic and ultramafic intrusive rocks of eastern Magerøy, which form an important syn-orogenic igneous complex.

In a study of the thrust-zone between the Magerøy Nappe and the Gjesvær migmatite complex, Ramsay & Sturt (1976) showed that the nappe was emplaced under metamorphic conditions which extended well into the amphibolite facies. They also recognized an extensive post-tectonic recrystallization of the mylonitized lithologies of the thrust zone, and concluded that the thrusting of the nappe had taken place during the $D_1$ event.

The work of Føyn (1967), Curry (1975) and Ramsay & Sturt (1976), together with a detailed structural analysis of a deformed conglomerate in eastern Magerøy (Ramsay & Sturt 1970), represented the only modern studies

*Fig. 1.* Geological map of Magerøy, compiled and simplified from the mapping by T. B. Andersen, C. J. Curry and K. Kjærsrud. The geological cross-section is shown in Fig. 3.

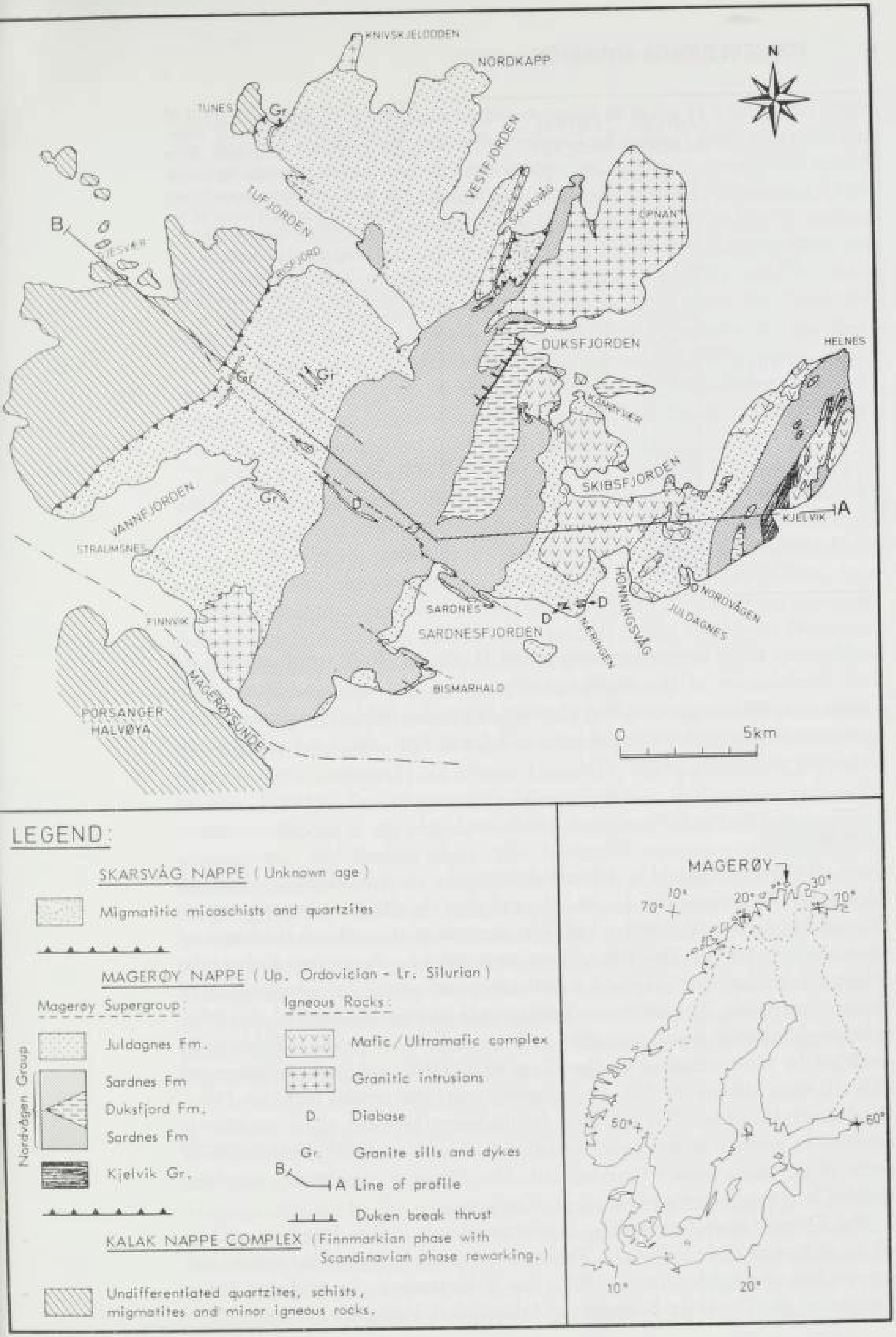
N
KNIVSKJELODDEN
NORDKAPP
TUNES
Gr
VESTFJORDEN
TUFJORDEN
SKARSVÅG
OPNAN
B
GJESVÆR
RISFJORD
DUKSFJORDEN
HELNES
KÅMØYVÆR
SKIBSFJORDEN
KJELVIK
A
VANNFJORDEN
STRAUMSNES
SARDNES
D
HONNINGSVÅG
NORDVÅGEN
JULDAGNES
NERINGEN
FINNVIK
SARDNESFJORDEN
BISMARHALD
MAGERØYSUNDET
PORSANGER HALVØYA
0
5km
LEGEND:
SKARSVÅG NAPPE (Unknown age)
Migmatitic micaschists and quartzites
MAGERØY NAPPE (Up. Ordovician - Lr. Silurian)
Magerøy Supergroup:
Igneous Rocks:
Nordvågen Group
Juldagnes Fm.
Sardnes Fm
Duksfjord Fm.
Sardnes Fm
Kjelvik Gr.
Mafic/Ultramafic complex
Granitic intrusions
D. Diabase
Gr. Granite sills and dykes
B A Line of profile
Duken break thrust
KALAK NAPPE COMPLEX (Finnmarkian phase with Scandinavian phase reworking.)
Undifferentiated quartzites, schists, migmatites and minor igneous rocks.
MAGERØY
10°
70°
20°
30°
70°
60°
60°
10°
20°

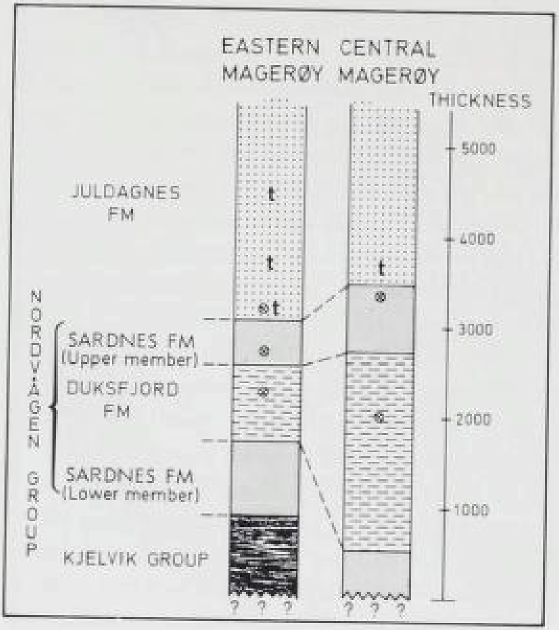


*Fig. 2.* Stratigraphic profiles of the Magerøy Supergroup showing thickness variations from the eastern (Kjelvik–Honningsvåg area) to the central part (Sardnes–Duksfjord area) of the island. Circled crosses and t's show stratigraphic levels at which body fossils and trace-fossils, respectively, have been recorded. All thicknesses in metres. For legend, see Fig. 1.

on Magerøy when the present author and K. Kjærsrud (in prep) commenced their investigation of the stratigraphy, structure and metamorphism in the central and western parts of the Magerøy Nappe in 1976. The present paper represents a shortened version of parts of a Cand. Real. thesis submitted at the University of Bergen, 1979.

## Stratigraphy

Curry (1975) established a lithostratigraphy in eastern Magerøy, between Kjelvik and Næringen (Fig. 1), and showed that the Magerøy Supergroup (as defined by Andersen (1979)) had a minimum stratigraphical thickness of approximately 5.5 km. This area was re-investigated by the present author who effected a further stratigraphical sub-division and partial re-interpretation of Curry's succession. The sedimentological interpretation of some of the lithostratigraphical units is still uncertain, and the preliminary model is liable to be modified by future detailed studies. Two stratigraphic columns are presented (Fig. 2), from eastern (Kjelvik–Honningsvåg area) and central (Sardnes–Duksfjord area) Magerøy. The variation in thickness between these profiles is ascribed to primary lateral facies variation, although tectonic modification of some of the units cannot be ruled out. The Magerøy Supergroup has been divided into two following units:

The *Kjelvik Group* (900 m, Fig. 2) is exposed only in the immediate vicinity of the village of Kjelvik (Fig. 1). This unit consists of interbedded pelites and greywackes, divided by Curry (1975) into 3 formations, the Midttind Pelite Formation, the Transition Formaton and the Kjelvik Psammite Formation. The

Kjelvik Group was by the same author regarded as being of a turbiditic origin. The sequence displays progressively coarser and thicker greywackes towards the top (Curry 1975), and this is thought to reflect a progressive upward shallowing, possibly on a prograding submarine fan system (Andersen 1979).

The stratigraphically overlying *Nordvågen Group* (2180 m, Fig. 2) contains a complex association of metasediments. These include lensoidal bands of conglomerates, limestones, quartzites and greywackes of variable thickness. Most of the unit, however, consists of pelitic and semi-pelitic rocks. The Nordvågen Group is subdivided into 2 formations, the *Sardnes Formation* and the *Duksfjord Formation*. The Duksfjord Formation is laterally discontinuous, and in the eastern and central parts of Magerøy it divides the Sardnes Formation into an upper (500 m) and a lower member (825 m). The stratigraphic thicknesses given here are estimated from eastern Magerøy.

The Duksfjord Formation contains laterally persistent limestone horizons which, in the type locality between Nordvågen and Kjelvik, have yielded a Lower Silurian shelly fauna (Henningsmoen 1961). The fossils recorded include crinoids, brachiopods, favositids, halysitids, heliolitids and rugose corals. Interpretation of the depositional environment of the Nordvågen Group is at present inconclusive, although it appears that much of the group represents shallow-marine sediments. This is most evident in the Duksfjord Formation, where colonial corals have been found in growth position (B. A. Sturt, pers. comm. 1978) together with abundant crinoid fragments.

The *Juldagnes Formation* (2400 m, Fig.2) is the youngest unit preserved in the Magerøy succession. At the base monograptids of Lower Llandoverian age (Monograptus sandersoni) have been found (D. Skevington, pers. comm. in Sturt et al. 1975). Trace fossils are relatively common in the lower part of the formation. Species of the ichnofauna which have been identified include Protopalaeodictyon and Scolitia plana. The formation represents a typical flysch sequence with turbidites of intermediate facies type. In the type area between Honningsvåg and Nordvågen, sedimentary structures typical of turbidite sedimentation are well preserved. These include complete Bouma sequences, soft sediment deformation structures and solemarks. No variation of the depositional environment has been discerned within this formation. The flysch sediments of the Juldagnes Formation probably formed as a consequence of rapid relief-producing processes, most likely associated with early orogenic activity during the Scandinavian phase of the Caledonian orogeny.

## Structural analysis

### INTRODUCTION

The area mapped by the present author extends from Duksfjord in the north to Magerøysundet in the south, and covers approximately 160 km$^2$. Data from the adjacent areas mapped by Curry (1975) and Kjærsrud (in prep.) have been used in the interpretation of the overall structure of the Magerøy Nappe.

Two main deformational events can be discerned in the lithologies of the

Magerøy Nappe, $D_1$ and $D_2$. There is some indication that $D_1$ can be subdivided into two episodes of deformation $D_{1a}$ and $D_{1b}$, separated by a short static interval. This is based mainly on textural evidence from the metamorphic assemblages. The following structural nomenclature symbols are used:

$S_0$ — Bedding.
$D_1$ — First deformational event.
$D_{1a}$ — Earliest phase of $D_1$.
$D_{1b}$ — Main phase of $D_1$.
$S_{1a}$ — Slaty cleavage developed during $D_{1a}$, now preserved in cores of porphyroblasts
$S_1$ — Main planar structure developed during $D_{1b}$ (schistosity in the west, slaty cleavage in the east).
$F_1$ — Folds developed during $D_1$.
$L_1$ — Lineations developed during $D_1$.
$D_2$ — Second deformational event.
$S_2$ — Cleavage (crenulation and pressure solution cleavage) developed during $D_2$.
$F_2$ — Folds developed during $D_2$.
$L_2$ — Lineations developed during $D_2$.

## THE $D_1$ STRUCTURAL PATTERN OF THE MAGERØY NAPPE

### Introduction

The internal $D_1$ structure of the Magerøy Nappe comprises 5 large overturned to recumbent folds (Fig. 3). In the eastern part of the nappe the folds verge towards east-southeast, while those in the west have a northwesterly vergence. This pattern of opposite vergence results in a domain of overall conjugate form in the central part of the island. In consequence 3 structural domains are identified:

1. East Magerøy (eastward vergence)
2. Central Magerøy (divergence of folds)
3. West Magerøy (westvard vergence)

## THE $D_1$ STRUCTURE OF EAST MAGERØY

The $D_1$ structure of this domain (Fig. 3) is formed by a major coupled fold, the *Kjelvik anticline* and the *Pollneset syncline*. Curry (1975) identified the existence of both structures on stratigraphical grounds. The present author, however, disagrees with her interpretation of the geometry and facing of the structures. Curry regarded both folds as downward facing, and held that this pattern was a primary $D_1$ phenomenon rather than a result of refolding. The present author asserts that this is an incorrect and unnecessary complication of the structural pattern. The $S_0/S_1$ relations in all areas where younging and the $F_2$ geometry are recognized, vergence of $D_1$ parasite folds and the preserved main folds closures show that both of the large folds were developed as upward-facing structures. The hinge area of the Pollneset syncline was, however,

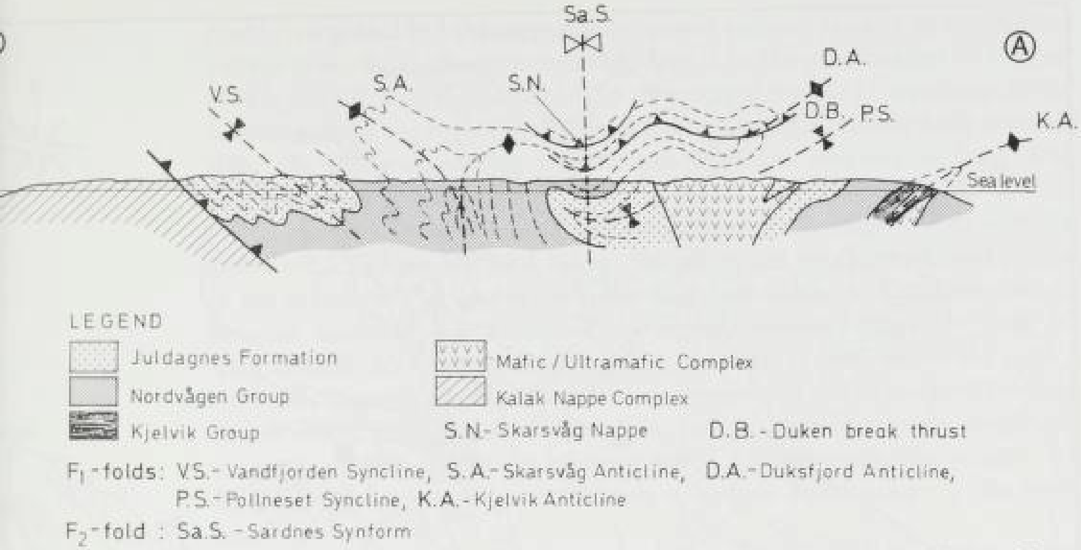


*Fig. 3.* Profile A–B of Fig. 1 showing the major fold structures of the Magerøy Nappe.

refolded during $D_2$ so that west of Sardnesfjorden (see Fig.s 3 and 4) it appears as an antiformal syncline. This is only the situation west of the axial surface of the $F_2$ Sardnes synform (se below and Fig. 5B) where the dip direction of $S_0$ and $S_1$ was changed during $D_2$.

The hinge zone of the Kjelvik anticline is located in the vicinity of the village of Kjelvik. It is not possible to observe the fully developed inverted limb because of the trend of the coastline. Parts of both the Kjelvik Group and the Nordvågen Group are, however, inverted northeast of Kjelvik. Much of the structural pattern of this area has been obliterated by the contact metamorphism associated with the gabbroic bodies of the mafic/ultramafic igneous complex. The common limb of the large coupled fold, is continuously exposed between Kjelvik and Næringen (Fig. 4). The degree of deformation varies considerably depending on the relative competence of the lithologies, as was also shown by Ramsay & Sturt (1970). The present steep dips of $S_0$ and $S_1$ are largely the result of $F_2$ refolding.

The $D_2$ deformation has considerably modified the geometry of the Kjelvik anticline, but as the $F_2$ folding of the area appears to be homoclinal (i.e. the original direction of dip is unchanged), the facing of the $F_1$ fold is preserved. By unfolding the effects of $D_2$, the $F_1$ fold appears to have been developed as an upward-facing anticline, with axial surface dipping 30° W. The plunge of the axis was 013°/7° prior to the $F_2$ refolding, the interlimb angle 27° and the approximate amplitude and wavelength was in the order of 7–7.5 km and 5 km, respectively. The unfolding of $D_2$ is an approximation as the pre-$D_2$ orientation of $S_0$ and $S_1$ is unknown. The easternmost area, however, is least affected by $D_2$ so the orientation of $S_1$ in this area is taken as the pre-$D_2$ orientation on which the unfolding is based. The reconstruction also assumes that $S_1$ had a subparallel development throughout the fold profile.

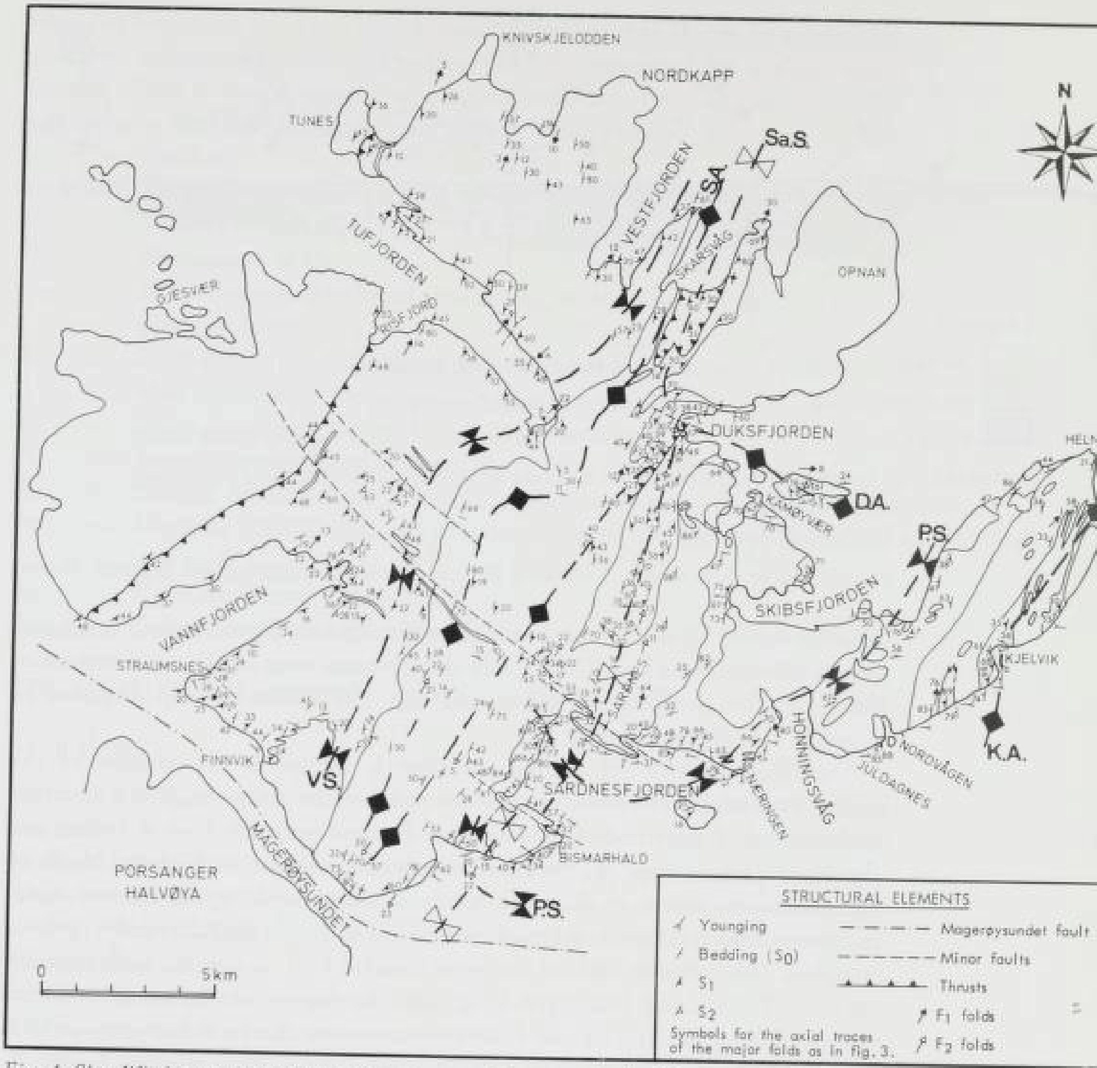


*Fig. 4.* Simplified map of representative structural elements in the Magerøy and Skarsvåg Nappes.

The Pollneset syncline is the complementary syncline to the Kjelvik anticline. The key area for establishing this fold is the shoreline exposure around Sardnesfjorden (Fig. 4), the hinge of the fold being well exposed in the Pollneset area, northwest of Sardnes. The existence of the structure was recognized by Curry (1975), but, as with the Kjelvik anticline, the original facing direction of the fold was misinterpreted. The relatively low metamorphic condition and deformational state of the metasediments in the Sardnes region accounts for good preservation of primary structures. This allows a good stratigraphic control around the closure of the fold from the normal to the inverted limb.

Unlike the area further to the east, the rocks of the Sardnesfjorden region have experienced strong $D_2$ overprinting. The $D_1$–$D_2$ interference pattern is readily recognized and the approximate co-axial surfaces produce an interference pattern (Fig. 5b, c) closely resembling *Type 3* in the classification of Ramsay (1967, p. 530). The change of the dip direction of the pre-$D_2$ structures in the western limb of the $F_2$ Sardnes synform has inverted the primary $S_0/S_1$ relationship. The Pollneset syncline in this area therefore now has the form of an antiformal syncline (Fig. 3).

The inverted limb of the Pollneset syncline is a common limb with the Duksfjord anticline described below. Owing to the gentle northward plunge of the axis (030°/10°), this particular fold limb forms an extensive tract of inverted strata in the Sardnes–Duksfjord–Karmøyvær region, an area of approximately 65 km². Much of the area, however, is occupied by the mafic/ultramafic igneous complex. Because of the presence of thick stratigraphic units, within which stratigraphic markers are lacking or only sparsely developed, mesoscopic parasite folds are rarely observed. Consequently, the vergence of the minor $F_1$ folds consistently shows a normal relationship to the main structures.

The dimensions of the Pollneset syncline are comparable to that of the Kjelvik anticline. The amplitude and wavelength are approximately 7.75 km and 5 km, respectively. Exact values for interlimb angle and attitude of axial surface are not given on account of the pronounced $D_2$ refolding, although it is clear that the fold is tight, i.e. interlimb angle 0–30° (Fleuty 1964), and originally approached a true recumbent fold.

## THE $D_1$ STRUCTURE OF CENTRAL MAGERØY

Divergence of the large-scale $F_1$ folds in central Magerøy produced a domain of overall conjugate form. The box-fold-like polycline of this domain is formed by two, opposite-facing, overturned to recumbent anticlines; *the Duksfjord anticline* and the *Skarsvåg anticline*. The eastward-verging Duksfjord anticline is the better preserved, while the geometry of the westward-verging Skarsvåg anticline is more speculative due to the level of erosion. The structural domain of central Magerøy has an elongated NW–SE-trending shape (Fig. 1). The combination of northerly plunge of both the $F_1$ and the $F_2$ fold axes provides a section through different structural levels of the polycline from north to south, although the topographic relief never exceeds 350 km. From Duksfjord to Magerøysundet (approximately 18 km) a vertical section through 2.5 km of the polycline is exposed. The preservation of the highest levels of the $D_1$ structure in the Duksfjord area is largely due to the later downbuckling in the Sardnes synform ($F_2$).

The core zone of the polycline is best exposed along Magerøysundet and is formed by steep to vertical dipping strata of the Nordvågen Group. The $D_1$ deformation is strong and $S_0$ is transposed in the sub-vertical $S_1$ cleavage. The steep zone ($S_0$ between 50° and 90°) can be traced northwards for approximately 5 km, but poor inland exposures make detailed structural observations difficult. The strong $D_1$ deformation localized in this zone has destroyed most of the primary structures, and younging evidence is not preserved. There are,

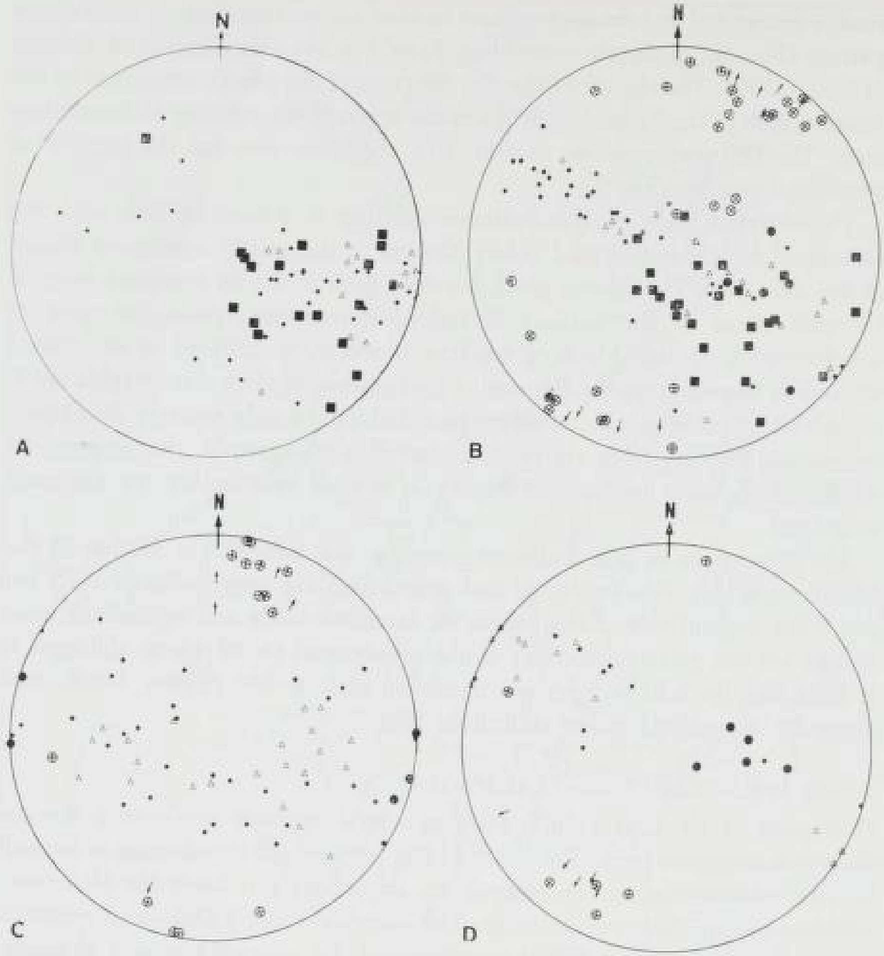


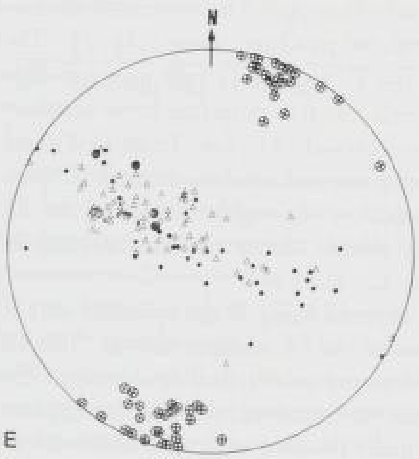


*Fig. 5.* Stereographic plots (equal area) of structural data. A. East Magerøy, B. Sardnesfjorden–Magerøysundet, C. Duksfjord–Sardnes, D. Magerøysundet, E. West Magerøy. Symbols: In A and B, squares—poles to normal $S_0$. Dots—poles to inverted $S_0$. In C, D and E, Dot—poles to unspecified $S_0$. In all plots, open tringles—poles to $S_1$. Heavy dots—poles to $S_2$. Circles with crosses—$F_1$ axes and $L_1$. Arrows—$F_2$ axes and $L_2$.

however, structures present in the transition zone between the Nordvågen Group and the Juldagnes Formation both to the east and to the west of the steep zone, which show that both stratigraphic boundaries are inverted.

In the Duksfjord area where the highest structural levels of the central polycline are preserved, the hinge of the Duksfjord anticline is highlighted by the outcrop pattern of the Duksfjord Formation. Relatively few primary structures are preserved, but the good stratigraphic markers provided by laterally persistent limestones allow correlations to be made over considerable distances. It is possible to extrapolate way-up from areas where evidence of younging can be found in close contact with the limestones. By using this method, in addition to the $S_0/S_1$ relationship, and taking the $F_2$ pattern into consideration, it can be seen that the entire area from Duksfjord to Sardnes is characterized by inverted strata on the inverted middle limb of the Pollneset syncline and the Duksfjord anticline. The lithologies cropping out to the west and north of Duksfjord form the upper, normal limb of the anticline. The outcrop pattern of the Duksfjord Formation indicates that a slide (Fig. 3) occurred between the two limbs. This tectonic break, the Duken break-thrust (Andersen 1979), was developed sub-parallel to the axial surface of the fold, enabling the upper, normal limb to translate further towards southeast over the inverted limb probably during late stages of $D_1$. Mylonitic fabrics are not observed, however, due to the penetrative post-$D_1$ recrystallisation in this part of the island.

The hinge zone of the Duksfjord anticline is characterized by a steep to sub-vertical sheet dip of $S_0$. Large-scale parasitic $F_1$ folds (amplitudes up to 500 m) have been observed in this area along the northern side of Duksfjord. In the closure of the $F_2$ Sardnes synform the pre-$D_2$ orientation of $S_0$ and $S_1$ has been retained. In this position the $S_1$ cleavage dips shallowly towards west. Away from the hinge of the $F_1$ anticline the upper and lower limbs are sub-parallel. This implies that the Duksfjord anticline had a pre-$D_2$, recumbent, sub-isoclinal profile. The restored axis of the Duksfjord anticline plunges at approximately 020°/15°. This is nearly coincident with the $S_0/S_1$ intersection lineation.

Only the lower limb of the Skarsvåg anticline is presently exposed, and this is responsible for the regionally inverted relationship between the Nordvågen Group and the Juldagnes Formation in west-central Magerøy. The sheet dip of $S_0$ on this limb is usually steep (40° E), while $S_1$ dips eastward between 20° and 30°. This $S_0/S_1$ relationship indicates inversion, in agreement with the evidence provided by sedimentary structures. The steep limb is strongly folded, and the long limb/short limb configuration of the parasites indicates that the main structure has a westward vergence. The abundant development of parasite folds on this limb indicates that the strain was strongly compressional. Parasitic structures of different orders of magnitude are developed, ranging in amplitude from centimetres to several metres. These folds are usually noncylindrical and have an incongruous (Ramsay & Sturt 1973) relationship to the main fold. The axis of the Skarsvåg anticline, in contrast to that of the Duksfjord anticline, appears to be sub-horizontal (020°/0°). The co-axial relation of $F_1$ and $F_2$ folds indicates that this was the primary trend of the $F_1$ fold. Because of the presence of the steep inverted limb with parasite folds of relatively low amplitude (compared to wavelength) it is likely that the Skarsvåg anticline was developed as an overturned, asymmetrical fold.

## RECONSTRUCTION OF THE PRE-$D_2$ MORPHOLOGY OF THE CENTRAL POLYCLINE

The difference in geometry and fold profile development in east and west Magerøy is an important factor when trying to reconstruct the original shape of the central polycline. Several uncertainties in this reconstruction exist, particularly for the higher structural levels which have been largely removed by erosion. The $F_2$ refolding and poor inland exposures add further uncertainties to the accuracy of the model presented.

The coupling of the Duksfjord and the Skarsvåg anticlines produced a structural culmination with two hinges; i.e. a polyclinal anticline. Folds of this kind are normally classified as box or conjugate folds (Ramsay 1967). The two anticlines which form the conjugate structure have considerable contrast in fold profile. The Duksfjord anticline is a tight, recumbent structure, while the Skarsvåg anticline probably developed as an overturned, asymmetrical, open fold. The eastward transport of material in relation to the Duksfjord anticline was thus larger than the westward transport associated with the Skarsvåg anticline. The non-uniform geometry of the two folds resulted in an asymmetry of the profile of the polycline. The axes of the two anticlines also differ in plunge (D. A. 020°/15°, S.A. 020°/0°). This, together with the difference in fold profiles, gives the large-scale 'mushroomlike' polycline a geometry which is probably best described as a non-cylindrical asymmetrical box-fold.

## THE SKARSVÅG NAPPE

East of the village of Skarsvåg a sequence of schists and quartzites crop out which are unlike the metasediments of the Magerøy Supergroup, both lithologically and in tectono-metamorphic development. This unit, the Skarsvåg Nappe, forms a relatively thin sheet-like body overlying the Magerøy Nappe. Presently it occupies a site within the core of the Sardnes synform, and in consequence of the northerly plunge of this fold it represents the highest structural level preserved on Magerøy. The lithologies of the nappe consist predominantly of variably migmatized mica schists, together with disrupted layers of quartzite. Work by K. Kjærsrud (pers. comm. 1979) indicates that these lithologies have suffered a more complex deformational history than those of the Magerøy Nappe, but a precise tectono-metamorphic history is not yet delineated. The contact with the Magerøy Nappe is characterized by high-strain fabrics. Particularly along the western margin of the Skarsvåg Nappe the lithologies have a mylonitic appearance. In this area rocks of the Magerøy Nappe, both metasediments and the granitic intrusion of Skarsvåg (Fig. 1), are strongly deformed towards the contact with the Skarsvåg Nappe. K-feldspar phenocrysts in the granitoid are augened in a strong schistosity developed parallel to the contact of the Skarsvåg Nappe. Kjærsrud (pers. comm. 1979) suggests that the intrusion of this igneous body occurred somewhat earlier (syn-$D_1$) than the emplacement of the Finnvik, Opnan and Knivskjelodden granites. The Scandinavian phase $S_2$ crenulation cleavage is penetratively developed in the Skarsvåg Nappe. The interpretation of the migmatitic mica schists and quartzites in the Skarsvåg area as a separate tectonic unit rests on the following arguments.

1) There is a strong contrast between the Magerøy Nappe metasediments and the Skarsvåg Nappe lithologies, and the present author cannot recognize these latter as part of the stratigraphy of the Magerøy Supergroup.
2) The structural development is apparently more complex and indicates a more involved tectono–metamorphic history than for the rocks of the Magerøy Supergroups.
3) The junction between the two units is the locus of high strains, which is characteristic of many thrust zones. This is best displayed along the western margin of the nappe.

Although detailed studies of these lithologies are not yet available, the present author proposes that the Skarsvåg rocks represent an individual tectono–stratigraphic unit (the Skarsvåg Nappe) separated from the Magerøy Nappe by a basal thrust zone. The Skarsvåg Nappe thus forms a higher nappe than the Magerøy Nappe in the tectono–stratigraphy of Finnmark, preserved as a small klippe within the core of the Sardnes synform.

Is is not possible to comment in absolute terms on the age of the lithologies of this nappe. Metasediments of similar character are well known from the type Sørøy succession (Ramsay 1971) of Eocambrian/Cambrian age (Holland & Sturt 1970). This sequence of metasediments forms a major constituent of the Kalak Nappe Complex. This nappe complex, however, also contains Precambrian elements (Brueckner 1973, Ramsay & Sturt 1977, Zwaan & Roberts 1978) and thus a possible Precambrian age for the rocks of the Skarsvåg Nappe cannot be ruled out.

## THE $D_1$ STRUCTURE OF WESTERN MAGERØY

The Skarsvåg anticline forms part of the structural domain characterized by westward-verging folds. This area includes the part of Magerøy west of the central polycline, and east of the Magerøy Nappe basal thrust. The $F_1$ pattern is characterized by the development of macroscopic, asymmetrical to overturned, coupled folds. The most significant of these fold pairs is that formed by the above-mentioned Skarsvåg anticline and the *Vandfjorden syncline*. The fold style of this syncline can be readily identified as both limbs and the hinge are preserved. The syncline, mirrored by the minor parasite folds on the normal, long limb of the fold, is overturned and asymmetrical with an attenuated long limb and thickened, strongly folded, steep short limb. As a result of the pronounced deformation and metamorphic recrystallization, primary

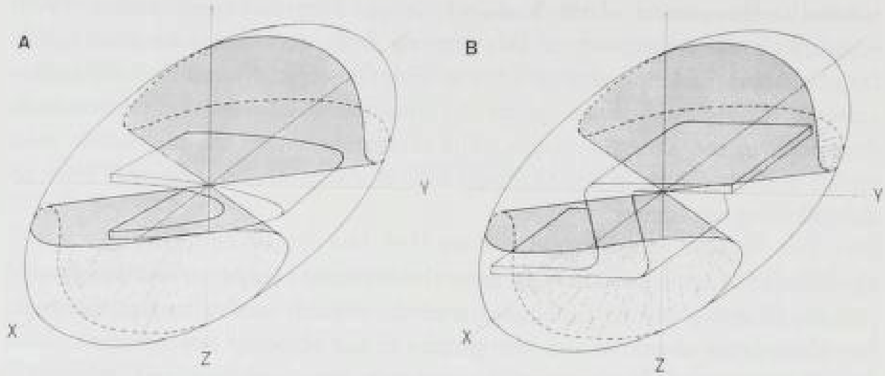


*Fig. 6.* A and B illustrate the difference in style of $F_1$ folds between eastern (A) and western (B) Magerøy. This is a result of different orientation of fold limbs in relation to the regional strain ellipsoid. The strain ellipsoids with surface of no finite longitudinal strain (shaded) shown for K-values of $\infty > K > 1$.

sedimentary structures are only sporadically preserved. Careful mapping was necessary to establish the mean dip of $S_0$, and thus locate the axial trace of the fold. The relatively simple $F_2$ refolding pattern, however, makes the $S_0/S_1$ relationship a valid criterion of younging. The large inter-limb angle of the large-scale asymmetrical folds produced a markedly different orientation of the limbs within the regional strain ellipsoid. This resulted in a marked contrast in the type of deformation observed in the limbs (Fig. 6). The steep short limbs were positioned in the field of compression which resulted in strong folding and tectonic thickening. The long limbs, however, were located within the extensional field and were strongly attenuated (Fig. 6b).

The structural pattern of $D_1$ is likely to have been produced through two successive stages with different orientation of the bulk strain ellipsoid.

1) An initial phase (early-$D_1$) with essentially tangential shortening with respect to the primary attitude of $S_0$. During this phase the present pattern of large-scale folds was set, though considerably modified during the late $D_1$ event.
2) The second phase (late-$D_1$) was characterized by strong flattening strains with attendant intense folding in the steep limbs and attenuation in the flat-lying limbs. This deformation may possibly have been associated with a process of 'gravity collapse', as a result of a combination of tectonic thickening of the nappe itself and a large overburden relating to higher nappe units.

This fold style in the western part of the Magerøy Nappe contrasts with that in the eastern part of the polycline. The development of relatively tight folds in the east produced an orientation of the limbs with approximately the same relative attitude in the bulk strain ellipsoid during the final flattening phase of strain. This resulted in a similar deformational pattern in both limbs of the

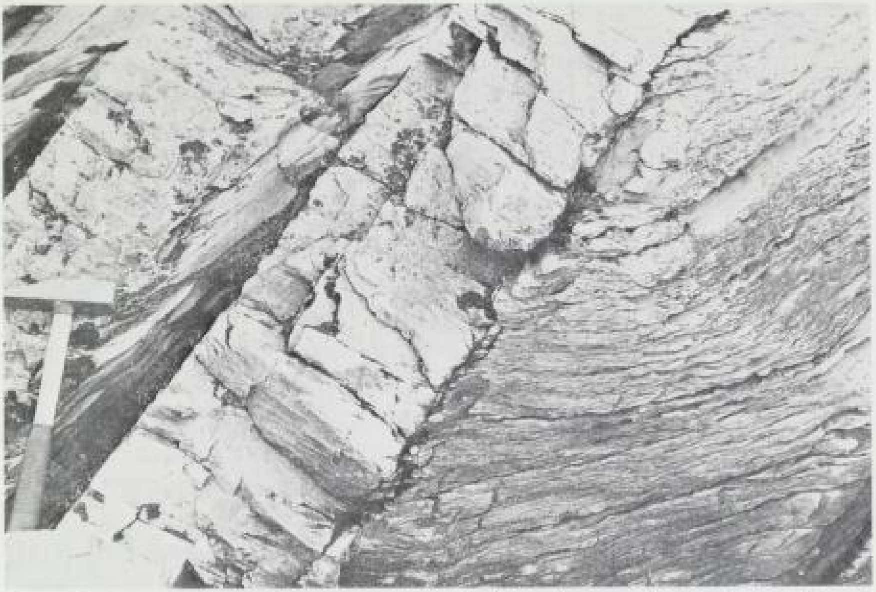

*Fig. 7.* $S_1$ cleavage refraction between coarse-grained sandstones and pelites/semi-pelites of the Sardnes Formation near the hinge of the Pollneset syncline, 2 km northwest of Sardnes.

$D_1$ folds. Accordingly, there is, apart from facing, no difference in fold style of the parasite folds in the normal and inverted limbs of the large-scale $D_1$ folds developed in eastern Magerøy.

THE $D_1$ EVENT: DISCUSSION

Based on mineralogical and textural studies it can be shown that the metamorphic conditions progressively increased during the $D_1$ event. In the east the metamorphic grade never exceeded biotite grade, the assemblages characterizing most of east Magerøy during $D_1$ probably belonged to the chlorite zone of low greenschist facies, and a slaty cleavage developed in the pelitic lithologies (Fig. 7). The study of the minerals characterizing the $S_1$ axial planar foliation indicates that the syn-$D_1$ metamorphism continuously increased towards the west, and by the closing stages of $D_1$ had attained the staurolite/kyanite zone of the amphibolite facies. This late stage of $D_1$ coincides with the final movements along the Magerøy Nappe basal thrust, and the emplacement of the nappe thus occurred during $D_1$ (Ramsay & Sturt 1976).

The study of inclusion patterns in syn-$D_1$ porphyroblasts, particularly garnets, suggests that the $D_1$ event was not a simple and continuous rhythm of rising and waning stress, but consisted of two discrete periods of active stress. These were separated by a short static interval. This suggestion is based essentially on the geometry of the syntectonic (Powell & Treagus 1970) garnet inclusion fabric, but is also supported by structural observations on the early boudinage pattern and its relationship to the stretching lineation in the Sardnesfjorden area (see p. 17). Where it is best developed the garnet inclusion

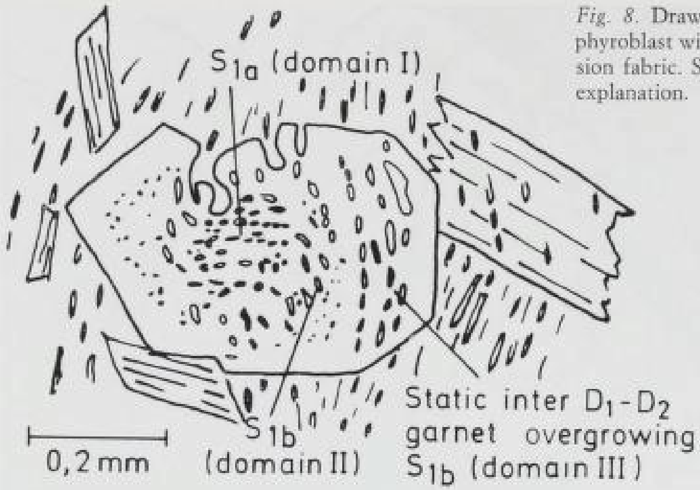


*Fig. 8.* Drawing of garnet porphyroblast with composite inclusion fabric. See text for further explanation.

pattern defines three domains within the porphyroblasts. These are illustrated in Fig. 8 and their characteristics can be summarized as:

Domain I. The inclusions are formed by quartz and opaque dust and are aligned in straight lines.

Domain II. The inclusions define curves, and are coarsened compared to those in domain I.

Domain III. The inclusions are further coarsened and are again, as in domain I, aligned in straight lines. These are parallel to the $S_1$ cleavage developed in the matrix.

The sequence of formation of this pattern of inclusions in garnets is considered to have originated as follows:

1. Tectonic stress produced an early planar structure ($S_{1a}$) in the rock prior to garnet crystallization. This structure $S_{1a}$ is preserved as relics in the core of porphyroblasts (Fig. 8).
2. The regional temperature increased and garnet growth was initiated. These porphyroblasts overgrew the $S_{1a}$ without rotation, probably in a static interval. The groundmass fabric gradually coarsened and this is reflected in the size of the individual inclusions. This stage of garnet crystallization is represented by domain I.
2. Further temperature increase under active stress caused rotational growth (syntectonic) of the garnets. This was accompanied by a general coarsening of the fabric, and represents domain II in the porphyroblasts.
4. The outer domain III was produced under static crystallization post-$D_1$. The garnets overgrew the $S_1$ cleavage, and the inclusions define straight lines parallel to the external $S_1$ cleavage.

Other explanations for the observed pattern are possible. A very rapid crystallization of garnet during the initial stage of growth, so that rotation was not recorded, may explain the straight inclusion trains of domain I. Electron microprobe analysis of garnets (Andersen 1979), however, shows a strong normal zonation (Atherton 1968) also within the innermost domain of the garnet porphyroblasts. This zonation is also continuous with that in the outer part of the porphyroblasts. There is therefore no evidence for particularly rapid growth of individual garnets in the early stages of their formation. The observed pattern of domains I, II and III is thus probably most satisfactorily explained through the stages 1 to 4 outlined above.

In the Sardnesfjorden area a pattern of boudinage in the competent sandstone beds is observed in which the boudin necks are aligned parallel to the axis of the Pollneset syncline. Boudinage in two directions (Chocolate-tablet boudinage, Ramsay (1967) has not been observed. This indicates that the k-values (Ramsay 1967) were considerably thigher than $k = 0$. The Sardnesfjorden boudin orientation appears to indicate that the principal direction of extension during the stage of the deformation history at which the boudins formed was at a high angle to the axis of the Pollneset syncline. This observation is in contradiction to other observations of stretching direction from the same area. The long axes of pebbles in deformed conglomerates, as well as the general mineral stretsching lineation, parallel the axis of the large-scale syncline. The rock-element stretching lineation thus indicates that the principal extensional axis was parallel to the fold axis. Examination of hydrothermal quartz in boudin necks also shows a rodding of quartz parallel to the $F_1$ fold axis.

When viewed in context with the observed inclusion pattern in garnet porphyroblasts, it is believed that the boudinage pattern in the Sardnesfjorden area has originated as a result of a polyphasal deformation history of the main $D_1$ event.

I) At early (low T) stages of $D_1$ ($D_{1a}$), the principal direction of extension was oriented at a high angle to the fold axis, indicated by the pattern of early boudins.
II) At later stages of $D_1$ ($D_{1b}$), the X-axis of the strain ellipsoid was orientated parallel to the axis of the main folds. Growth of minerals and deformation/rotation of pebbles took place under this phase of $D_1$ which occurred at more elevated T-conditions as seen from the syn-tectonic mineral assemblages.

The polyphasal pattern of $D_1$ is only detectable in the area of Magerøy with eastward vergence of the large-scale folds. If this pattern developed in the west it appears to have been completely obliterated by the late-$D_1$ deformation and subsequent metamorphic recrystallization. The significantly higher syn-$D_1$ metamorphic conditions in the west show a different and deeper crustal level for this part of the nappe during $D_1$. The difference in crustal level might be attributed to a continued stacking of higher nappe from the west on to the Magerøy

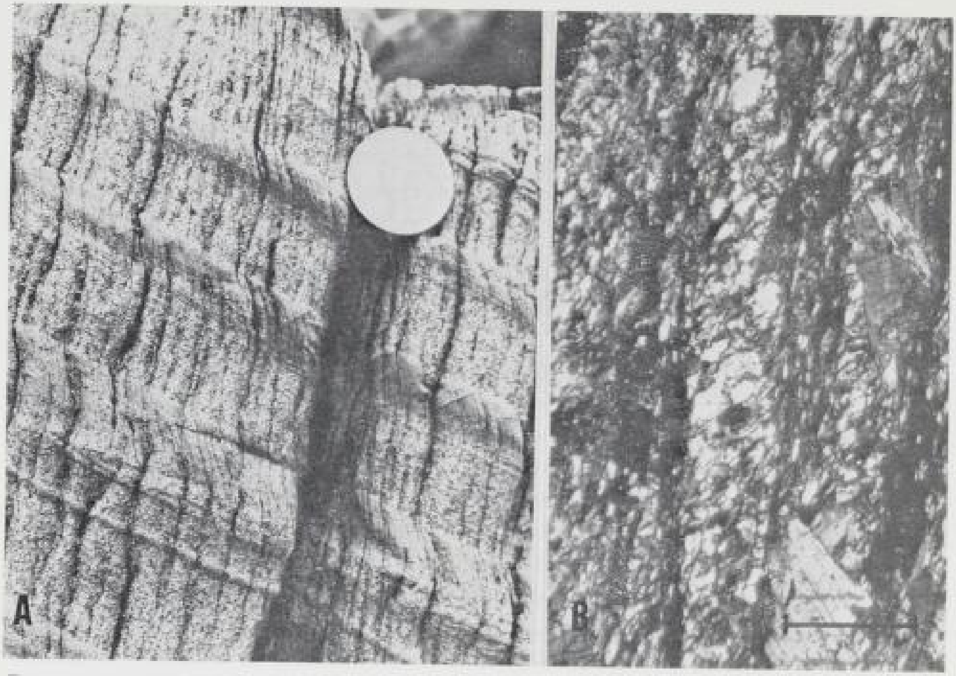

*Fig. 9.* (A) $S_2$ cleavage showing refraction in an alternating shale and sandstone lithology of the Juldagnes Formation, from the west side of Sardnesfjord. The coin measures 3 cm. (B) Photomicrograph of the pelite in (A) showing the $S_2$ pressure solution cleavage. The microlithons contain a relict $S_1$ cleavage and interkinematic (post-$D_1$/pre-$D_2$) biotite porphyroblasts. Bar scale, 0.2 mm.

Nappe which immediately overlies the Finnmarkian basement, as indicated by the presence of the Skarsvåg Nappe. These higher grade conditions were further amplified during the inter $D_1$–$D_2$ period. The difference in both deformational pattern and metamorphism between the western and eastern parts of the nappe is thus attributed to difference in crustal level for the two parts of the nappe

STRUCTURAL PATTERN PRODUCED DURING $D_2$

The second major fold phase ($D_2$) affecting the Ordovician–Silurian metasediments and also the igneous rocks which were intruded inter $D_1$–$D_2$, was less penetrative than $D_1$. The deformation took place under waning metamorphic conditions, which nowhere in Magerøy exceeded middle greenschist facies. The folds that developed form a set of essentially upright open structures. The $S_2$ crenulation and pressure solution cleavage is developed with a variable intensity (Fig. 9). The most intense $D_2$ strains are localized in the relatively incompetent lithologies of the Nordvågen Group, particularly in the Duksfjord Formation, which has a spatial distribution along the core of the Sardnes synform.

THE SARDNES SYNFORM

The dominant $D_2$ structure on Magerøy is the Sardnes synform. Although large

*Fig. 10.* Stereographic plot (equal area) of $D_2$ structural elements from southern Magerøy. The variation in $S_2$ orientation is a result of macroscopic convergent cleavage fanning across the Sardnes synform. Symbols: Dots—poles to $S_2$. Arrows—$F_2$ axes and $L_2$.

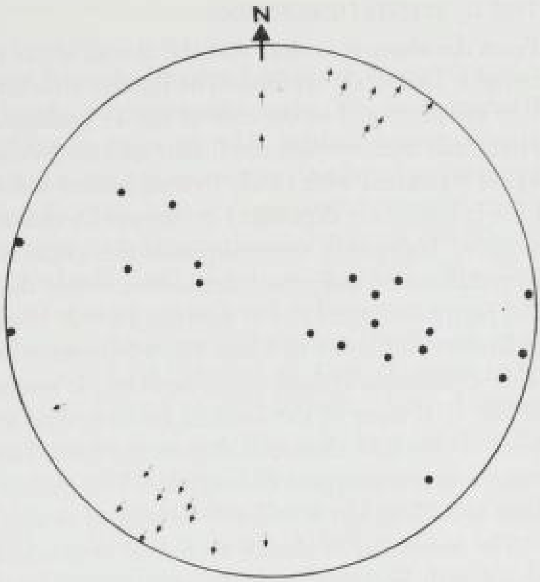


$F_2$ folds exist both east and west of the axial trace of this structure they are developed as parasitic folds on the large-scale central synform. This parasite/host relationship is illustrated by the overall attitude of $S_2$, which forms a macroscopic convergent cleavage fan (Fig. 10). The axial trend of the Sardnes synform is on average sub-parallel to that of the major $F_1$ folds. Locally, however, the trend of the axis varies considerably between 045° and 350°. For most of its observable distance the trend is approximately 010°–020°. The local deflections of the axis probably result from a primary non-plane, non-cylindrical folding of an inhomogeneous rock body. This inhomogeneity is expressed by variable competence of the sediments and also by the presence of the intrusive Skarsvåg and Opnan granitoids. There is no sign of later folding, and the irregularities in direction and plunge of the axis have probably developed as a primary feature of the synform. The axial surface of the synform is vertical to steeply westward dipping (80°–90°). The gentle eastward overturning of the synform is most pronounced in the southern segment of the area towards Magerøysundet (Fig. 4).

Several major $F_2$ folds can be discerned on both limbs of the main synform. On the eastern limb Curry (1975) recognized two major $F_2$ folds forming an asymmetrical fold pair. This is mirrored in the western limb. The long limb/short limb relationship of these flexures relative to the Sardnes synform is consistent with a normal parasite/host fold relationship. Curry (1975) showed the asymmetrical fold pair on the eastern limb to have a non-coaxial relationship to the host. Those developed on the western limb are essentially co-axial, but die out when traced along their axes in the northerly direction.

THE $D_2$ EVENT: DISCUSSION

From the above it is clear that the overall effect of $D_2$ was the formation of an upright, large-scale synform. The highest structural levels of the $D_1$ fold structure are preserved in the core of the $F_2$ synform. This event took place under retrograde metamorphic conditions and the locally intense $S_2$ crenulation cleavage is associated with newly formed biotite and white mica. The development of $S_2$ is essentially dependent on the pre-$D_2$ characteristics of the lithologies. In areas of high-grade metamorphism the grain coarsening produced by static recrystallization and neomineralization during the metamorphic peak (inter $D_1$–$D_2$) partly destroyed the $S_1$ foliation, which is necessary for a subsequent crenulation cleavage to develop. Fig. 10 shows a non-uniform orientation of $S_2$. This variation in attitude of $S_2$, however, is systematic in the sense that $S_2$ east of the axial trace of the Sardnes synform dips towards the west while to the west of this fold closure it dips to the east. The cleavage, therefore, forms a macroscopic convergent cleavage fan. This pattern is not explicable in terms of later re-folding, but is probably developed as a primary $D_2$ feature.

The formation of the $D_2$ synformal structure is probably a result of large-wavelength buckling in the basement. This folding produced open antiforms and synforms with axes trending approximately 010°–030°. The Magerøy Nappe and the Skarsvåg Nappe, which represent the highest tectonic units in the nappe sequences in Finnmark (Sturt et al. 1978, Kjærsrud, in prep.) are situated within the core of the major Sardnes synform. As such they partly owe their preservation from erosion to this folding, although more important is the downfaulting of the northern block on the Magerøysundet fault. A relatively extensive tract of Finnmarkian basement is exposed in the Gjesvær area (Fig. 1). This area represents a preserved part of a complementary antiform to the west of the $F_2$ Sardnes synform. The basal thrust of the Magerøy Nappe was thus folded during $F_2$ into its present attitude with a dip of 40°–50° to the south-east.

None of the major structures, $D_1$ or $D_2$, can be directly correlated across the Magerøysundet fault. There has been a considerable post-$D_2$ movement along this structure. This involves both normal dip-slip and also dextral strike-slip components (Zwaan & Roberts 1978). It is not possible, however, to quantify this movement. On the mainland in west Finnmark there are recorded several large-scale flexures. These structures post-date the Finnmarkian $D_2$ event, and fold the Finnmarkian thrust planes (Sturt, pers. comm. 1979). Associated with this late folding there are kink bands that cut all Finnmarkian structures (Jansen 1976). It is suggested that the folds of this generation form the dome-like structures in which the windows of low-grade Karelian rocks are exposed (Komagfjord and Alta–Kvænangen windows).

Both trend and style of the late folds of the mainland closely correspond with the $D_2$ pattern observed in the Magerøy Nappe and its substrate in western Magerøy. It is therefore suggested that the late buckling of the Finnmarkian nappes and substrate in west Finnmark occurred during the Scandinavian phase of the Caledonian orogeny, and probably at a late stage of this phase.

## Faulting

The Magerøy Nappe is separated from the Finnmarkian Kalak Nappe Complex of Porsangerhalvøya (Fig. 1) by the Magerøysundet fault. This fault transects and thus post-dates the Scandinavian phase $F_2$ folds in the Magerøy Nappe. Faults of similar trend and relative age are commonly developed on Magerøy north of the main fault. The trend of this fault set is essentially parallel to the major fault in the Varanger area of east Finnmark known as the Trollfjord–Komagelv fault (Siedlecka & Siedlecki 1967, Kjøde et al. 1978). The final large-scale movements along this structure are believed to have occurred before late Devonian times. This conclusion is based on K/Ar dating (Beckinsale et al. 1975) of dolerite dykes that occur on both sides of the fault (Roberts 1975) and which have given ages of around $355 \pm 10$ m.y. A mafic dyke of similar characteristics and which post-dates the movement along faults parallel to the Magerøysundet fault occurs in central Magerøy. Although no conclusive evidence is available concerning the age of the faulting, the similarity to the Trollfjord–Komagelv fault situation is evident. It is therefore likely that the Magerøysundet fault forms part of an extensive fault system related to the Trollfjord–Komagelv structure.

## Summary and conclusion

The emplacement of the Magerøy Nappe occurred during the Silurian, Scandinavian phase of the Caledonian orogeny (Ramsay & Sturt 1976). The earliest orogenic activity which relates to this phase is probably represented by the development of the 2.4 km-thick flysch sequence of the Juldagnes Formation.

The tectono–metamorphic features of this orogenic phase are imprinted on the lithologies of the nappe as two deformational events with attendant regional metamorphism. The metamorphism reached its peak during the interkinematic period ($D_1$–$D_2$), and was accompanied by important syn-orogenic magmatism. This included both acid and mafic/ultramafic intrusions. The Finnvik granite, intruded coevally with the metamorphic peak, has given a Rb/Sr whole rock isochron age of $417 \pm 11$ m.y. B.P. ($Rb^{87} = 1.42 \times 10^{-11}$). As such, it dates the age of the Scandinavian phase metamorphism (Sturt et al. in prep.). Recent geochronological studies from the Gjesvær migmatite complex (H. Austrheim, pers. comm. 1979) indicate that this metamorphism also resulted in an isotopic homogenization in the Finnmarkian basement, as shown by a Rb/Sr whole rock isochron of $409 \pm 28$ m.y. for this complex. The high $Sr^{87}/Sr^{86}$ ratios, 0.7111 for the Finnvik granite and the exceptionally high 0.7547 for the Gjesvær migmatites, imply a long crustal history prior to the final isotope homogenization.

There are indications of early low-T deformation during the initial stages of $D_1$. The increasing regional metamorphism which accompanied $D_1$ shows that the lithologies were depressed to progressively deeper crustal levels. This is considered by the author to be the result of a continued stacking of higher nappe units onto the Magerøy Nappe, such as is represented by the Skarsvåg Nappe. The strong metamorphic zonation which had developed at the closing stages of $D_1$, and which was further amplified in the inter $D_1$–$D_2$ period, indicates that the western basal parts of the nappe were positioned at deeper crustal levels than the eastern parts. This may have been a result of a combination of a relatively steep westward dip of the thrust and therefore a considerable overburden from the higher structural levels of the Magerøy Nappe and probably also from nappes in a structurally more elevated position.

The tectono–thermal environment during the second deformational event, $D_2$, was clearly different from that which prevailed during $D_1$. By the onset of $D_2$ the temperatures had dropped to a level characterized by lower greenschist facies metamorphism. This event, producing the open, upright folds, probably occurred during the early stages of the uplift-cooling history of the area. The basal thrust plane developed its present orientation, with a dip towards the southeast, as a result of strong upbuckling of the Finnmarkian basement to the west.

*Acknowledgements.* – The author is particularly grateful for the critical advice and help given by Prof. B. A. Sturt, Univ. of Bergen, during the course of this work. Thanks also to Prof. D. M. Ramsay, Univ. of Dundee, and Cand. Real. A. Thon, Univ. of Bergen, for their critical reading and improvement of the manuscript. E. Irgens and J. Ellingsen are thanked for the drafting of maps and illustrations.

International Geological Correlation Programme.
Norwegian contribution No. 38 to Project Caledonian Orogen.

## REFERENCES

Andersen, T. B. 1979: *The geology of south-western Magerøy; with special reference to the tectono–metamorphic development.* Unpubl. Cand. Real. thesis, Univ. of Bergen. 338 pp.

Atherton, M. P. 1968: Variation in garnet, biotite and chlorite composition in medium grade pelitic rocks from the Dalradian, Scotland, with particular reference to zonation in garnet. *Contrib. Mineral. Petrol. 18*, 347–371.

Beckinsale, R. D., Reading, H. G. & Rex, D. C. 1975: Potassium–Argon ages for basic dykes from East-Finnmark: Stratigraphical and structural implications. *Scott. J. Geol. 12*, 51–65.

Brueckner, H. K. 1973: Reconnaissance Rb–Sr investigation of salic, mafic and ultramafic rocks in the Øksfjord area, Seiland province, northern Norway. *Norsk geol. Tidsskr. 53*, 11–23.

Curry, C. J. 1975: *A regional study of the geology of the Magerøy basic igneous complex and its envelope.* Unpubl. Ph. D. thesis, Univ. of Dundee. 244 pp.

Fleuty, M. J. 1964: The description of folds. *Proc. Geol. Ass. 75*, 461–492.

Føyn, S. 1967: Stratigraphical consequences of the discovery of Silurian fossils on Magerøy, the island of North Cape. *Norges geol. Unders. 347*, 208–222.

Henningsmoen, G. 1961: Cambro–Silurian fossils in Finnmark, northern Norway. *Norges geol. Unders. 213*, 93–95.

Holland, C. H. & Sturt, B. A. 1970: On the occurrence of archaeocyathids in the Caledonian metamorphic rocks of Sørøy, and their stratigraphic significance. *Norsk geol. Tidsskr. 50*, 345–355.

Holtedahl, O. 1944: On the Caledonides of Norway. *Skr. Norske Vidensk.-Akad. i Oslo. Mat.-Naturv. Kl. 4, no. 1.*

Jansen, Ø. 1976: *Strukturell og metamorf utvikling i den vestlige del av Komagfjord-vinduet og overliggende dekker.* Unpubl. Cand. Real. thesis, Univ. of Bergen, 198 pp.

Kjøde, J., Storetvedt, K. M., Roberts, D. & Gidskehaug, A. 1978: Palaeomagnetic evidence for large-scale dextral movement along the Trollfjord–Komagelv Fault, Finnmark, North Norway. *Phys. Earth. Plan. Int. 16*, 132–144.

Lønne, W. & Sellevoll, M. A. 1975: A reconnaissance gravity survey of Magerøy, Finnmark, Northern Norway. *Norges geol. Unders. 319*, 1–15.

Powell, D. & Treagus, J. E. 1970: Rotational fabrics in metamorphic minerals. *Min. Mag. 37*, 801–814.

Ramsay, D. M. 1971: Stratigraphy on Sørøy. *Norges geol. Unders. 269*, 314–317.

Ramsay, D. M. & Sturt, B. A. 1970: Polyphase deformation of a polymict Silurian conglomerate from Magerøy, Norway. *J. Geol. 78*, 264–280.

Ramsay, D. M. & Sturt, B. A. 1973: An analysis of non-cylindrical and incongrous fold pattern from Eo-Cambrian rocks of Sørøy, Northern Norway. *Tectonophysics 18*, 81–107.

Ramsay, D. M. & Sturt, B. A. 1976: The syn-metamorphic emplacement of the Magerøy Nappe. *Norsk geol. Tidsskr. 56*, 291–307.

Ramsay, D. M. & Sturt, B. A. 1977: A sub-Caledonian unconformity within the Finnmarkian nappe sequence and its regional significance. *Norges geol. Unders. 334*, 107–116.

Ramsay, J. G. 1967: Folding and fracturing of rocks. McGraw Hill, New York, 568 pp.

Roberts, D. 1974: Hammerfest. Description of the 1:250,000 geological map. *Norges geol. Unders. 301*, 66 pp.

Siedlecka, A. & Siedlecki, S. 1967: Some new aspects of the geology of Varanger Peninsula (northern Norway), preliminary report. *Norges geol. Unders. 247*, 288–306.

Sturt, B. A., Pringle, I. R. & Roberts, D. 1975: Caledonian nappe sequence in Finnmark, northern Norway, and timing of orogenic deformation and metamorphism. *Geol. Soc. Am. Bull. 86*, 710–718.

Sturt, B. A., Pringle, I. R. & Ramsay, D. M. 1978: The Finnmarkian phase of the Caledonian orogeny. *Geol. Soc. London 135*, 597–610.

Zwaan, K. B. & Roberts, D. 1978: Tectonostratigraphic succession and development of the Finnmarkian nappesequence, North Norway. *Norges geol. Unders. 343*, 53–71.

# Geochemistry and Petrology of Dolerite Dykes of Probable Late Caledonian Age from the outer Sunnfjord Region, West Norway

F. J. SKJERLIE & M. TYSSELAND

Skjerlie, F. J. & Tysseland, M. 1981: Geochemistry and petrology of dolerite dykes of probable late Caledonian age from the outer Sunnfjord region, West Norway. *Norges geol. Unders. 363*, 25–43.

Major and trace element abundances from dolerite dykes in the outer Sunnfjord region show an overall compositional similarity to continental tholeiites. The dyke rocks exhibit a fractionated nature, especially with respect to a strong enrichment in total Fe and in Ti. The fractionation apparently took place in a deep-seated magma chamber where plagioclase and clinopyroxene were formed as phenocrysts. During ascent of the magma, suspended pyroxene phenocrysts underwent marginal growth and strong resorption of plagioclase primocrysts took place. The PT variation trend during intertelluric crystallization of the Sunnfjord dolerite magmas has been outlined on the basis of textural features and mineral compositions. The geological relationships in the area indicate that the emplacement of the dyke swarm took place in the Lower Devonian and may thus represent the youngest igneous event in the outer Sunnfjord region.

*F. J. Skjerlie & M. Tysseland, Geologisk Institutt, Avd. A, Allégt. 41, Universitet i Bergen, 5014 Bergen, Norway*

## Introduction

Dolerite dykes in the outher Sunnfjord region were first reported from Kinn by Reusch (1881) and subsequently described both from Kinn and Moldvær by Kolderup (1928). Two more dykes, at Sandvik and Gronevik, were noted by Kildal (1969) and a further dyke has been observed at Haukå by Bryhni (pers. comm. 1979).

The present authors believed that these dykes could be members of an extensive dyke swarm in this region and a systematic search for dolerites was carried out. Thirty dolerite dykes have been sampled from various localities (Fig. 1) and their whole rock and mineral geochemistry investigated.

## Geological setting

The Vevring Complex (Fig. 1), which consists of eclogite-bearing amphibolites, gneisses and schists, represents the deepest exposed level in this region and is of Precambrian age (Furnes et al. 1976, Skjerlie & Pringle 1978). It is bounded by major faults with E–W trends (Fig. 1). These faults are considered by Steel (1976) to represent parts of a Devonian graben/wrench fault system. The most complete structural sequence within the graben areas occurs in the southern part of the region. The lowermost unit here is the Askvoll Group which is a parautochthonous sequence of supposed Lower Palaeozoic age (Skjerlie 1969,

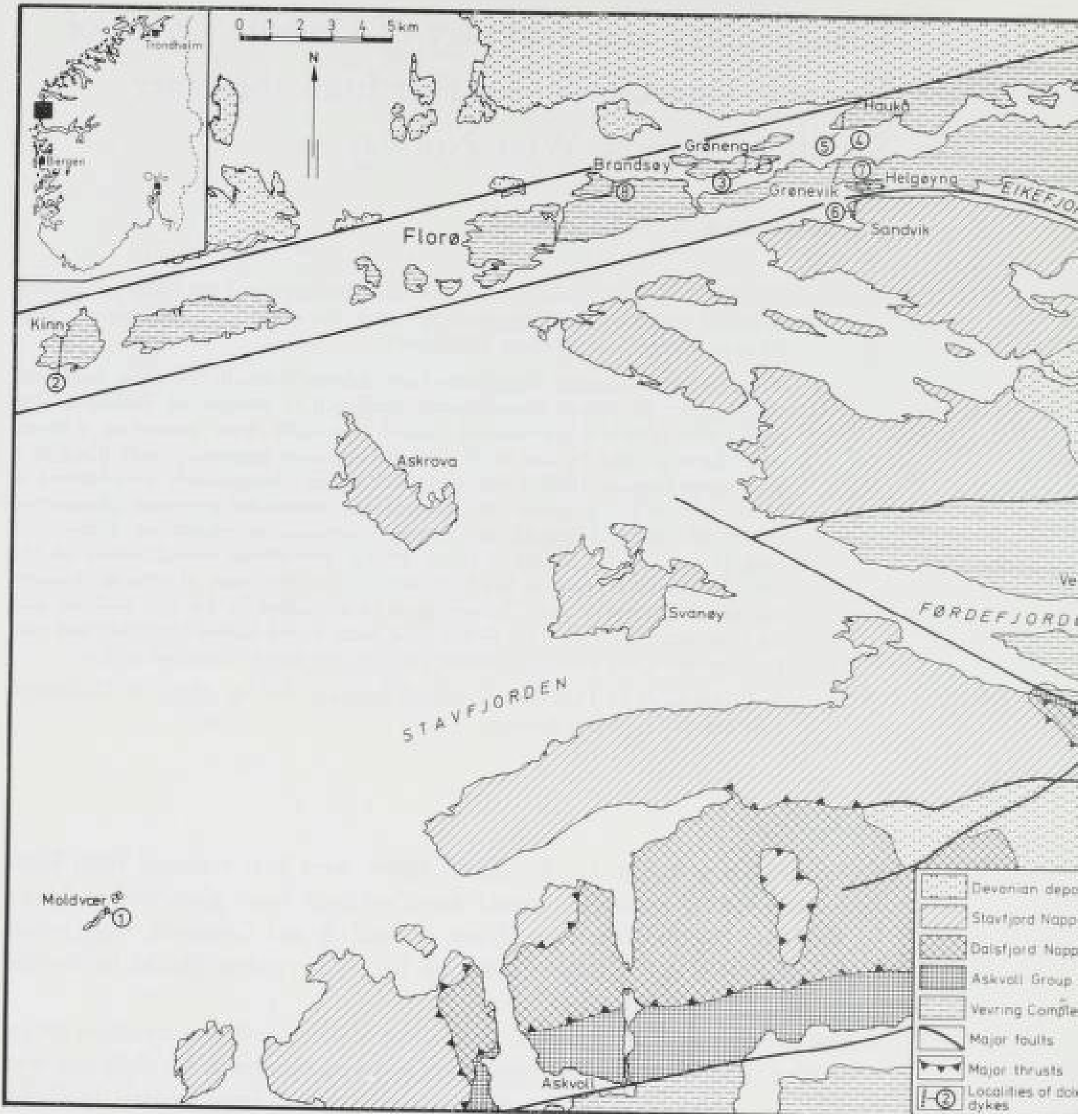


*Fig. 1.* Simplified geological map of the outher Sunnfjord region showing the locations of the dolerite dykes.

Furnes et al. 1976). This unit is tectonically overlain by the Dalsfjord Nappe which consists of Precambrian charnokitic rocks. The charnokitic rocks are in turn overthrust by the rocks of the Stavfjord Nappe (Skjerlie 1969). The uppermost unit comprises deposits of Devonian age. In the northern part of the region only parts of this succession are present.

## Field relationships

The thirty dolerite dykes which have been found to date in the outer Sunnfjord region occur in zones where there is a high incidence of jointing in the host rocks. Twenty-five of the dykes intrude the Precambrian Vevring Complex and are concentrated in the area between Kinn and Haukå-Helgøyna. Five of the dykes, however, intrude rocks of the Stavfjord Nappe (Fig. 1, localities 1 and 6).

Widths of the dykes range from 10 cm to 10 m, but the majority are from 50 cm to 2 m in thickness. They strike consistently NNE–SSW and are either vertical or dip steeply to the WNW regardless of the structure of the country rocks. The dykes exhibit chilled margins, and apophyses and host rocks xenoliths are rather common.

The dykes at Haukå (Fig. 1, loc. 5) do not extend into the Devonian rocks to the north, nor have dolerite dykes been observed to cut Devonian deposits anywhere else in the outer Sunnfjord region. Some of the dykes on Helgøyna (loc. 7) and on Brandsøy (loc. 8) end abruptly at faults trending parallel to the major dislocations, and the dykes have locally been strongly fractured as a result of movements along these structures. The authors consider that the emplacement of the dolerite dykes pre-dated the major faulting which controlled the deposition of the Middle Devonian sediments (Skjerlie 1971). A further line of evidence for a late Caledonian emplacement is that dykes which cut the rocks of the Stavfjord Nappe, the latter presumably metamorphosed during the Caledonian orogeny, show no signs of metamorphism.

Although the geological relationships indicate a possible Lower Devonian emplacement age for the dykes, preliminary age determinations (K/Ar) show a spread of values from 480–990 Ma (Macintyre pers. comm. 1980), and no unequivocal pattern has yet emerged. Obviously the true age of these dykes will be of considerable importance in any geotectonic reconstruction of the area; work is in progress on the geochronology of the dykes by Macintyre (K/Ar) and Råheim (Rb/Sr).

## Petrography

The dolerite dykes are fine-grained melanocratic rocks containing plagioclase and pyroxene phenocrysts and glomerocrysts up to 5 mm across. Under the microscope the dykes show a very uniform mineralogy dominated by plagioclase, clinopyroxene and opaques. Reddish-brown biotite and apatite occur as accessories, and quartz has been detected in some of the dykes by microprobe analysis. The ore minerals are essentially titanomagnetite with small amounts of pyrite.

The dykes usually exhibit a glomeroporphyritic texture. Clinopyroxene occurs as phenocrysts in addition to plagioclase. The plagioclase is twinned according to the albite, Carlsbad and pericline laws and the plagioclase phenocrysts commonly show oscillatory zoning. The clinopyroxene is an augite and may exhibit a visible zoning. Both simple and polysynthetic twinning are common in the clinopyroxene phenocrysts.

The cores of the plagioclase phenocrysts show varying degrees of resorption, and may be deeply embayed along their margins and along Carlsbad twin planes (Fig. 2). The less intensely resorbed crystals clearly show that the cores were originally euhedral and tabular. The shapes of the outer zones have, however, been influenced by neighbouring mineral grains during their growth. The margins of the plagioclase phenocrysts also carry poikilitic inclusions of pyroxene. The plagioclase phenocrysts, therefore, appear to have originated during two stages of crystal growth.

Among the groundmass minerals there appears to be some textural evidence that pyroxene began to crystallize before plagioclase. Even though the plagioclase grains are generally elongated in the [001] zone direction, their shape is irregular due to interference with

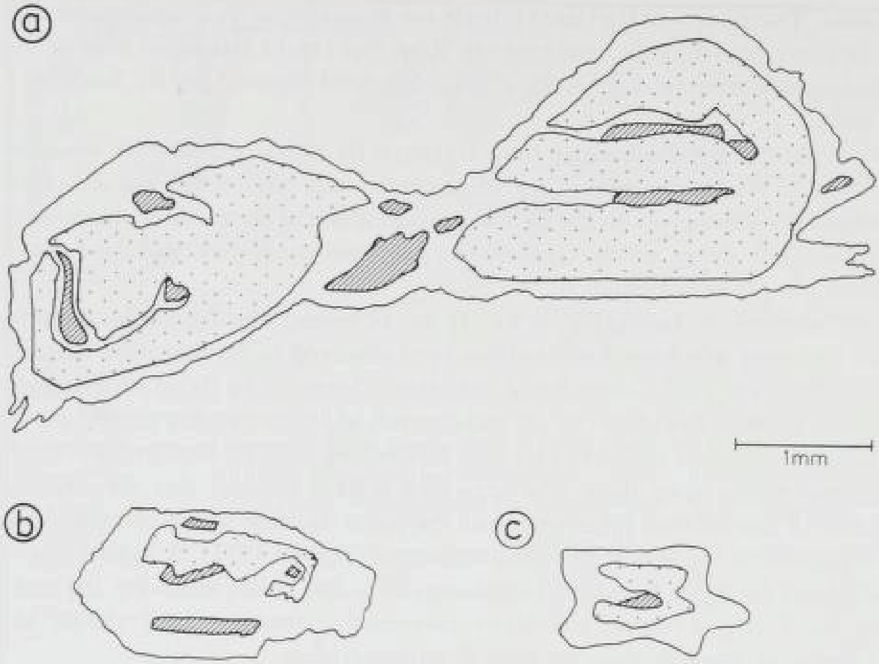


*Fig. 2.* Plagioclase crystals from the Sunnfjord dolerites. Primocrysts (stippled) have been partly resorbed along their margins and twin planes. Their outer zones carry poikilitic inclusions of clinopyroxene (hatched). a – Plagioclase from dyke 7b; b – Plagioclase from dyke 5d; c – Plagioclase from dyke 8b.

neighbouring pyroxene grains. Poikilitic inclusions of pyroxene in plagioclase also imply that the groundmass pyroxene commenced crystallization before plagioclase.

The titanomagnetite almost certainly commenced crystallization as the last of the major phases and tends to be moulded around the pyroxene and plagioclase grains. Even though there is some suggestion of mutual intergrowth of pyroxene and titanomagnetite, and the plagioclase may have small amounts of titanomagnetite as poikilitic inclusions, the sequence of groundmass crystallization appears to have been pyroxene-plagioclase-titanomagnetite.

The dolerite dykes are as a rule extremely fresh. In a few of the dykes, however, the clinopyroxene is altered to biotite to a minor degree. A weak sericitization of the plagioclase phenocrysts may also be seen in some of the dykes. One of the dykes (6a) exhibits a pervasive sericitization.

## Analytical techniques

Major elements were determined by XRF, using glass beads prepared according to the method of Padfield & Gray (1970) except for sodium for which pressed powder pellets were employed. Twenty international standards and the recommended values of Flanagan (1973), refined by least-squares procedures and matrix corrections, were used for calibration. Ferrous iron was determined titrimetrically using potassium dichromate.

The trace elements were determined by XRF using pressed powder pellets. Twelve international standards and the recommended values of Flanagan (1973) refined by least-squares procedures were used for calibration.

The mineral analyses were made with an ARL-SEMO electron microprobe using a series of natural and synthetic standards an ZAF correction procedures.

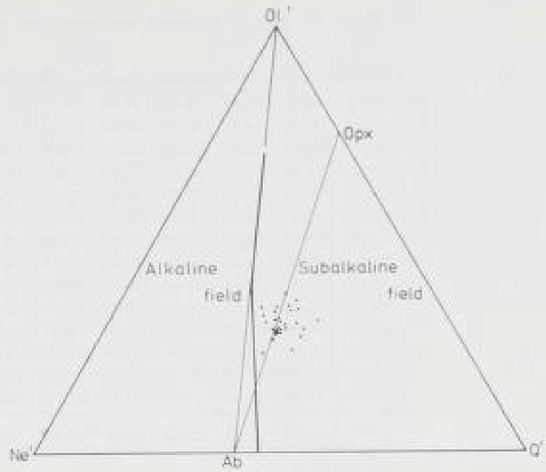


*Fig. 3.* Ol'–Ne'–Q' projection of the Sunnfjord dolerites plotted in % cation equivalents based on the cation norm. The heavy solid line is Irvine & Baragar's (1971) dividing line between alkaline and subalkaline series.

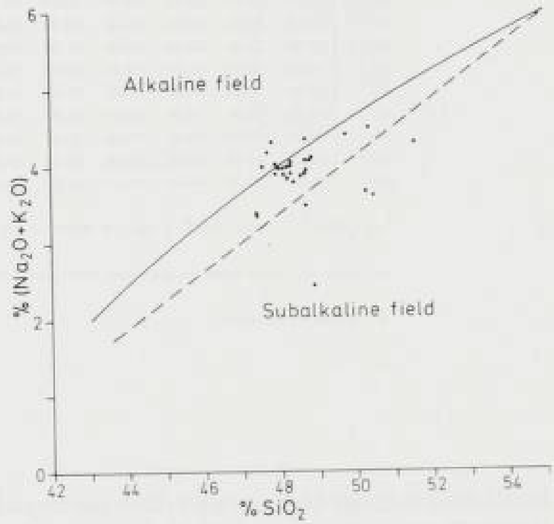


*Fig. 4.* Alkali–silica plot of the Sunnfjord dolerites. The solid curve is the dividing line after Irvine & Baragar (1971). The dashed line is MacDonald's (1968) dividing line.

## Whole rock chemistry

### MAJOR ELEMENTS

Major element analyses of the dykes together with cation norms are given in Table 1. The norm calculations were made after adjustments of the analytical data as recommended by Irvine & Baragar (1971): (1) $Fe_2O_3$ was limited according to the equation % $Fe_2O_3$ = % $TiO_2 + 1.5$, the excess being converted to FeO; (2) the analyses were recalculated to 100% volatile free. The cation norm was obtained from the CIPW norm using the conversion factors calculated by Hutchinson (1975).

Although neither orthopyroxene nor pigeonite has been identified in the thin-sections, and all the modal pyroxene appears to be augite, the dyke rocks

Table 1. Major element composition and cation norms of dykes in the outer Sunnfjord regic

| Dyke No. | 1a | 1b | 1c | 2 | 3 | 4a | 4b | 4c | 4d | 4e | 4f | 4g | 5a | 5b |
|---|---|---|---|---|---|---|---|---|---|---|---|---|---|---|
| $SiO_2$ | 51.07 | 48.64 | 49.07 | 49.40 | 49.87 | 47.42 | 48.02 | 47.94 | 48.24 | 47.54 | 48.13 | 47.41 | 47.93 | 46.89 |
| $Al_2O_3$ | 13.12 | 14.46 | 14.03 | 12.65 | 13.15 | 12.94 | 13.45 | 13.21 | 12.85 | 13.01 | 13.36 | 12.84 | 13.28 | 13.03 |
| $TiO_2$ | 2.70 | 2.72 | 2.66 | 3.19 | 3.26 | 3.30 | 3.35 | 3.28 | 3.29 | 3.34 | 3.19 | 3.28 | 3.26 | 3.20 |
| $Fe_2O_3$ | 5.57 | 2.77 | 3.13 | 3.93 | 5.52 | 5.61 | 5.04 | 5.49 | 5.39 | 5.37 | 5.21 | 3.92 | 5.22 | 3.14 |
| FeO | 9.09 | 10.82 | 10.67 | 11.76 | 10.05 | 10.62 | 11.32 | 11.42 | 11.42 | 11.02 | 11.32 | 12.77 | 11.32 | 13.14 |
| MgO | 4.60 | 5.59 | 4.99 | 4.48 | 5.25 | 5.34 | 5.14 | 4.91 | 4.99 | 5.04 | 4.94 | 5.12 | 5.29 | 5.07 |
| CaO | 8.24 | 7.89 | 7.95 | 8.26 | 7.84 | 8.56 | 8.85 | 8.49 | 8.46 | 8.61 | 8.72 | 8.76 | 8.60 | 8.88 |
| $Na_2O$ | 3.00 | 2.92 | 2.86 | 2.74 | 2.59 | 2.85 | 2.21 | 3.09 | 2.78 | 2.88 | 2.54 | 2.84 | 3.05 | 2.85 |
| $K_2O$ | 1.27 | 1.41 | 1.53 | 0.78 | 1.06 | 0.88 | 0.21 | 0.90 | 1.11 | 1.11 | 0.91 | 0.96 | 0.91 | 1.39 |
| MnO | 0.22 | 0.23 | 0.21 | 0.24 | 0.33 | 0.22 | 0.18 | 0.21 | 0.21 | 0.19 | 0.18 | 0.19 | 0.18 | 0.18 |
| $P_2O_5$ | 0.38 | 0.39 | 0.41 | 0.46 | 0.47 | 0.44 | 0.40 | 0.43 | 0.43 | 0.44 | 0.48 | 0.44 | 0.73 | 0.40 |
| $H_2O$ | 0.42 | 1.47 | 1.67 | 0.94 | 1.35 | 1.50 | 2.32 | 1.20 | 1.22 | 1.88 | 1.47 | 1.54 | 1.20 | 1.31 |
| TOTAL | 99.68 | 99.31 | 99.18 | 98.83 | 100.74 | 99.68 | 100.49 | 100.57 | 100.39 | 100.43 | 100.45 | 100.07 | 100.97 | 99.48 |
| FM[1] | 75.69 | 70.78 | 73.30 | 77.62 | 74.51 | 74.85 | 75.73 | 77.14 | 76.76 | 76.09 | 76.62 | 76.31 | 75.38 | 76.11 |
| Cation Norms | | | | | | | | | | | | | | |
| Q | 4.22 | ----- | 0.84 | 5.02 | 5.40 | 1.22 | 6.62 | 0.46 | 1.82 | 0.79 | 3.07 | ----- | 0.61 | ----- |
| Or | 7.77 | 8.67 | 9.49 | 4.90 | 6.54 | 5.49 | 1.29 | 5.56 | 6.86 | 6.90 | 5.64 | 5.92 | 5.55 | 8.64 |
| Ab | 27.98 | 27.29 | 26.91 | 26.07 | 24.24 | 26.98 | 21.03 | 28.86 | 26.05 | 27.10 | 23.94 | 26.74 | 28.35 | 26.83 |
| An | 19.28 | 23.14 | 21.96 | 21.06 | 21.98 | 20.92 | 27.74 | 20.29 | 20.21 | 20.25 | 23.44 | 20.42 | 20.54 | 19.57 |
| Mt | 4.55 | 3.02 | 3.42 | 4.34 | 5.18 | 5.27 | 5.37 | 5.20 | 5.23 | 5.30 | 5.13 | 4.30 | 5.15 | 3.44 |
| Il | 3.90 | 3.94 | 3.89 | 4.71 | 4.73 | 4.83 | 4.94 | 4.75 | 4.79 | 4.88 | 4.65 | 4.80 | 4.70 | 4.68 |
| Ap | 0.81 | 0.86 | 0.90 | 1.02 | 1.01 | 0.97 | 0.89 | 0.93 | 0.95 | 0.97 | 1.06 | 0.97 | 1.58 | 0.89 |
| Cpx | 16.45 | 11.97 | 13.27 | 15.34 | 12.27 | 16.61 | 12.83 | 16.50 | 16.56 | 17.21 | 14.85 | 17.70 | 14.91 | 19.16 |
| Opx | 15.04 | 18.54 | 19.32 | 17.54 | 18.65 | 17.71 | 19.29 | 17.45 | 17.53 | 16.60 | 18.22 | 18.43 | 18.61 | 7.83 |
| Ol | ----- | 2.57 | ----- | ----- | ----- | ----- | ----- | ----- | ----- | ----- | ----- | 0.72 | ----- | 8.96 |

[1] FM = [(FeO* + MnO)/(FeO* + MnO + MgO)] x 100

M: Mean of thirty dykes in the outer Sunnfjord region

S: Standard deviation

are all comparatively high in opx in their norm and commonly also have Q (21 dykes). This is typical for subalkaline rocks, and in the Ol'–Ne'–Q' projection (Irvine & Baragar 1971) all the dykes plot within the subalkaline field (Fig. 3). In the alkali–silica diagram (Fig. 4), however, only five of the dykes plot in the subalkaline field of MacDonald (1968); the others lie within the alkaline field. Using the dividing line of Irvine & Baragar (1971) twenty-five of the dykes plot in the subalkaline field, the majority of them, however, plotting very close to the dividing line. From the alkali–silica diagram alone we might draw the conclusion that the dyke rocks have neither typical subalkaline nor alkaline compositions; i.e. they are transitional rocks. We must bear in mind, however, that interstitial silica has been detected in some dykes by microprobe analysis, and that all the dyke rocks are comparatively high in opx in their norm and commonly also have small amounts of Q. The conclusion must be, therefore, that the dolerite dykes are saturated and of subalkaline affinity.

The major element chemistry (Table 1) demonstrates that the dyke rocks

| | 5e | 5f | 6a | 6b | 7a | 7b | 7c | 7d | 8a | 8b | 8c | 8d | 8e | 8f | M | σ |
|---|---|---|---|---|---|---|---|---|---|---|---|---|---|---|---|---|
| .67 | 46.80 | 47.14 | 48.33 | 47.69 | 48.30 | 47.71 | 48.06 | 48.22 | 46.12 | 47.19 | 47.53 | 47.65 | 46.48 | 47.86 | 47.94 | 0.98 |
| .27 | 12.88 | 13.17 | 13.08 | 13.28 | 13.29 | 13.24 | 13.16 | 13.36 | 12.24 | 12.41 | 12.50 | 13.09 | 12.09 | 13.02 | 13.09 | 0.46 |
| .26 | 3.23 | 3.22 | 3.23 | 3.22 | 3.21 | 3.30 | 3.15 | 3.17 | 3.26 | 3.25 | 3.36 | 3.23 | 3.27 | 3.27 | 3.20 | 0.18 |
| .70 | 3.82 | 4.89 | 5.96 | 6.56 | 4.73 | 5.94 | 5.29 | 4.21 | 4.50 | 5.51 | 5.07 | 4.21 | 5.27 | 6.78 | 4.93 | 0.96 |
| .95 | 12.81 | 11.47 | 9.70 | 9.92 | 11.84 | 10.48 | 10.84 | 12.14 | 11.84 | 11.50 | 11.80 | 10.80 | 11.76 | 10.28 | 11.25 | 0.93 |
| .04 | 5.07 | 4.95 | 5.46 | 5.27 | 5.11 | 5.00 | 5.04 | 5.05 | 6.43 | 5.98 | 5.82 | 5.89 | 6.77 | 5.74 | 5.28 | 0.50 |
| .79 | 8.74 | 8.84 | 8.38 | 7.36 | 8.57 | 8.93 | 8.34 | 8.04 | 9.01 | 8.73 | 8.71 | 8.50 | 8.51 | 8.45 | 8.49 | 0.37 |
| .01 | 2.99 | 2.84 | 2.99 | 2.39 | 2.76 | 3.02 | 2.18 | 2.23 | 2.84 | 3.18 | 2.86 | 2.30 | 2.48 | 2.98 | 2.77 | 0.28 |
| .00 | 1.10 | 0.95 | 1.09 | 1.59 | 1.10 | 0.94 | 2.12 | 1.82 | 0.46 | 0.76 | 1.02 | 1.56 | 0.79 | 0.99 | 1.09 | 0.38 |
| .20 | 0.19 | 0.19 | 0.27 | 0.20 | 0.20 | 0.19 | 0.28 | 0.22 | 0.25 | 0.25 | 0.26 | 0.25 | 0.25 | 0.25 | 0.22 | 0.04 |
| .54 | 0.42 | 0.42 | 0.64 | 0.43 | 0.43 | 0.38 | 0.42 | 0.61 | 0.45 | 0.45 | 0.44 | 0.46 | 0.44 | 0.45 | 0.46 | 0.08 |
| .23 | 1.48 | 1.72 | 1.40 | 2.54 | 1.01 | 1.47 | 1.36 | 1.37 | 1.40 | 0.90 | 1.20 | 1.30 | 1.20 | 0.90 | 1.38 | 0.38 |
| .76 | 99.63 | 99.80 | 100.53 | 100.45 | 100.55 | 100.58 | 100.24 | 100.44 | 98.80 | 100.21 | 100.57 | 99.24 | 99.32 | 100.97 | 100.10 | |
| .47 | 76.54 | 76.44 | 73.74 | 75.25 | 76.13 | 76.21 | 75.93 | 76.18 | 71.51 | 73.64 | 74.06 | 71.59 | 71.22 | 74.34 | | |
| — | — | 0.60 | 1.33 | 2.35 | 1.43 | 0.29 | 1.40 | 2.00 | — | — | — | 1.29 | 0.03 | — | 1.37 | |
| .16 | 6.83 | 5.92 | 6.69 | 9.97 | 6.78 | 5.79 | 13.10 | 11.27 | 2.80 | 4.68 | 6.28 | 9.68 | 4.94 | 6.03 | 6.71 | |
| .00 | 28.26 | 26.93 | 27.92 | 22.78 | 25.73 | 28.27 | 20.56 | 20.95 | 26.44 | 29.66 | 26.70 | 21.74 | 23.45 | 27.59 | 26.06 | |
| .76 | 19.39 | 21.45 | 19.80 | 22.01 | 21.43 | 20.65 | 20.84 | 22.07 | 19.95 | 17.98 | 18.94 | 21.87 | 20.52 | 19.07 | 20.38 | |
| .09 | 4.20 | 5.20 | 5.15 | 5.23 | 5.11 | 5.23 | 5.10 | 4.60 | 4.87 | 5.35 | 5.29 | 4.63 | 5.74 | 5.15 | 5.15 | |
| .72 | 4.72 | 4.72 | 4.67 | 4.74 | 4.65 | 4.79 | 4.60 | 4.62 | 4.70 | 4.70 | 4.86 | 4.74 | 4.79 | 4.70 | 4.66 | |
| .17 | 0.93 | 0.93 | 1.40 | 0.95 | 0.93 | 0.92 | 0.92 | 1.33 | 0.97 | 0.97 | 0.95 | 0.99 | 0.97 | 0.97 | 0.99 | |
| .66 | 18.64 | 17.52 | 15.22 | 10.94 | 15.87 | 18.30 | 15.78 | 12.46 | 18.62 | 19.38 | 18.40 | 15.52 | 16.70 | 16.29 | 15.98 | |
| .19 | 10.51 | 16.75 | 17.82 | 21.03 | 18.07 | 15.86 | 17.70 | 20.70 | 19.01 | 12.52 | 17.82 | 19.54 | 23.36 | 18.12 | 18.10 | |
| .25 | 6.52 | — | — | — | — | — | — | — | 2.64 | 5.36 | 0.76 | — | — | 1.28 | — | |

exhibit a fractionated nature especially with respect to an enrichment in total Fe and Ti. In classifying the fractionated tholeiitic suite of eastern Iceland, Wood (1978) used a combination of phenocryst assemblages and a chemical parameter, the FM ratio, where:

$$FM = \frac{FeO^x + MnO}{FeO^x + MnO + MgO} \times 100$$

All oxides are in wt. pr. cent and $FeO^x$ refers to total Fe expressed as FeO.

The FM ratio of the dolerite dykes (Table 1) classifies the majority of them as ferrobasalt (FM = 74 to 77) and a few of them fall within the range of low magnesia basalt (FM = 66 to 73). The dyke rocks have been plotted in the MgO versus $FeO^x$ diagram of Wood (1978). The Sunnfjord dykes are relatively enriched in Fe compared to the aphyric Thingmuli lavas (Carmichael 1964) (Fig. 5).

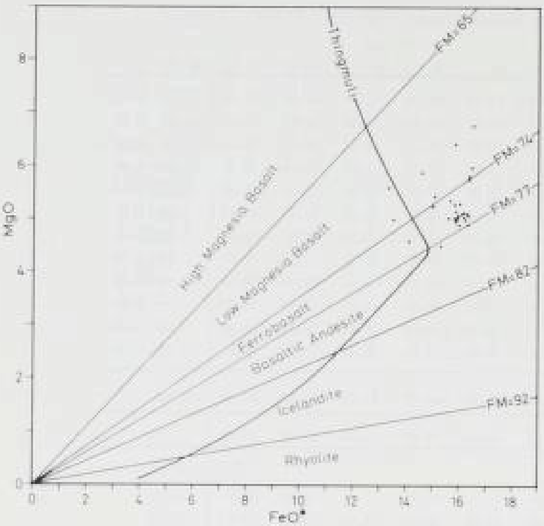


*Fig. 5.* MgO versus FeO* for the Sunnfjord dolerites. Oxides as wt %, total iron as FeO*. The field boundaries separating different volcanic rocks are after Wood (1978). The trend defined by the aphyric lavas of the Thingmuli complex is included (Carmichael 1964).

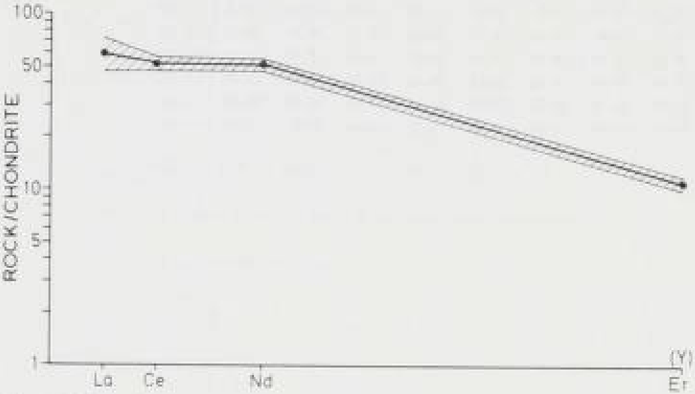


*Fig. 6.* Mean chondrite-normalized rare-earth distribution for 30 dolerites from Sunnfjord (chondrite data from Frey et al. 1968). Hatched field is 2 standard deviations wide.

## TRACE ELEMENTS

Trace element analyses and selected element ratios of the Sunnfjord dolerite are given in Table 2.

According to Pearce and Cann (1973) Y/Nb ratios for within-plate basalts are less than 1.0 for alkalic rocks and greater than 2.0 for tholeiitic rocks. The Y/Nb ratios for the Sunnfjord dolerites vary between 1.0 and 1.53 (mean 1.24) and thus suggest a transitional nature. Yet continental basaltic rocks having a typical tholeiitic geochemistry, e.g. the Karroo dolerites (Cox et al. 1967), exhibit the same range in Y/Nb ratios as do the Sunnfjord dolerites, and the tholeiitic Vestfjella dolerite dykes in Antarctica have an average Y/Nb ratio of 1.28 (Furnes, pers. comm. 1980).

The elements La, Ce, Nd and Y (the latter proxying for Er) have been taken as representative members of the rare arth series. The REE distribution pattern

Table 2. Trace element concentrations (ppm) of dykes in the outer Sunnfjord region

| Dyke No. | Rb | Sr | Ba | Y | Zr | Nb | La | Ce | Nd | Y/Nb | K/Rb | Ba/Rb | Ca/Sr | Sr/Ba | K/Sr | Rb/Sr | K/Ba |
|---|---|---|---|---|---|---|---|---|---|---|---|---|---|---|---|---|---|
| 1a | 36 | 240 | 326 | 20 | 140 | 20 | 19 | 50 | 36 | 1.0 | 292 | 9 | 245 | 0.74 | 44 | 0.15 | 32 |
| 1b | 52 | 241 | 417 | 23 | 148 | 23 | 17 | 50 | 36 | 1.0 | 225 | 8 | 234 | 0.58 | 49 | 0.22 | 28 |
| 1c | 57 | 232 | 443 | 23 | 143 | 22 | 15 | 45 | 35 | 1.05 | 225 | 8 | 245 | 0.52 | 55 | 0.25 | 29 |
| 2 | 19 | 297 | 460 | 22 | 134 | 17 | 19 | 47 | 34 | 1.29 | 337 | 24 | 199 | 0.65 | 22 | 0.06 | 14 |
| 3 | 27 | 163 | 355 | 20 | 135 | 16 | 18 | 46 | 32 | 1.25 | 326 | 13 | 344 | 0.45 | 54 | 0.17 | 25 |
| 4a | 28 | 260 | 386 | 20 | 138 | 17 | 21 | 44 | 28 | 1.18 | 263 | 14 | 235 | 0.67 | 28 | 0.11 | 19 |
| 4b | 3 | 193 | 301 | 20 | 139 | 17 | 20 | 42 | 30 | 1.18 | 567 | 100 | 328 | 0.64 | 9 | 0.02 | 6 |
| 4c | 12 | 197 | 464 | 21 | 140 | 16 | 26 | 48 | 32 | 1.31 | 625 | 38 | 308 | 0.42 | 38 | 0.06 | 18 |
| 4d | 20 | 186 | 474 | 20 | 139 | 16 | 21 | 56 | 38 | 1.25 | 460 | 24 | 322 | 0.40 | 49 | 0.11 | 19 |
| 4e | 18 | 184 | 456 | 20 | 140 | 16 | 25 | 48 | 31 | 1.25 | 511 | 25 | 335 | 0.40 | 50 | 0.10 | 20 |
| 4f | 20 | 184 | 344 | 21 | 137 | 16 | 23 | 48 | 31 | 1.31 | 375 | 17 | 339 | 0.53 | 41 | 0.11 | 22 |
| 4g | 14 | 199 | 415 | 20 | 138 | 16 | 22 | 52 | 35 | 1.25 | 571 | 30 | 315 | 0.48 | 40 | 0.07 | 19 |
| 5a | 11 | 204 | 422 | 20 | 139 | 17 | 29 | 46 | 33 | 1.18 | 682 | 38 | 301 | 0.48 | 37 | 0.05 | 18 |
| 5b | 26 | 190 | 432 | 19 | 132 | 16 | 20 | 50 | 28 | 1.19 | 442 | 17 | 334 | 0.44 | 60 | 0.14 | 26 |
| 5c | 10 | 212 | 441 | 20 | 139 | 16 | 26 | 50 | 37 | 1.25 | 740 | 44 | 296 | 0.48 | 35 | 0.05 | 17 |
| 5d | 12 | 211 | 471 | 21 | 137 | 16 | 29 | 50 | 37 | 1.31 | 691 | 39 | 298 | 0.45 | 39 | 0.06 | 18 |
| 5e | 17 | 211 | 401 | 21 | 136 | 15 | 21 | 47 | 33 | 1.40 | 535 | 24 | 296 | 0.53 | 43 | 0.08 | 23 |
| 5f | 16 | 208 | 377 | 20 | 137 | 17 | 20 | 48 | 32 | 1.18 | 494 | 23 | 304 | 0.55 | 38 | 0.08 | 21 |
| 6a | 30 | 231 | 423 | 21 | 137 | 15 | 18 | 45 | 30 | 1.31 | 300 | 14 | 259 | 0.55 | 39 | 0.13 | 21 |
| 6b | 31 | 198 | 440 | 21 | 139 | 17 | 17 | 50 | 29 | 1.24 | 426 | 14 | 266 | 0.45 | 66 | 0.16 | 30 |
| 7a | 13 | 191 | 445 | 20 | 139 | 16 | 19 | 57 | 33 | 1.25 | 700 | 34 | 321 | 0.43 | 47 | 0.07 | 20 |
| 7b | 13 | 198 | 359 | 20 | 134 | 16 | 20 | 42 | 27 | 1.25 | 600 | 27 | 321 | 0.55 | 40 | 0.07 | 22 |
| 7c | 45 | 190 | 424 | 22 | 137 | 17 | 12 | 40 | 27 | 1.29 | 391 | 9 | 313 | 0.45 | 93 | 0.24 | 41 |
| 7d | 26 | 190 | 656 | 21 | 138 | 16 | 23 | 41 | 30 | 1.31 | 580 | 25 | 302 | 0.29 | 80 | 0.14 | 23 |
| 8a | 8 | 201 | 356 | 26 | 136 | 17 | 19 | 39 | 27 | 1.53 | 475 | 45 | 320 | 0.56 | 19 | 0.04 | 11 |
| 8b | 11 | 202 | 395 | 20 | 134 | 17 | 15 | 39 | 24 | 1.18 | 573 | 36 | 309 | 0.51 | 31 | 0.05 | 16 |
| 8c | 25 | 212 | 398 | 25 | 134 | 17 | 16 | 39 | 25 | 1.47 | 340 | 16 | 294 | 0.53 | 40 | 0.12 | 21 |
| 8d | 45 | 226 | 451 | 20 | 145 | 18 | 16 | 37 | 24 | 1.11 | 287 | 10 | 289 | 0.50 | 57 | 0.20 | 29 |
| 8e | 21 | 182 | 319 | 20 | 139 | 17 | 18 | 37 | 29 | 1.38 | 314 | 9 | 334 | 0.57 | 36 | 0.12 | 30 |
| 8f | 26 | 197 | 379 | 20 | 140 | 17 | 16 | 44 | 26 | 1.18 | 315 | 15 | 306 | 0.52 | 42 | 0.13 | 22 |
| M | 23 | 207 | 414 | 21 | 138 | 17 | 20 | 46 | 31 | 1.24 | 455 | 25 | 296 | 0.51 | 44 | 0.11 | 22 |
| S | 13 | 27 | 66 | 1 | 3 | 2 | 4 | 5 | 4 | 0.11 | 153 | 18 | 36 | 0.09 | 17 | 0.06 | 7 |

M Mean of thirty dykes in the outer Sunnfjord region

S Standard deviation

for the dyke swarm shows significant enrichment in light over heavy REE (Fig. 6). The slope of the light REE is similar to those of the Grande Ronde (Reidel 1978), the Ice Harbor flows (Helz et al. 1974), Deccan trap basalts (Alexander & Gibson 1977) and the Vestfjella dolerites (Furnes pers. comm. 1980) and, therefore, appears to be common for continental tholeiites.

The K/Rb ratios for the Sunnfjord dolerites lie within the range 225–700, averaging 455. This is distinctly higher than that observed for tholeiitic dolerites from Tasmania and Antarctica (Compston et al. 1968) and is somewhat higher than for most of the basalts of the Columbia River Group (McDougall 1976)

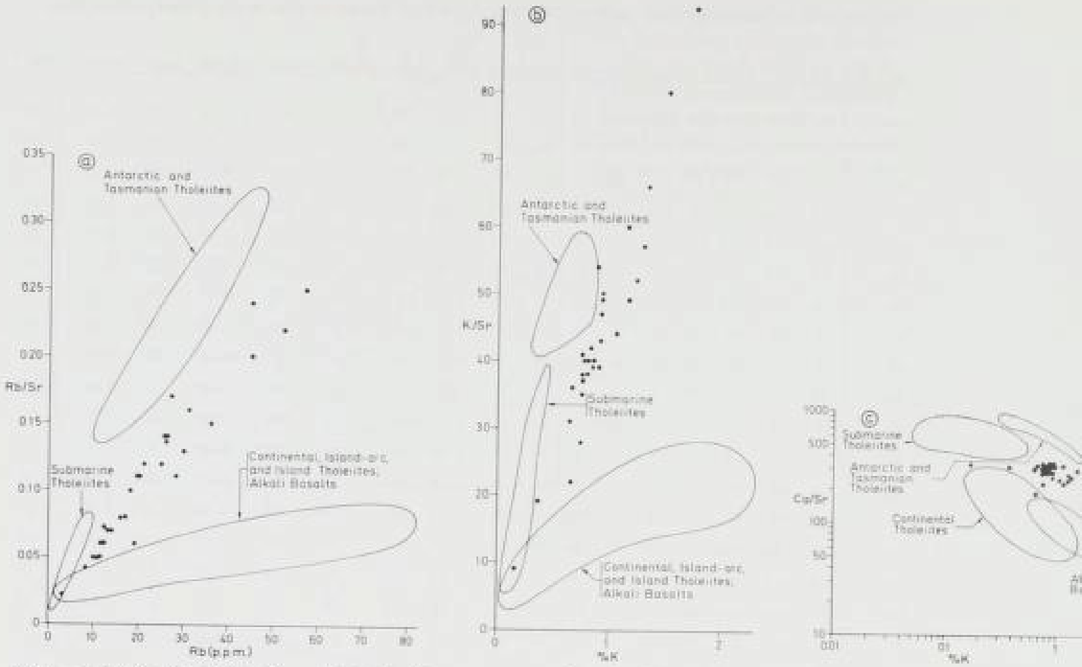


*Fig. 7.* Rb/Sr–Rb, K/Sr–K, and Ca/Sr–K scattergrams for the Sunnfjord dolerites, with field boundaries after Condie et al. (1969).

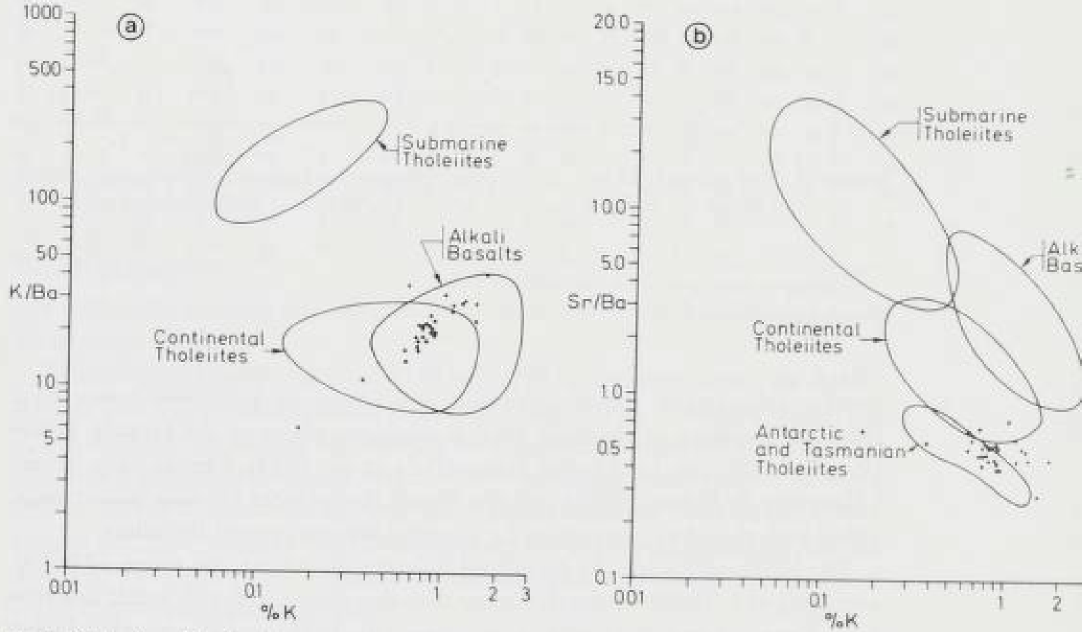


*Fig. 8.* K/Ba–K and Sr/Ba–K scattergrams for the Sunnfjord dolerites, with field boundaries after Condie et al. (1969).

except for the Picture George Basalt which shows higher K/Rb ratios than those of the Sunnfjord dykes. The Karroo dolerites, however, have K/Rb ratios in the range 303–609, and the average of 465 (Erlank & Hofmeyer 1966) is nearly the same as that of the Sunnfjord dolerites. An average K/Rb ratio of 465 is also observed for the tholeiitic Vestfjella dykes from Antarctica (Furnes, pers. comm. 1980).

The average Sr content in the Sunnfjord dykes is distinctly lower han the average (428 ppm) for continental tholeiites in general (Condie et al. 1969), yet higher than for Antarctic tholeiites (Compston et al. 1968) and some of the Karroo dolerites (Cox et al. 1967, Woolley et al. 1979). The Rb/Sr ratios of the Sunnfjord dolerites lie within the range 0.02–0.25; the average of 0.11 is distinctly lower than that observed for tholeiitic dolerites from Antarctica and Tasmania (Compston et al. op. cit.) but shows greater similarity with the Columbia River Group, especially the Yakima Basalt (McDougall op. cit.).

In Fig. 7 the Rb/Sr ratios are plotted as a function of Rb, and the K/Sr and Ca/Sr ratios as functions of K. The fields occupied by the major basalt types are after Condie et al. (1969). The Rb/Sr ratios increase linearly with Rb (Fig. 7a) and the K/Sr ratios increase linearly with K (Fig. 7b), features which indicate that K, Rb and Sr cannot have been affected by alteration to any significant extent. The rate of increase in Rb/Sr with Rb and K/Sr with K follows the Sr-depletion fractionation trend typical of submarine tholeiites and Sr-depleted continental tholeiites (Condie e al. 1969). The Ca/Sr ratios which occupy the area between continental tholeiites and Antarctic and Tasmanian tholeiites (Fig. 7c), follow the same trend; i.e. depleted in Sr relative to Ca compared to continental tholeiites.

The K/Ba ratios plotted as a function of K illustrate the similarity of the Sunnfjord dolerites to continental tholeiites as well as to alkali basalt (Fig. 8a). However, in the Sr/Ba versus K diagram all analyses plot exclusively in the field of continental tholeiites, showing in particular similarities with Antarctic and Tasmanian tholeiites (Fig.8b).

## Mineral chemistry

### PLAGIOCLASE

Microprobe analyses of phenocryst and groundmass plagioclase are given in Table 3. The margins of the plagioclase phenocrysts display pronounced normal zoning. The cores, which show varying degrees of resorption (Fig. 2), are relatively homogeneous with An contents between 63 and 64 per cent. The innermost parts of the marginal zones very between 55 and 59% An whilst the outermost parts of the phenocrysts have compositions varying between An 41 and 52.

The groundmass plagioclase also show normal zoning. The cores have An contents of 54 to 59 whilst the margins vary from An 41 to 52 per cent. The compositional variations of the groundmass plagioclase correspond, therefore, with those of the margins of the plagioclase phenocrysts. The groundmass

Table 3. Representative microprobe analyses of plagioclase from dykes in the outer Sunnfjord reg

| Dyke No. | 4a | | | | | 5c | | | | | |
|---|---|---|---|---|---|---|---|---|---|---|---|
| | Phenocrysts | | | Matrix | | Phenocrysts | | | Matrix | | |
| | P | Mp | R | Mc | R | P | Mp | R | Mc | R | Mc |
| CaO | 12.52 | 11.36 | 9.75 | 11.73 | 9.61 | 12.30 | 11.66 | 9.90 | 11.67 | 9.80 | 11.42 |
| $Na_2O$ | 3.82 | 4.42 | 5.41 | 4.43 | 5.27 | 3.85 | 4.68 | 5.15 | 4.80 | 5.22 | 4.63 |
| $K_2O$ | 0.27 | 0.53 | 0.29 | 0.29 | 0.36 | 0.12 | 0.00 | 0.06 | 0.20 | 0.50 | 0.20 |
| $SiO_2$ | 54.53 | 56.95 | 56.61 | 55.24 | 57.49 | 53.79 | 54.35 | 58.21 | 55.02 | 56.55 | 56.16 |
| $Al_2O_3$ | 27.71 | 26.98 | 26.13 | 26.97 | 26.33 | 28.79 | 27.34 | 26.23 | 26.95 | 26.99 | 25.68 |
| TOTAL | 98.85 | 100.24 | 98.19 | 98.66 | 99.06 | 98.85 | 98.23 | 99.75 | 98.64 | 99.06 | 98.09 |
| Number of ions on the basis of 24 oxygens | | | | | | | | | | | |
| Ca | 1.83 | 1.64 | 1.43 | 1.72 | 1.39 | 1.80 | 1.72 | 1.43 | 1.72 | 1.42 | 1.68 |
| Na | 1.01 | 1.15 | 1.44 | 1.18 | 1.36 | 1.02 | 1.25 | 1.34 | 1.27 | 1.37 | 1.23 |
| K | 0.05 | 0.09 | 0.05 | 0.05 | 0.06 | 0.02 | 0.03 | 0.04 | 0.03 | 0.08 | 0.03 |
| Si | 7.46 | 7.66 | 7.75 | 7.56 | 7.79 | 7.36 | 7.49 | 7.62 | 7.55 | 7.68 | 7.72 |
| Al | 4.47 | 4.28 | 4.22 | 4.35 | 4.20 | 4.64 | 4.44 | 4.16 | 4.36 | 4.32 | 4.16 |
| Mol Proportions | | | | | | | | | | | |
| An | 63.16 | 56.87 | 49.04 | 58.04 | 48.94 | 63.39 | 57.26 | 50.71 | 56.68 | 49.40 | 57.04 |
| Ab | 34.86 | 40.00 | 49.23 | 39.68 | 48.58 | 35.88 | 41.59 | 47.70 | 42.15 | 47.63 | 41.79 |
| Or | 1.98 | 3.13 | 1.73 | 2.28 | 2.48 | 0.73 | 1.15 | 1.59 | 1.17 | 2.97 | 1.17 |

Abbreviations: P: Cores of partly resorbed primocrysts
Mp: Innermost marginal zone of the phenocrysts
Mc: Core of the matrix plagioclase
R: Rim of the phenocrysts and the matrix plagioclase.

plagioclase may also have small cores of irregular shape with compositions from 63 to 64% An. These cores probably represent strongly resorbed phenocrysts which have acted as nucleii during the later crystallization of the groundmass plagioclase.

The plagioclase appears to have crystallized in two different magmatic environments. The phenocryst cores were formed as primocrysts suspended in a slowly cooling magma, and the phenocrysts suffered subsequent resorption though prior to the growth of the rims. The margins of the phenocrysts, on the other hand, formed simultaneously with the groundmass plagioclase after the emplacement of the magma as dykes.

CLINOPYROXENE

Microprobe analyses from four samples (5c, 6a, 7a, 8b) show that the single

| 7a | | | | | | | 8b | | | | | | | |
|---|---|---|---|---|---|---|---|---|---|---|---|---|---|---|
| Phenocrysts | | | Matrix | | | | Phenocrysts | | | Matrix | | | | |
| P | Mp | R | Mc | R | Mc | R | P | Mp | R | P | Mc | R | Mc | R |
| .84 | 11.27 | 8.22 | 10.71 | 8.43 | 10.65 | 8.53 | 12.75 | 12.35 | 10.60 | 12.70 | 11.56 | 10.73 | 11.84 | 10.61 |
| .90 | 4.99 | 6.09 | 4.82 | 6.29 | 4.77 | 5.87 | 3.92 | 4.46 | 5.23 | 3.85 | 4.25 | 5.18 | 4.60 | 5.16 |
| .15 | 0.27 | 0.54 | 0.28 | 0.31 | 0.20 | 0.40 | 0.20 | 0.25 | 0.22 | 0.21 | 0.14 | 0.31 | 0.19 | 0.26 |
| .01 | 56.78 | 59.59 | 56.67 | 58.66 | 57.06 | 58.38 | 54.92 | 55.22 | 57.33 | 55.18 | 55.95 | 57.72 | 55.11 | 56.36 |
| .41 | 27.35 | 23.69 | 26.50 | 24.67 | 26.21 | 26.27 | 28.01 | 27.61 | 25.97 | 27.44 | 28.07 | 26.74 | 27.76 | 25.93 |
| .31 | 100.66 | 98.13 | 98.98 | 98.36 | 98.89 | 99.45 | 99.80 | 99.89 | 99.35 | 99.38 | 99.97 | 100.68 | 99.50 | 98.32 |
| | | | | | | | | | | | | | | |
| .90 | 1.62 | 1.20 | 1.56 | 1.23 | 1.55 | 1.22 | 1.85 | 1.79 | 1.54 | 1.85 | 1.67 | 1.54 | 1.72 | 1.56 |
| .04 | 1.30 | 1.61 | 1.27 | 1.66 | 1.26 | 1.52 | 1.03 | 1.17 | 1.37 | 1.02 | 1.11 | 1.34 | 1.21 | 1.37 |
| .02 | 0.05 | 0.09 | 0.05 | 0.05 | 0.03 | 0.07 | 0.04 | 0.04 | 0.04 | 0.04 | 0.02 | 0.05 | 0.03 | 0.05 |
| .44 | 7.61 | 8.12 | 7.70 | 7.99 | 7.75 | 7.81 | 7.45 | 7.49 | 7.77 | 7.51 | 7.54 | 7.72 | 7.49 | 7.73 |
| .45 | 4.32 | 3.81 | 4.25 | 3.96 | 4.20 | 4.14 | 4.48 | 4.41 | 4.15 | 4.40 | 4.46 | 4.21 | 4.45 | 4.19 |
| | | | | | | | | | | | | | | |
| .86 | 54.67 | 41.37 | 54.18 | 41.78 | 54.57 | 43.50 | 63.48 | 59.61 | 52.13 | 63.29 | 59.56 | 52.39 | 58.07 | 52.38 |
| .04 | 43.76 | 55.39 | 44.16 | 56.42 | 44.23 | 54.10 | 35.32 | 38.97 | 46.56 | 34.72 | 39.59 | 45.81 | 40.82 | 46.07 |
| .10 | 1.57 | 3.24 | 1.66 | 1.80 | 1.20 | 2.40 | 1.20 | 1.42 | 1.31 | 1.99 | 0.85 | 1.80 | 1.11 | 1.55 |

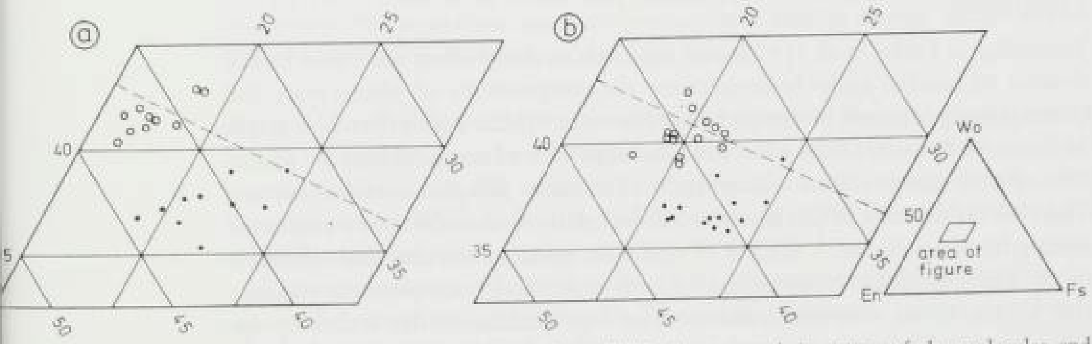


*Fig.* 9. Plots of clinopyroxenes from Table 4 expressed in terms of the molecular end members enstatite (En: $Mg_2Si_2O_6$), ferrosilite (Fs: $Fe_2Si_2O_6$), and wollastonite (Wo: $Ca_2Si_2O_6$). The dashed line separates pyroxenes from alkaline (above) and subalkaline volcanic rocks (below) (Le Bas 1962). *a* – Clinopyroxene phenocrysts; circles—core; dots—rim. *b* – Groundmass clinopyroxene; circles—core; dots—rim.

pyroxene present in the dykes is an augite. Representative analyses from cores and rims of phenocryst and groundmass pyroxenes are given in Table 4.

The phenocrysts are characterized by relatively homogeneous cores constituting the larger parts of the grains, and strongly zoned margins. The compositional zoning in the phenocrysts consists of Fe increasing and Ca decreasing from core to rim (Fig.9a), and Al and Ti increasing in the same direction (Fig. 10 a-b).

The cores of the groundmass pyroxenes are somewhat richer in Fe and poorer in Ca than the cores of the phenocrysts, but the compositional zoning follows the same trend with respect to these elements, Fe increasing and Ca decreasing from core to rim (Fig. 9b). Unlike the phenocrysts, however, the compositional zoning of the groundmass pyroxene shows that Al and Ti decrease from core to rim (Fig. 10c-d). The difference between the rims of the phenocrysts and the cores of the groundmass pyroxenes is, therefore, that the latter are richer in Ca and poorer in Fe (Fig. 9a-b). On the other hand there are no significant differences between the groundmass pyroxene cores and the rims of the phenocrysts with respect to the content of Al and Ti (Fig. 10a-d).

Kushiro (1960) and Le Bas (1962) showed that the amounts of Al and Ti which enter clinopyroxene depend on the degree of alkalinity of the parent magma, and that the Al and Ti contents in clinopyroxene could be used to distinguish between alkaline and non-alkaline magmas. Barberi et al. (1971) considered, however, that the physical conditions under which the pyroxene crystallized are at least of the same importance as the composition of the parent magma, and hence the pyroxene cannot be regarded as diagnostic of parental magma type. This view is substantiated by Fig. 10a-d; in these plots the cores of the phenocrysts lie within the non-alkaline field and the margins within the alkaline field of Le Bas (1962). The groundmass pyroxenes show the opposite trend, their cores falling within the the alkaline and their rims within the non-alkaline fields.

## Discussion

According to Fodor et al. (1975) one approach to deciphering the liquid line of descent of basaltic rocks is to compare the compositions of phenocrysts and groundmass pyroxenes in one and the same rock. These will reflect two stages in the crystallization of the melt, provided that mineral compositions are a function of melt compositions and crystallization takes place in a closed system. The bulk chemistries of the Sunnfjord dolerites show that the dykes originated from a fractionated basalt magma of tholeiitic affinity. The chemical similarity of the different dykes with respect to both major and trace elements suggests that all the dykes were emplaced more or less simultaneously, and from the same source. The compositional zoning of the phenocryst and groundmass pyroxenes might, therefore, provide a record of the nature of the crystallization of the melts both before and after emplacement of the dykes.

It appears reasonable to suppose that the melts which produced the Sunn-

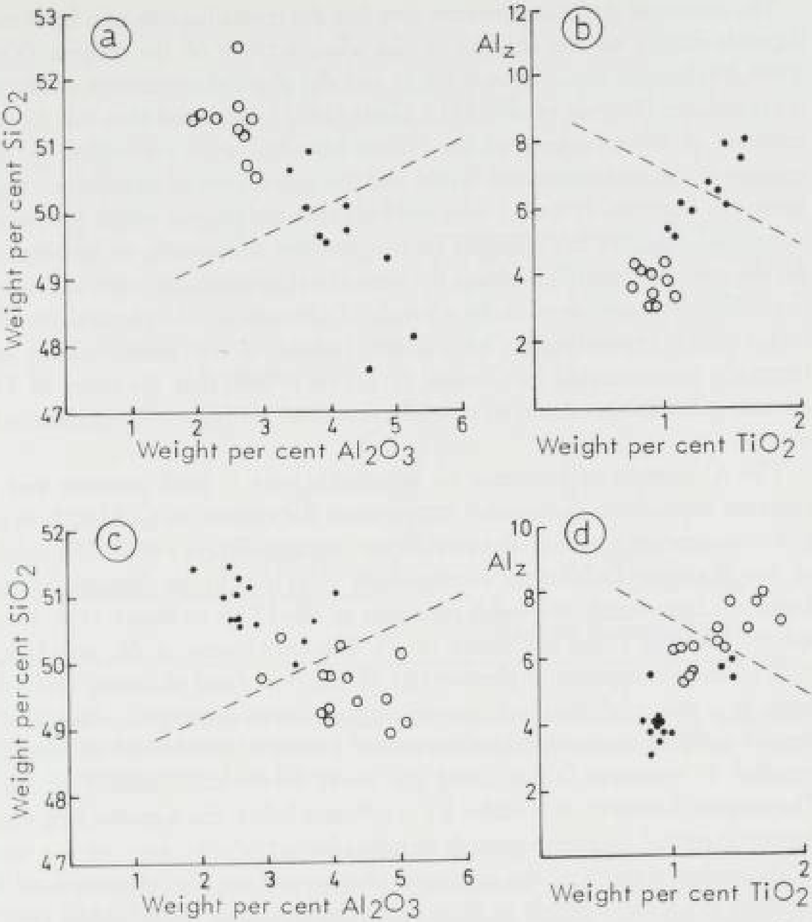


*Fig. 10.* Plots of clinopyroxene compositions from Table 4. Symbols as in Fig. 9. *a* and *c*: $SiO_2$ versus $Al_2O_3$ plots of phenocrysts and groundmass pyroxene, respectively. The dashed line separates pyroxenes from subalkaline (above) and alkaline volcanic rocks (below) (Le Bas 1962). *b* and *d*: $Al_z$ versus $TiO_2$ plots of phenocrysts and groundmass pyroxene, respectively. The dashed line separates pyroxenes from alkaline (above) and subalkaline volcanics (below) (Le Bas 1962).

fjord dolerites originated by fractionation of a primitive tholeiitic parent magma which occupied a deep-seated magma chamber. At a certain stage in the fractionation history of this magma, both plagioclase and clinopyroxene were liquidus phases. Plagioclase with a composition from An 63 to 64 commenced crystallization before clinopyroxene (Wo 40.4–42.7).

The enrichment of $Al_z$ in the rims of the clinopyroxene phenocrysts is undoubtedly related to an increase in Ti content (Table 4). Verhoogen (1962) showed on the basis of thermodynamic considerations, that the entry of Ti into clinopyroxene is favoured by high temperature and is directly controlled by silica activity. The compositions of clinopyroxenes from volcanic rocks are consistent with this interpretation (Le Bas 1962).

The nature of the clinopyroxene trend in the crystallization of a basic magma depends mainly on the changes in the silica activity of the magma (Kushiro 1960, Verhoogen 1962, Brown 1967) and the physical conditions under which it crystallizes (Barberi et al. 1971). Gibb (1972) suggested that the Al and Ti contents of clinopyroxene of the Shiant Isles Sill were controlled by the Ti content of the undersaturated liquid and the appearance of titaniferous magnetite on the liquidus. It would seem unlikely that the magma which produced the Sunnfjord dolerites has changed its composition sufficiently to be responsible for the compositional differences between the clinopyroxene cores and margins; the differences are more likely a result of changes in the physical conditions under which crystallization took place. Indeed, it has recently been experimentally demonstrated by Gamble & Taylor (1980) that the entry of Ti and Al into the clinopyroxene is strongly favoured by high cooling rates of the magma.

The Al content of pyroxene in subsolidus runs is both pressure and temperature dependent; at constant temperature the content of $CaAl_2SiO_6$ in clinopyroxene reaches a maximum at moderate pressures (Hays 1967). The solubility of the titanium Tschermack's component ($CaTiAl_2O_6$) in diopside increases, however, from nearly nil under pressures of 10–25 kb to about 11% at atmospheric pressure (Yagi & Onuma 1967). The enrichment of $Al_z$ and Ti in the rims of the clinopyroxene phenocrysts of the Sunnfjord dolerites may, therefore, be a result of marginal growth during ascent of magma. Ascent of the magma carrying suspended phenocrysts of basic plagioclase and clinopyroxene resulted in pressures falling along the trend drawn schematically in Fig. 11. The magma, however, was under PT conditions below the liquidus long enough for the marginal pyroxene growth to take place.

The marginal parts of the pyroxene phenocrysts are also characterized by a decrease in Ca and increase in Fe towards the rim. This is probably a result of depletion of the magma in Ca due to simultaneous crystallization of plagioclase. The growth of the zoned margins of the pyroxene phenocrysts, therefore, probably took place under decreasing pressure and mainly under PT conditions within the stability field of Pl + Cpx + L, with the exception of the outermost rims (Fig. 11). By a further fall in pressure, plagioclase was no longer a liquidus phase and resorption of plagioclase phenocrysts took place.

There exists an unquestionable relationship between water pressure ($pH_2O$) and the order of appearance of the mineral phases in basaltic magmas (Yoder & Tilley 1962, Nesbitt & Hamilton 1970). The sequence of groundmass crystallization in the Sunnfjord dolerites, which appears to have been pyroxene–plagioclase–titanomagnetite, probably took place under relatively high $pH_2O$; under these conditions pyroxene will crystallize before plagioclase.

Fodor et al. (1975) established that the ratio FeO/(FeO + MgO + CaO) for groundmass clinopyroxenes in Hawaiian tholeiitic rocks is dependent on the same ratio in the liquid by the onset of the pyroxene crystallization. The strong resorption of plagioclase phenocrysts which took place prior to the crystallization of the groundmass clinopyroxene within the Sunnfjord dolerites led to a

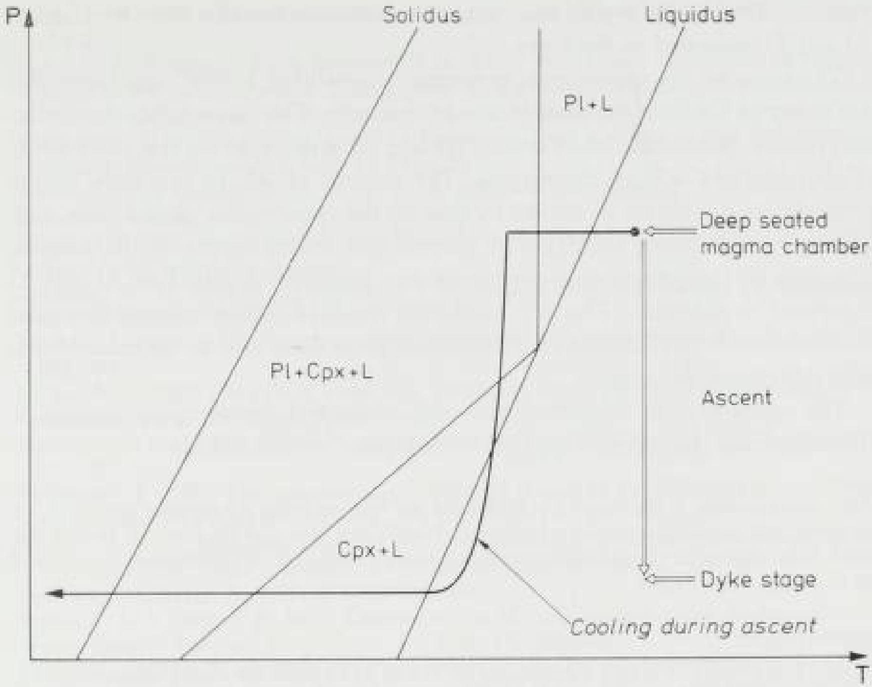


*Fig. 11.* Hypothetical PT diagram (S. Maaloe pers. comm. 1979) showing the suggested evolution of phenocrysts based on textural features and mineral compositions. Pl — plagioclase; Cpx — clinopyroxene; L — liquid.

decrease in the ratio $FeO/(FeO+MgO+CaO)$ in the magma; hence the groundmass pyroxene cores were richer in Ca than the rims of the phenocrysts. The high content of $Al_z$ in the groundmass pyroxene clearly demonstrates that the magma temperature at which their cores commenced crystallization was of the same order as during the growth of the margins of the pyroxene phenocrysts (Verhoogen 1962, Boyd & England 1964, Akela & Boyd 1973). The decrease in the $Al_z$ content in the marginal part of the groundmass pyroxene was a function of falling temperatures, the simultaneous crystallization of groundmass plagioclase and an increase in the activity of $SiO_2$ consequent upon titanomagnetite crystallization.

## Summary and conclusion

The major part of the investigated dolerite dykes from Sunnfjord are subalkaline, strongly fractionated ferrobasalts that show many geochemical similarities with continental tholeiitic basalts. Textural and mineralogical compositions of plagioclase and clinopyroxene phenocrysts suggest that crystal fractionation started at relatively high pressure. During ascent of the plagioclase- and clinopyroxene–phyric magma, plagioclase was partially resorbed, a phenomenon ascribed to rapid decrease in pressure without any significant reduction in temperature. During the evolutionary stage the pyroxene margins were enriched in Al and Ti compared to the cores.

The cores of the groundmass pyroxenes crystallized before plagioclase and are richer in Ca than the rims of the phenocrysts. This is probably due to resorption of plagioclase phenocrysts, leading to a decrease in the ratio FeO/(FeO+MgO+CaO) of the magma. The content of $Al_z$ in the cores of the groundmass pyroxenes is similar to that of the rims of the phenocrysts, suggesting no significant reduction in temperature during ascent of the magma. The rims of the groundmass pyroxenes are, however, depleted in Al and Ti compared to the cores. This is a combined result of falling temperatures, the simultaneous crystallization of groundmass plagioclase and an increase in the $SiO_2$ activity of the magma.

The crystallization of groundmass plagioclase and the marginal growth of the plagioclase phenocrysts apparently took place simultaneously.

*Acknowledgements.* – We thank Dr. B. Robins for help with the microprobe work and for criticism and comments on the manuscript. Thanks are also due to Prof. S. Maaloe for helpful discussions on phase diagrams relevant to this work. The illustrations were prepared be E. Irgens and J. Lien.

REFERENCES

Akella, J. & Boyd, F. R. 1973: Partitioning of Ti and Al between coexisting silicates, oxides, and liquids. *Proc. Fourth Lunar Sci. Conf., Geochim. Cosmochim. Acta*, Suppl. 4, Vol. 1, 1049–1059.

Alexander, P. O. & Gibson, I. L. 1977: Rare earth abundances in Deccan trap basalts *Lithos 10*, 143–147.

Barberi, F., Bizouard, H. & Varet, J. 1971: Nature of the Clinopyroxene and Iron Enrichment in Alcalic and Transitional Basaltic Magmas. *Contr. Mineral. Petrol. 33*, 93–107.

Boyd, F. R. & England, J. L. 1964: The System Enstatite–Pyrope. *Carnegie Inst. Washington. Yearbook 63*, 157–161.

Brown, G. M. 1967: Mineralogy of basaltic rocks (103–162). *In* Hess, H. H. & Poldervaart, A. (eds.). *Basalts, vol. 1.* Interscience Publishers.

Carmichael, I. S. E. 1964: The petrology of Thingmuli, a Tertiary volcano in eastern Iceland. *J. Petrol. 5*, 435–460.

Compston, W., McDougall, I. & Heier, K. S. 1968: Geochemical comparison of the Mesozoic basaltic rocks of Antarctica, South Africa, South America and Tasmania. *Geochim. Cosmochim. Acta, 32*, 129–149.

Condie, K. C., Barsky, C. K. & Mueller, P. A. 1969: Geohemistry of Precambrian diabase dikes from Wyoming. *Geochim. Cosmochim. Acta, 33*, 1371–1388.

Cox, K. G., MacDonald, R. & Hornung, G. 1967: Geochemical and petrographic provinces in the Karroo basalts of Southern Africa. *Am. Min. 52*, 1451–1474.

Erlank, A. J. & Hofmeyer, P. K. 1966: K/Rb and K/Cs Ratios in Karroo Dolerites from South Africa. *J. Geophys. Res. 71*, 5439–5445.

Flanagan, F. J. 1973: 1972-values for international geochemical reference standards. *Geochim. Cosmochim. Acta 37*, 1189–1200.

Fodor, R. V., Keil, K. & Bunch, T. E. 1975: Contributions to the Mineral Chemistry of Hawaiian Rocks. IV. Pyroxenes in Rocks from Haleakala and West Maui Volcanoes, Maui, Hawaii. *Contr. Mineral. Petrol. 50*, 173–195.

Furnes, H., Skjerlie, F. J. & Tysseland, M. 1976: Plate tectonic model based on greenstone geochemistry in the late Precambrian–Lower Palaeozoic sequence in the Solund–Stavfjorden areas, West Norway. *Norsk geol. Tidsskr. 56*, 161–186.

Gamble, R. P. & Taylor, L. A. 1980: Crystal/liquid partioning in augite; effects of cooling rate. *Earth Planet. Sci. Lett. 47*, 21–33.

Gibb, F. G. F. 1973: The Zoned Clinopyroxenes of the Shiant Isles Sill, Scotland. *J. Petrol. 14*, 203–230.

Hays, J. F. 1967: Lime-alumina-silica. *Carnegie Inst. Washington. Yearbook 65–66*, 234–236.

Heltz, R. T., Wright, T. L., & Swanson, D. A. 1974: Petrogenetic significance of chemical trends in the youngest unit of Yakima basalt on the Columbia Plateau, Northwest U.S.A. *Proc. of the Symposium on Andean and Antarctic Volcanology Problems, Santioga, Chile.*

Hutchinson, C. S. 1975: The Norm, its Variations, their Calculation and Relationships. *Schweiz. Mineral, und Pet. Mitt. 55*, 243–256.

Irvine, T. N. & Baragar, W. R. A. 1971: A guide to the chemical classification of the common volcanic rocks. *Can. J. Earth Sci. 8*, 523–548.

Kildal, E. S. 1969: Geologisk kart over Norge, berggrunnskart. Måløy, blad 20, 1 : 250 000. *Nor. Geol. Unders. Norsk utgave.*

Kolderup, N. H. 1928: Fjellbygningenn i kyststrøket mellom Nordfjord og Sognefjord. *Bergens Mus. Årbok, Naturv.rekke 1.* 221 p.

Kushiro, I. 1960: Si-Al relation in clinopyroxenes from igneous rocks. *Am. J. Schi. 258*, 548–554.

Le Bas, M. J. 1962: The role of aluminium in igneous clinopyroxenes with relation to their parentage. *Am. J. Sci. 260*, 267–288.

MacDonald, G. A. 1968: Composition and Origin of Hawaiian Lavas. *Geol. Soc. Am. Mem. 116*, 477–522.

McDougall, I. 1976: Geochemistry and origin of basalt of the Columbia River Group, Oregon and Washington. *Geol. Soc. Am. Bull. 87*, 777–792.

Nesbitt, R. W. & Hamilton, D. L. 1970: Crystallization of an alkali olivine basalt under controlled $PO_2$, $PH_2O$ conditions. *Phys. Earth Planet. Interiors 3*, 309–315.

Padfield, T. & Gray, A. 1970: Phillips Bulletin.

Pearce, J. A. & Cann, J. R. 1973: Tectonic setting of basic volcanic rocks determined using trace element analyses. *Earth Planet. Sci. Lett. 19*, 290–300.

Reidell, S. P. 1978: *Stratigraphy and Petrogenesis of the Grande Ronde Basalt in the Lower Salmon and adjacent Snake River Canyons.* Ph. D. thesis, Washington State University.

Reusch, H. 1881: Konglomerat-Sandsteinsfelterne i Nordfjord, Søndfjord og Sogn. *Nyt Magazin for Naturvitenskaberne 26*, 93–170.

Skjerlie, F. J. 1969: The pre-Devonian Rocks in the Askvoll–Gaular Area and adjacent Districts, Western Norway. *Nor. Geol. Unders. 258*, 325–359.

Skjerlie, F. J. 1971: Sedimentasjon og tektonisk utvikling i Kvamshestens devonfelt, Vest-Norge. *Norges geol. Unders. 270*, 77–108.

Skjerlie, F. J. & Pringle, I. R. 1978: A Rb/Sr whole-rock isochron date from the lowermost gneiss complex of the Gaular area, west Norway and its regional implications. *Nor. Geol. Tidsskr. 58*, 259–265.

Steel, R. J. 1976: Devonian basins of western Norway – sedimentary response to tectonism and to varying tectonic context. *Tectonophysics 36*, 207–224.

Verhoogen, J. 1962: Distribution of titanium between silicates and oxides in igneous rocks. *Am. J. Sci. 260*, 211–220.

Wood, D. A. 1978: Major and Trace Element Variations in the Tertiary Lavas of Eastern Iceland and their Significance with respect to the Iceland Geochemical Anomaly. *J. Petrol. 19*, 393–436.

Woolley, A. R., Bevan, J. C. & Elliot, C. J. 1979: The Karroo dolerites of southern Malawi and their regional geochemical implications. *Mineral. Mag. 43*, 487–495.

Yagi, K. & Onuma, K. 1967: The join $CaMgSi_2O_6$–$CaTiAl_2O_6$ and its bearing on the titanaugites. *Contr. Fac. Sci. Hokkaido Univ., No. 1064*, 463–483.

Yoder, H. S., Jr. & Tilley, G. E. 1962: Origin of basalt magma: an experimental study of natural and synthetic rock systems. *J. Petrol. 3*, 342–352.

# Rundingens og petrografiens innflytelse på sprøhet og flisighet av naturlige grusforekomster, belyst ved eksempler fra noen norske dalfører

KARL ANUNDSEN, TORLEIV MOSEID & REIDAR TRØNNES

Anundsen, K., Moseid, T. & Trønnes, R. 1981: The influence of roundness and petrography on brittleness and flakiness in natural gravel deposits, illustrated by examples from some Norwegian valleys. *Norges geol. Unders. 363*, 45–77.

Gravel deposits in five Norwegian valleys have been investigated with regard to petrographic composition, roundness, transport directions, brittleness and flakiness. These parameters are all found to be very complex. However, the brittlenes and flakiness along Surnadalen are more consistent in the fluvial than in the glacifluvial material, but this is not the case in Suldalen. The glacifluvial material is normally less rounded than the fluvial, which is however influenced by the petrographic composition. The brittleness is found to be influenced by the petrographic composition of the gravel, but perhaps more by the roundness. This latter is presumably due not only to enrichment of the strongest particles by continued fluvial treatment, but also to the roundness itself.

*K. Anundsen, Geologisk Institutt avd. B, Universitetet i Bergen, N–5014 Bergen – Universitetet, Norway*
*T. Moseid & R. Trønnes, Geologisk Institutt, Norges Tekniske Høgskole, N–7034 Trondheim – NTH, Norway*

## Innledning

Med midler fra Norges Teknisk-Naturvitenskapelige Forskningsråd, har Karl Anundsen drevet et forskningsprosjekt med det mål å finne eventuelle relasjoner mellom en grusforekomsts dannelsesbetingelser/geografiske beliggenhet på den ene siden, og dens styrke-parametere på den andre, for om mulig å oppnå et hjelpemiddel til å lokalisere gode grusforekomster. Det legges her fram resultater av de undersøkelser som ble foretatt mens Anundsen var ansatt ved NTH.

Styrke er her definert ved sprøhet (utført ved fallprøven), og flisighet, hvis ikke annet er nevnt. I teksten forkortes sprøhet til S og flisighet til f.

Det er tidligere funnet en sammenheng mellom et stein/grusmateriales petrografi og dets styrke (Anundsen 1977). I Sverige er en liknende sammenheng funnet ved sammenstilling av et stort antall resultater (Høbeda 1977). Relasjonene som Høbeda (1977) finner må imidlertid være meget grove, idet det under forfatternes arbeide viste seg å eksistere mange lokale forhold som ga store styrkevariasjoner innen et begrenset område. Slike forhold vil i det foreliggende arbeide bli tatt fram for om mulig å gi et mer nøyaktig lokaliserings-hjelpemiddel. Moseid og Trønnes har tatt sine siv.ing.-grader på prosjeket, h.h.v. i Surnadalen og i Sunndalen. Anundsen har vært leder av prosjektet, veileder for Moseid og utformet oppgaven for Trønnes, undersøkt de øvrige områder, og delvis viderebearbeidet Moseid's og Trønnes' materialer og resultater. Ragnar Dahl har vært veileder for Trønnes, og gitt gode råd i forbindelse med arbeidet i Sunndalen.

## Problemstilling

Undersøkelsene har tatt utgangspunkt i følgende hypotese: Det må være en sammenheng mellom sprøhet og petrografi. Da bergartstypen endrer seg fra sted til sted, må det finnes en sammenheng mellom en grusforekomsts beliggenhet og dets styrke. Dette er også påvist ved å sammenstille en del data fra div. hovedoppgaver (Fig. 2), og ikke minst ved sammenstillingen av et stort antall data fra Sverige (Høbeda 1977).

Fra forskjellige steder har fragmenter av fast fjell blitt ført med av breer, breelver og «normale» elver, og blitt avsatt som grusforekomster. Dette materialet er videre blitt utsatt for erosjon, transport og akkumulasjon. De svakeste partiklene slites fortest ned, og det må etter hvert bli en prosentvis økning av sterke bergartsbruddstykker i grusfraksjonen, forutsatt intet nytt tilskudd av svakere korn. Derfor må en regne med at den relasjon en har funnet mellom beliggenhet og styrke er meget grov. Det har vært et siktemål å forsøke å finne årsaken til interne variasjoner (av kvalitet) innen et begrenset område, og om mulig lage et redskap til å anta en kvalitet med større presisjon. For å oppnå dette må en foreta meget detaljerte undersøkelser av transportretning, petrografisk sammensetning, runding, sprøhet og flisighet.

Det må presiseres at undersøkelsene ikke gjelder massenes egnethet til f. eks. betongformål. Hvorvidt styrkesten (fallprøven) er relevant for å vurdere masser til betong, vil bli tatt opp av Anundsen i et senere arbeid.

## Metoder

Skal en kunne avsløre eventuelle korrelasjoner som nevnt, må en løse transportspørsmålet, d.v.s. gjøre undersøkelser over transportretningene til forekomstenes enkelte bestanddeler. I Surnadalen, Sunndalen, Sogndalsdalen Suldalen og og Setesdalen (Fig. 1) er følgende jordarter undersøkt: morene, glasifluvialt og fluvialt materiale. Hele dalfører med sidedaler er valgt for å kunne kontrollere hva som skjer med et grusmateriale under transport, og hvor det skjer forandringer med det. Dalfører som er innbyrdes ulike m.h.t. bergartstyper, isavsmeltningshistorie og dreneringstype er undersøkt. Det er foretatt analyser av sprøhet, flisighet, runding og petrografisk sammensetning. Runding og petrografi er vesentlige for å spore 1) transportretninger og -måter, 2) tilførsler til dalen fra sidedaler. Prinsipielt burde man foreta petrografi- og rundingsanalysene også på den fraksjon som brukes i sprøhets- og flisighetsanalysene. Det er foretatt noen analyser av runding og petrografi på flere fraksjoner for å se på variasjonene. Rundingsanalyser viser klart at der er en bestemt fraksjon hvor rundingen er optimal, og at rundingen i grovere og finere fraksjoner er lavere. Dette er i overensstemmelse med resultatene til Kaitanen & Strøm

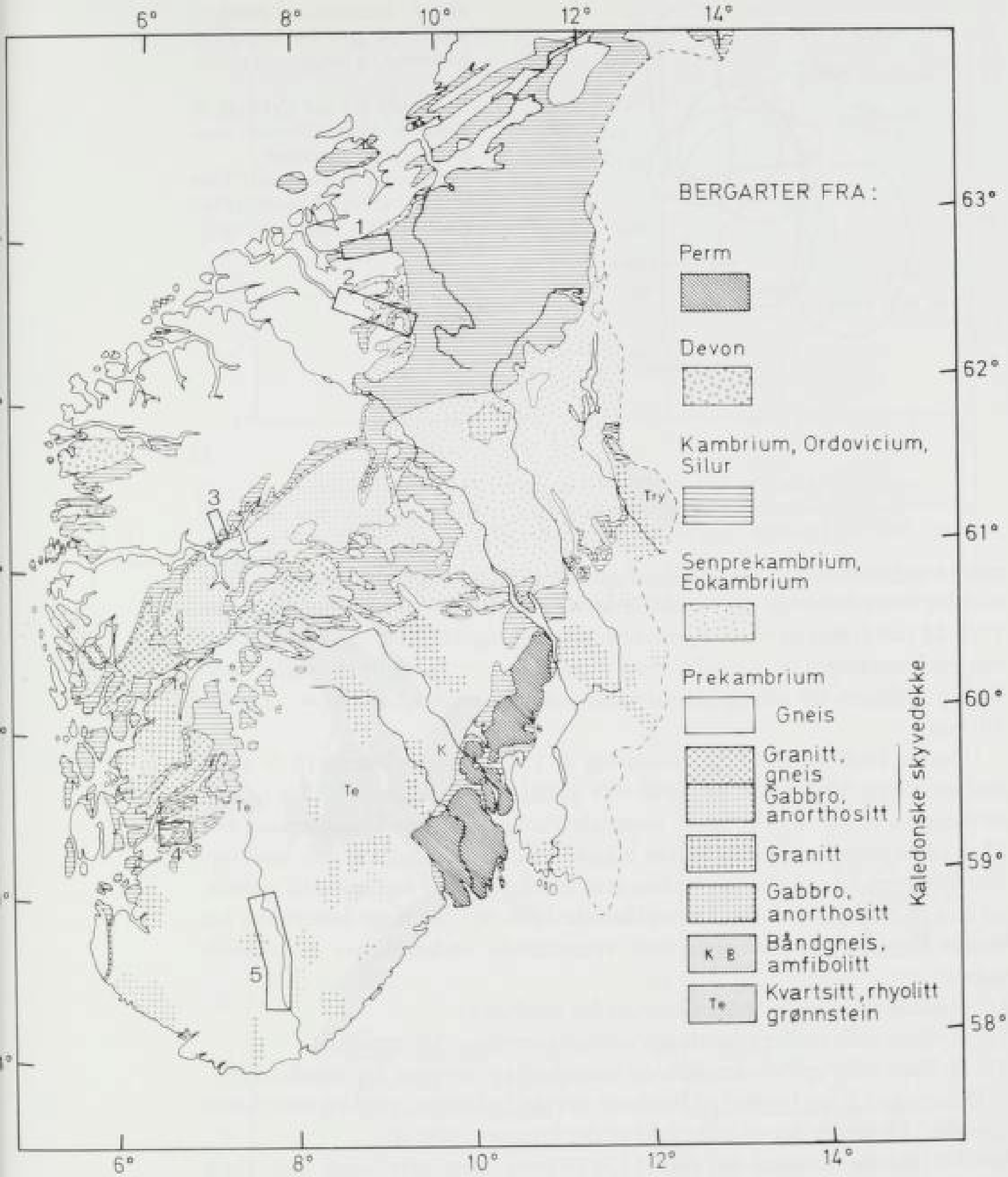


Fig. 1. Beliggenheten av de undersøkte områder. (Berggrunnsgeologisk kart modifisert etter Holtedahl & Dons (1960).
*Location of the investigated areas. Geological map modified from Holtedahl & Dons (1960).*
1: Surnadalen, 2: Sunndalen, 3: Sogndalsdalen, 4: Suldalen, 5: Setesdalen.

(1978). For særlig grove fraksjoner, og for fraksjoner mindre enn 2 mm, viser egne resultater at rundingen blir tilnærmet den samme i alle typer avsetninger. 25–37 mm er derfor meget nær den fraksjon som forteller mest om et mate-

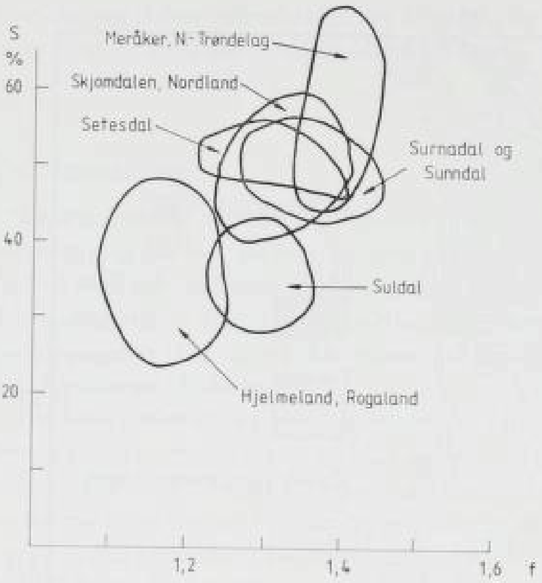


Fig. 2. Sprøhets- og flisighetsverdier på grus fra forskjellige landsdeler og berggrunns-provinser.
*Brittleness (S) and flakiness (f) numbers from different areas and bedrock provinces.*
Sammenstilt fra/*compiled from* Hugdahl (1976), Moseid (1976), Rake (1976), Stokke (1976), Anundsen (1977).

riales transporthistorie. Da det 1) ikke er noen lovmessig endring av petrografi med kortstørrelsen, 2) er vanskeligere å identifisere bergartstypen i f. eks. 11,2–16 mm fraksjonen enn i grovere fraksjoner, og 3) er umulig å identifisere dreneringsretningen i 11,2–16 mm fraksjonen, er for letthets skyld brukt samme fraksjon til petrografianalysene som til rundingsanalysene, 19/25–37 mm.

I Norge brukes både 11,2–16 mm og 8–11,2 mm fraksjonene til S- og f-analyse, tilsatt 50% knust overgrus (NS 1962, Statens Vegvesen 1966). Bruk av overgrus er logisk, idet grovt materiale i en naturlig forekomst knuses ned til en passe størrelse, og dels brukes blandet med naturgrus, men dels også som rent knuseprodukt. I Sverige bruker man imidlertid kun naturgrus til testene, og kun på fraksjonen 8–11,2 mm (Høbeda 1966:48). Så langt forfatterne har kunnet finne, er det ikke gjort noen systematiske undersøkelser av følgende forhold:

1) Hvilken rolle spiller testfraksjonen for resultatet?
2) Hvilken rolle spiller tilsettingen av knust overgrus for resultatet?
3) Hvilken rolle spiller mengden og størrelsen av overgrus for resultatet?

Det er gjort S- og f-tester på begge de nevnte fraksjoner, med og uten knust overgrus. De steder det er undersøkt er det kommet fram at:

1) 8–11,2 mm er sterkere enn 11,2–16 mm, men ofte også mer flisig (fig. 3, 4 og 5).
2) tilsetting av knust overgrus øker materialets styrke i begge fraksjoner i ett område (Fig. 5), men senker den i et annet (Fig. 3b).
3) spredningen i resultatene er størst for 11,2–16 mm naturgrus (Fig. 5).

Man kan imidlertid ikke si om den ene fraksjonen/metoden kan fortelle mer om et materiale enn den andre før man har prøvd dem alle i veg- og betongundersøkelser, og sett om man får fram de samme kvalitetsforskjeller der.

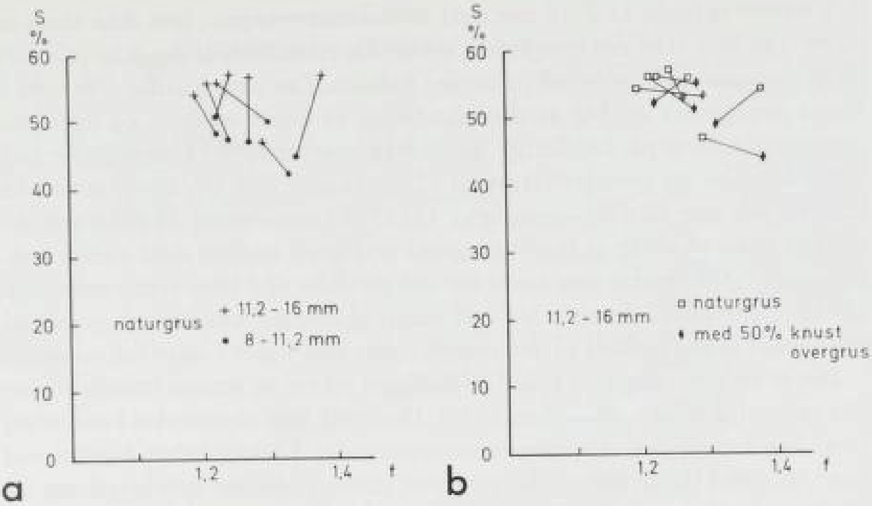


Fig. (3 a). Sprøhet – flisighet på naturgrus 8,0–11,2 og 11,2–16,0 mm, Setesdalen.
*Brittleness and flakiness on natural gravel, different fractions, Setesdalen valley.*
3 (b). Sprøhet/flisighet på 11,2–16,0 mm, naturgrus og med tilsetting av 50% overgrus, Setesdalen.
*Brittleness/flakiness (11,2–16,0 mm fraction) on natural gravel, and on a mixture of 50% natural gravel and 50% crushed stones (Conventional method), Setesdalen.*

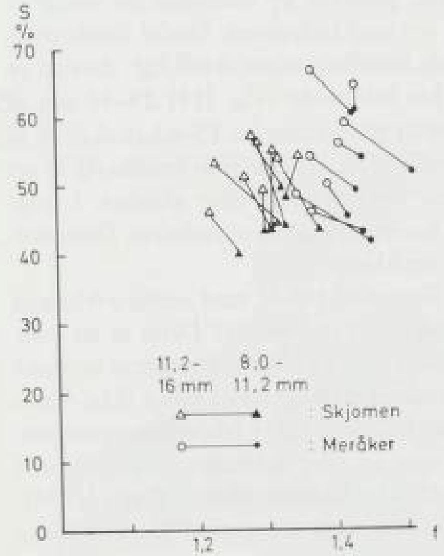


Fig. 4. S–f i div. fraksjoner, med overgrustilsetting, i Meråker og Skjomen.
*Brittleness/flakiness on different fractions (mixture), Meråker (Trøndelag) and Skjomen (North Norway).*
Sammenstilt fra/*compiled from* Hugdahl (1976) & Stokke (1976), *in* Anundsen (1977).

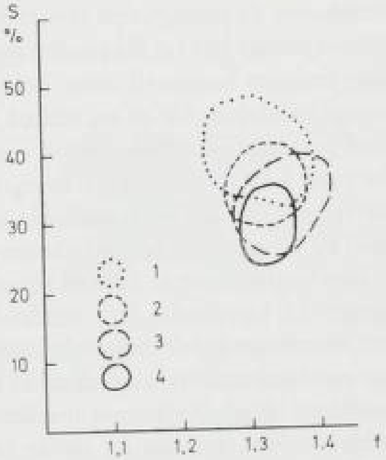


Fig. 5. S–f etter ulike metoder, Suldalen: 1: 8.0–11.2 mm tilsatt 50% knust overgrus, 2: 8.0–11.2 mm naturgrus, 3: 11.2–16.0 mm tilsatt overgrus, 4: 11.2–16.0 mm naturgrus. (Etter Anundsen 1977).
*Brittleness/flakiness according to different methods, Suldalen. 1: 8.0–11.2 mm conv., 2: 8.0–11.2 mm natural gravel, 3: 11.2–16.0 mm conv., 4: 11.2–16.0 mm natural gravel. (After Anundsen 1977).*

I testene er brukt 11,2–16 mm med 50% knust overgrus, hvis ikke annet er nevnt. Det kan, etter det foregående, synes som en svakhet at det ikke er utført S- og petrografi-undersøkelser på samme fraksjon. Det mest logiske ville være å foreta petrografisk analyse av den blandingen av knust overgrus og naturgrus som testen utføres på. Imidlertid, der er ikke stor forskjell i kornstørrelse mellom S-fraksjon og petrografi-fraksjon (11,2–16 mm mot 19/25–37 mm), der tilsettes like stor partikkel-mengde av 19/25–37 mm som av 11,2–16 mm, resultater tyder på at der er liten variasjon i petrografi mellom disse snevre fraksjonene, 11,2–16 mm er som nevnt for små partikler til å finne transport-retninger fra. Hensynet til det siste har veid tungt, og den feil som derved gjøres, må være svært liten i forhold til den unøyaktighet som ligger i selve fall-metoden.

Det er en kjent sak at de enkelte S-målinger på ett og samme materiale viser stor spredning (f. eks. Anundsen 1977). Dette må bety at metoden bare meget grovt kan fortelle om et aggregats knusemotstand. Undersøkelser foretatt ved Geol. inst. ved Universitetet i Bergen viser videre at det har stor betydning for resultatet hvilken type knuser man bruker, idet flisigheten på knuseproduktet varierer fra den ene knuseren til den andre.

I foreliggende arbeid er bl. a. søkt etter korrelasjoner mellom S (8–11,2/11,2–16 mm) og runding (19/25–37 mm). Selv om rundingen har sitt maksimum omtrent ved 25–37 mm, vil en slik korrelasjon fortsatt være meningsfylt, da 1) rundingen enda ikke er «visket» ut i S/f-fraksjonen, og 2) rundingen i 25–37 mm forteller noe generelt om transportlengde og -måte.

Det er sannsynlig at testresultatet kan påvirkes av størrelsen av overgrusfraksjonen, da petrografien ofte endrer seg med fraksjonen. Derfor burde overgrusen strengt tatt tas fra en stor mengde materiale (flere ti-tall kg), dersom en grov fraksjon brukes til dette. Derfor har forfaterne valgt (19) 25–37 mm til overgrusfraksjon, for at en ved en rimelig prøvestørrelse (5–6 kg) skal få så bred petrografisk representasjon som mulig. Derved står man imidlertid i fare for også å få påvirkning av overgrusens rundingsgrad, eller glatthet, i langt større grad enn om overgrusen ble tatt fra en mye grovere fraksjon. Dette forhold vil bli nærmere belyst i slutten av artikkelen.

Rundingsanalyser er foretatt visuelt (Bergersen 1964), med rundingsklassene kantet (k), kantrundet (kr), rundet (r), og godt rundet (gr). Dette er en etablert kvartærgeologisk undersøkelsesmetode, men i tidligere publiserte arbeider om grusforekomsters anvendbarhet til veg- og betongformål synes ikke denne metodens betydning å være trukket inn. Imidlertid er i laboratorietester forholdet mellom runding og styrke tatt opp av flere forskere, f. eks. Høbeda (1966), Grønhaug (1964, 1967), Woolf (1937), Moavenzadeh & Goetz (1963). Når et korn har høg rundingsgrad, vil dette også være glatt (se Grønhaug 1967), forutsatt at det er uforvitret.

En kan ikke se bort fra at subjektive vurderinger har betydning for rundingsfastsettelsen. En kan derfor ikke ta rundingsgraden som et absolutt mål for rundheten, og heller ikke sammenligne runding fra ett område (én persons vurdering) til et annet. De variasjoner en finner i rundingsgrad i ett område vil imidlertid være reelle.

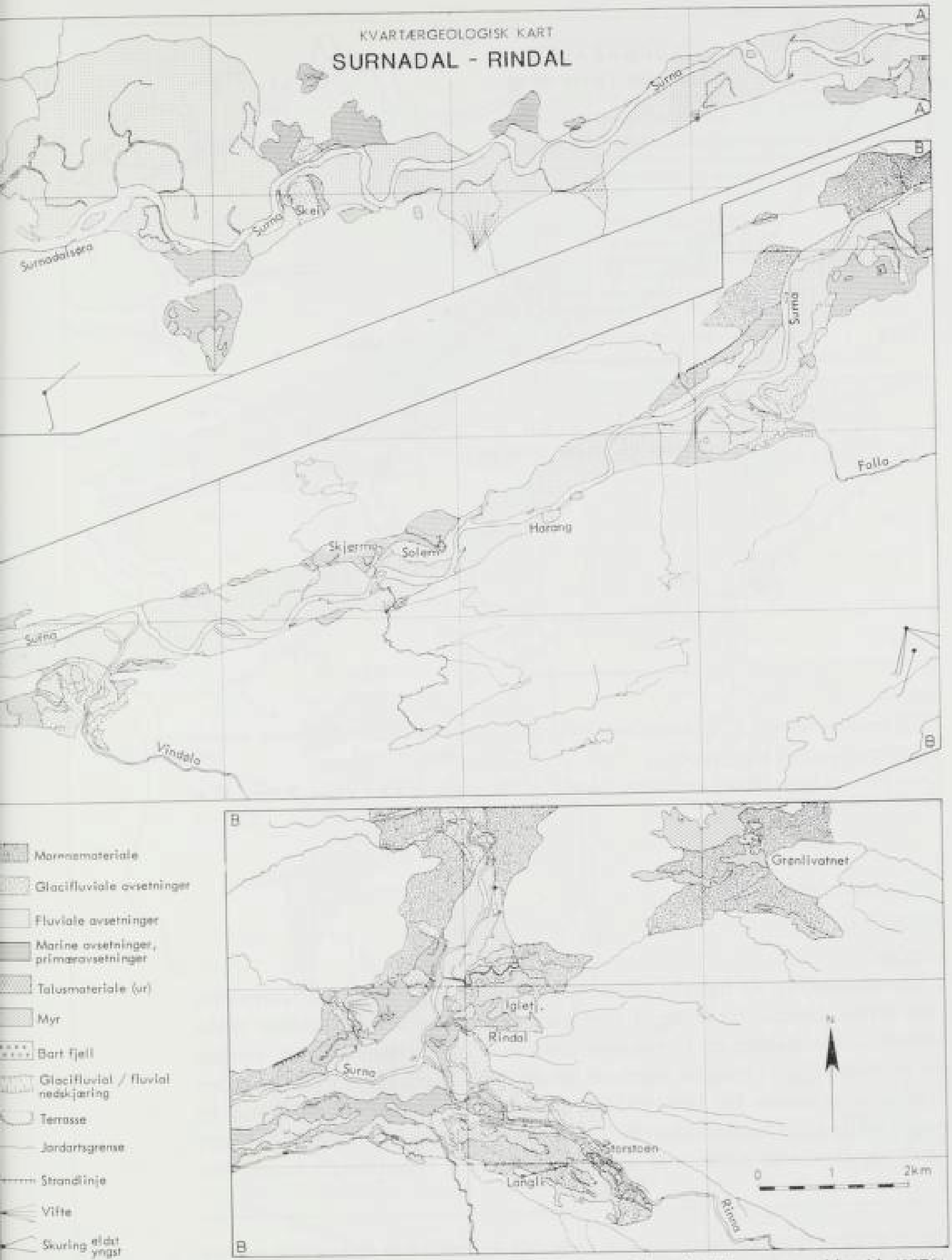


Fig. 6. Fordelingen av de ulike jordarter i Surnadalen. Modifisert etter Moseid (1976). A og B er profilene på fig 7.
*Distribution of the different types of deposits, Surnadalen valley. Modified from Moseid (1976). A and B are the profiles in Fig. 7.*

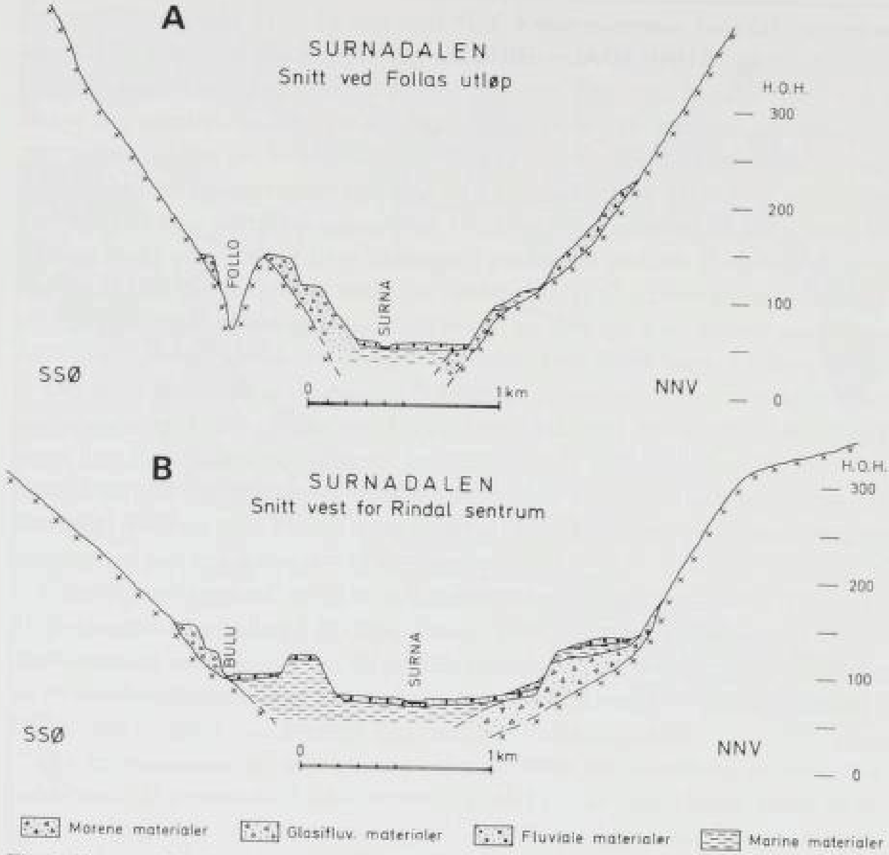


Fig. 7. Tverrprofiler fra Surnadalen.
*Cross profiles from Surnadalen valley. Above: At the outlet of river Folla. Below: W of Rindal village.*

# Regionale beskrivelser

## SURNADALEN

### *Geologi*

I Surnadalen (Fig. 6) fins det store løsavsetninger. Fig. 7 viser et tverrprofil, med typisk løsmassefordeling. I den østlige delen er det i dalsidene tykke masser av hardpakket og forholdsvis finstoffrik bunnmorene. I den vestlige del av dalen (Fig. 7) mangler stort sett bunnmorene. Generelt er morene sjelden nyttbar som ressurs for betongtilslag direkte. Bunnmorene er imidlertid en meget viktig kilde for dannelsen av betong- og vegmaterialer, ved at de har vært utsatt for fluvial og glasifluvial erosjon og sortering. Glasifluviale masser fins

---

Fig. 8. Berggrunnsgeologi (modifisert etter Holtedahl & Dons 1960) og isskuring omkring Surnadalen–Sunndalen.
*The bedrock geology (modified from Holtedahl & Dons 1960) and glacial striae around Surnadalen and Sunndalen valleys.*

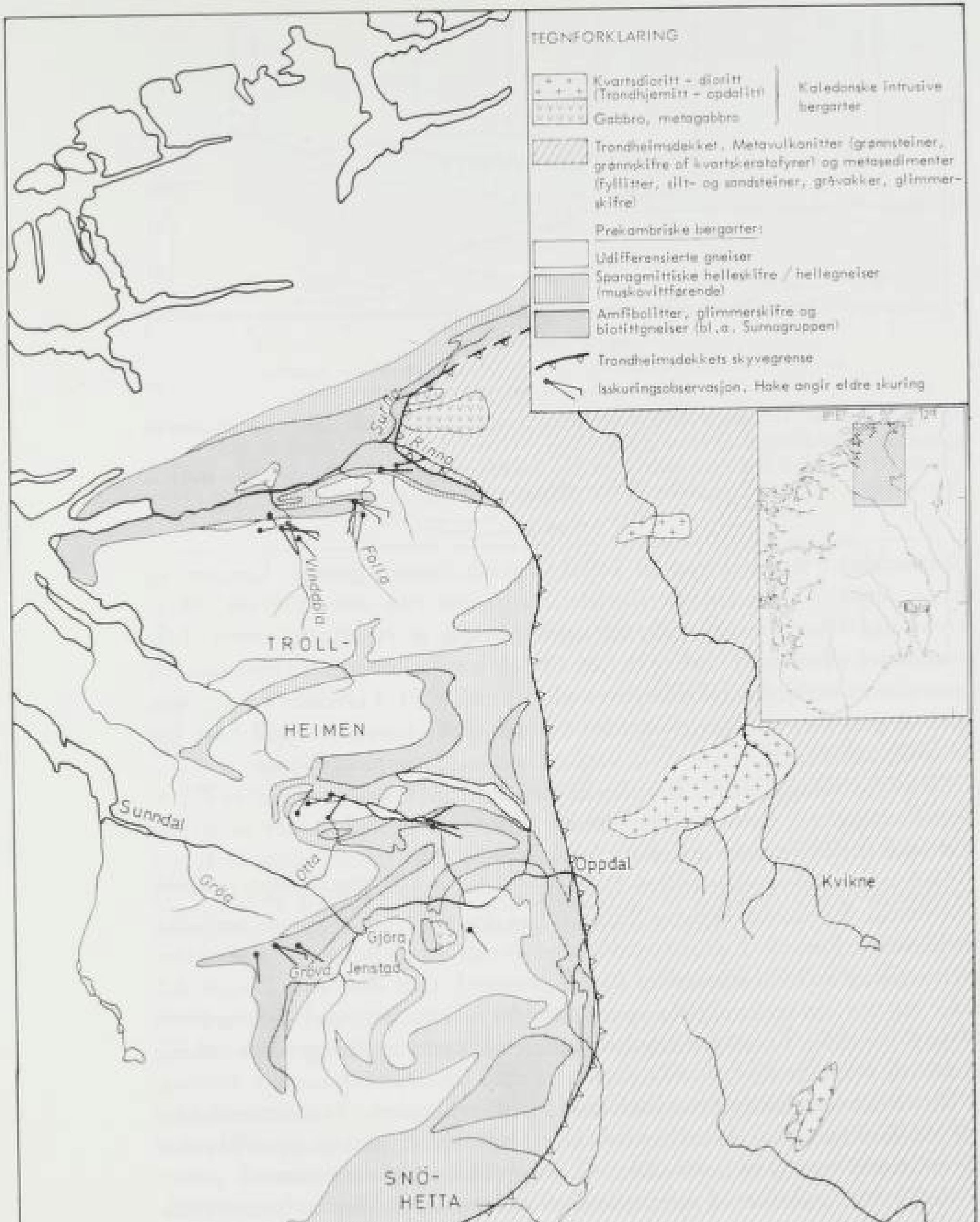
TEGNFORKLARING
Kvartsdioritt – dioritt (Trondhjemitt – opdalitt)
Gabbro, metagabbro
Kaledonske intrusive bergarter
Trondheimsdekket. Metavulkanitter (grønnsteiner, grønnskifre af kvartskeratofyrer) og metasedimenter (fyllitter, silt- og sandsteiner, gråvakker, glimmerskifre)
Prekambriske bergarter:
Udifferensierte gneiser
Sparagmittiske helleskifre / hellegneiser (muskovittførende)
Amfibolitter, glimmerskifre og biotittgneiser (bl.a. Surnagruppen)
Trondheimsdekkets skyvegrense
Isskuringsobservasjon. Hake angir eldre skuring
Surna
Rinna
Folla
Vindøla
TROLL-
HEIMEN
Sunndal
Grøa
Otta
Oppdal
Kvikne
Gjøra
Grøva
Jenstad
SNÖ-
HETTA
0
10
20
30km
Dombås

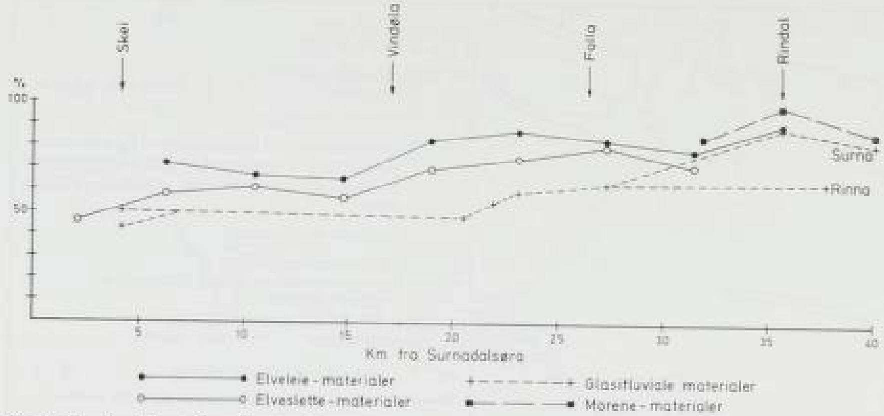


Fig. 9. Innhold av Trondheimsfeltets bergarter (lengdeprofiler) i de ulike avsetningstyper, Surnadalen. Modifisert etter Moseid (1976).
*Content of volcanics and sediments from the Trondheim region in the different types of deposits (long profiles) Surnadalen valley. Modified from Moseid (1976).*

i Surnadalen i terrasser opp til 140–147 m o.h. (marin grense). Utenom, og delvis under, de glasifluviale/fluviale avsetninger fins ofte leire/silt. På et lavere nivå finner man fluviale terrasserester som er ytterligere sortert. Like over elvens nåværende nivå er der en til dels ganske bred slette med sand og grus, ofte av beskjeden tykkelse, over silt/leire (Fig. 7). I elveleiet vil det være sand og grus som er i mer eller mindre kontinuerlig transport. Også høye terrasser kan helt bestå av leire/silt, særlig i områdene nærmest fjorden.

De berggrunnsgeologiske hovedtrekkene i Surnadalsområdet er vist på Fig. 8. Trondheimsfeltets lavmetamorfe basiske vulkanitter og sedimenter overlagrer tektonisk det NV-norske gneiskomplekset.

Den vestlige skyvegrensen for Trondheimdekket går i følge Råheim (1979) ved Rindal. Surnadalen vest for Rindal følger den VSV–ØNØ-gående Surnadal-synklinalen. Sentralt i denne synklinalen finnes amfibolitter, glimmerskifre, marmorer og kalksilikatbergarter (Surna-gruppen). I en smal sone i begge dalsider opptrer sen-prekambriske sparagmittiske hellegneiser, og i fjellområdene N og S for dalen finnes gneiser med varierende sammensetning (hovedsakelig diorittisk – granittisk).

Under den kaledonske metamorfosen og innskyvningen av Trondheimsdekket ble imidlertid endel av de prekambriske amfibolittene i Surna-gruppen påvirket og undergikk retrograd omvandling til grønnskifre og grønnsteiner.

Ved isskuringsstriper og retningsanalyse av morenestein har en funnet «matnings»-retningen av morene-materiale til dalen. På et tidlig tidspunkt har isen i Surnadal-området kommet fra Trollheimen i syd, og derfor matet dalen med Trollheims-gneis. På et senere tidspunkt har isen kommet fra SØ, og derfor i de østligste deler matet dalen med Trondheimsfelt-bergarter. På et enda senere tidspunkt har isen beveget seg vestover, og langs, hoveddalen (Moseid 1976). Den glasifluviale og fluviale transport har foregått fra sidedalene og ut til hoveddalen, og langs hoveddalen.

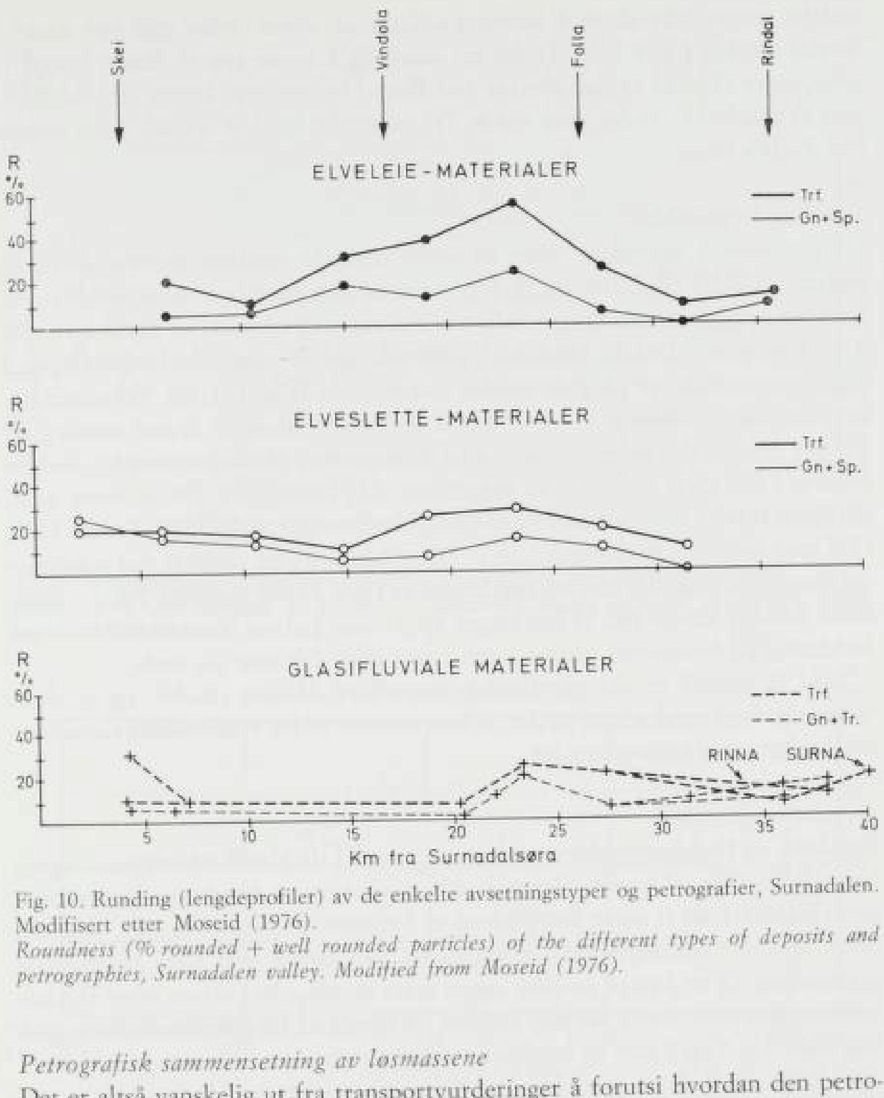


Fig. 10. Runding (lengdeprofiler) av de enkelte avsetningstyper og petrografier, Surnadalen. Modifisert etter Moseid (1976).
*Roundness (% rounded + well rounded particles) of the different types of deposits and petrographies, Surnadalen valley. Modified from Moseid (1976).*

*Petrografisk sammensetning av løsmassene*

Det er altså vanskelig ut fra transportvurderinger å forutsi hvordan den petrografiske sammensetningen vil være i massene i Surnadalen. Unntak danner 1) morenematerialet i den østlige delen, som består av mye Trondheimsfelt-bergarter (Fig. 9), 2) det glasifluviale materialet i øst som derfor også inneholder meget Trondheimsfelt-bergarter (Trf.), 3) den nåtidige dreneringen fra sidedalene som ventelig skulle gi Trollheimsgneis til hoveddalen, ved erosjon i fast fjell.

Det glasifluviale materialet blir fattigere på Trf umiddelbart nedstrøms Folla (Fig. 9). Dette er rimelig, da en må vente at smeltevann fra Folla har forsynt dalen med gneis. Det er derfor overraskende at fluvialt materiale, særlig elveleiemateriale, inneholder mye Trf også nedstrøms Folla's tilløp. Det fluviale materialet må derfor ha kommet nedover hoveddalen. Men da Trf-innholdet i elvematerialet er høgere enn i både det glasifluviale og det øvrige fluviale materialet, synes ikke dette å kunne forklares på annen måte enn ved nåtidig fluvial erosjon i fast fjell, da det er vanskelig å tenke seg at denne bergartsgruppen er så sterk at den anrikes ved fluvial behandling. Dette forhold kommer vi tilbake til, da det viser seg at Trf-materialet også er spesielt godt rundet ved Folla's tilløp.

*Runding av partikler*

De *glasifluviale* materialer viser en svakt stigende runding nedover dalen til nedstrøms Folla (Fig. 10), og skyldes ventelig den naturlige transportslitasjen. Den brå nedgangen nedstrøms Folla skyldes ventelig tilskudd av mindre rundet Trollheimsgneis. Det er imidlertid overraskende at også *alle* bergartstyper i elveleie-materialer er så godt rundet akkurat her (Fig. 10), da Trf-materialet her som nevnt må være kommet østfra. En skulle vente en lavere runding av Trf her dersom det høge innholdet av Trf-bergarter i elveleie-materialer skyldes erosjon i fast fjell umiddelbart oppstrøms. Og hvorfor er Trf-begatene igjen dårligere rundet nedstrøms Folla når det ikke kommer tilskudd av Trf fra Folla (Trf som kunne være dårlig rundet)? Dette kan være en svakhet ved rundingsanalysen som metode, idet en må huske at (19) 25–37 mm ved Folla's tilløp betyr kanskje 40–50 mm få km lenger oppstrøms i elven (Goede 1975). Noen forklaring på fenomenet utover dette synes ikke å kunne gis enda.

Med få unntak er det glasifluviale materialet dårligst rundet, og elveleiematerialet best rundet, som er det en kunne vente ut fra materialenes dannelsesbetingelser og transportlengder.

*Sprøhet og flisighet*

Sprøhets- og flisighetsverdiene endrer seg meget i de glasifluviale avsetningene langs dalen (Fig. 11), men tilsynelatende uavhengig av bergartssammensetningen (Fig. 9). I de fluviale materialene er verdiene *jevnere* (Fig. 11), selv om bergartssammensetningen endrer seg minst like meget som i de glasifluviale materialene. Dette kan på en eller annen måte skyldes det faktum at de fluviale massene har vært utsatt for den lengste transporten. Ved sammenligning mellom Figs. 11, 9 og 8 kan en konkludere at der er ingen trekk som umiddelbart viser hvor en (i dette området) kan finne materialet med lavest sprøhet og flisighet ut fra berggrunnskartlegging og petrografiske undersøkelser alene. Det er imidlertid mulig at det kan spores en svak avtagende sprøhet (logaritmisk petrografi-skala) med tiltagende Trf-innhold, på bekostning av gneis, i de glasifluviale materialene (Fig. 12). (Trf er her glimmerskifer, grønnstein m. fl.). Spredningen er imidlertid stor, og rundingen er meget varierende (Fig. 13).

Ved undersøkelse av forholdet gneis-sprøhet, Trf-sprøhet hver for seg, finner en at økende innhold av gneis øker sprøheten omtrent like meget som økende Trf reduserer den. Hver parameters innvirkning er derfor vanskelig å skille ut. Dersom det eksisterer en forskjell i sprøhet mellom de enkelte jordartstyper (Fig. 11 og 12), tross ens sammensetning, må dette i stor grad ha ikke-petrografiske årsaker. Det er derfor nærliggende at forskjellig transportmåte eller -lengde kan ha betydning, dvs enten 1) at det ved fluvial transport skjer en

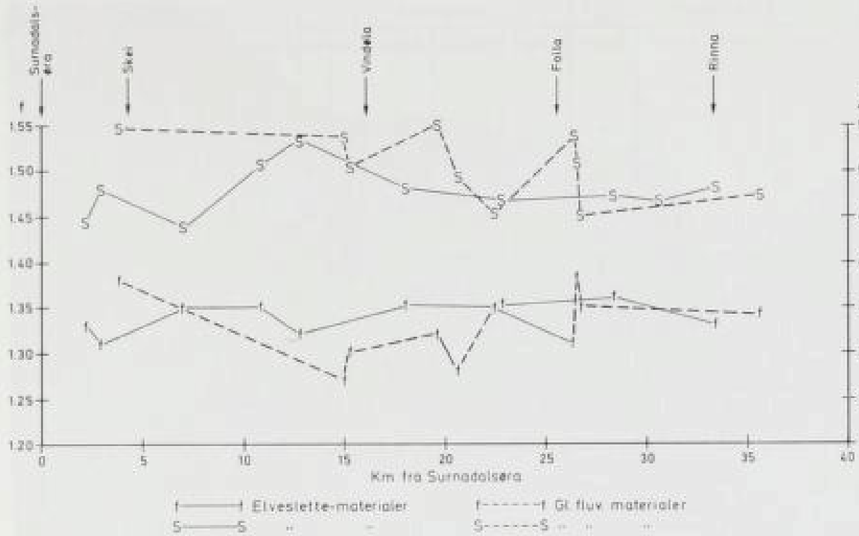


Fig. 11. Lengdeprofiler av prøhet og flisighet, Surnadalen. Etter Anundsen (1977).
*Brittleness (S) and flakiness (f) of the glacifluvial and fluvial deposits, Surnadalen. From Anundsen (1977).*

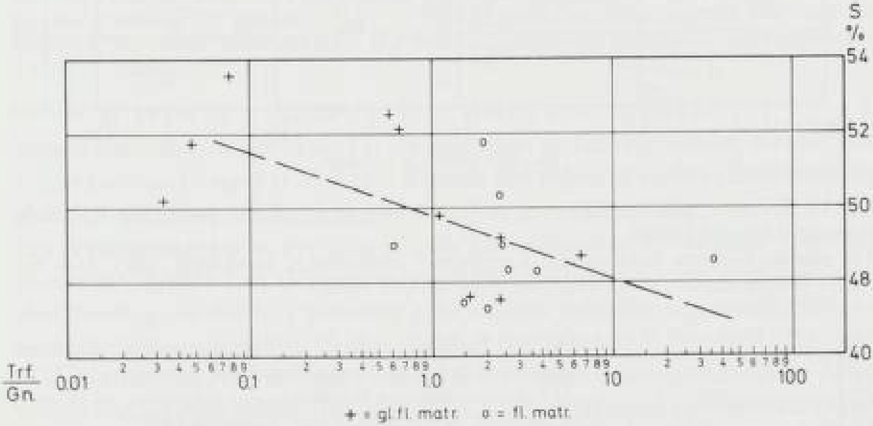


Fig. 12. Sprøhet og petrografi, Surnadalen. Forholdet mellom Trondheimsfeltets bergarter (Trf) og Trollheimsgneis (Gn) er framstilt logaritmisk. Modifisert etter Moseid (1976).
*The relation between brittleness, and petrographic composition, in glacifluvial (+) and fluvial (o) deposits, Surnadalen valley. Trf. are the volcanics and sediments from the Trondheim area, and Gn the gneisses from the Trollheimen area. Logarithmic horisontal scale. Modified frm Moseid (1976).*

knusing av de svake, og dermed anrikning av sterke korn, eller 2) at avrundingen av kornene influerer på sprøheten. Fluviale materialer er ofte bedre rundet enn de glasifluviale (Fig. 13).

*Sprøhet og runding*

Ved undersøkelse av sprøhet og runding spesielt (se over), finner man klart en økende styrke av grusmaterialer med øket runding, for alle jordarter og

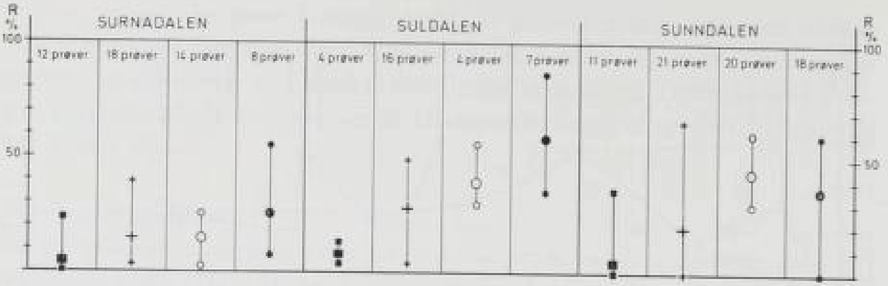


Fig. 13. Rundingen av forskjellige avsetningstyper i Surnadalen, Sunndalen og Suldalen. Middelverdien (uthevet) og variasjonsbredden er vist.
*The roundness of different deposits in the valleys of Surnadalen, Sunndalen and Suldalen.* ▣ *Morainic deposits,* + *Glacifluvial deposits,* o *Fluvial terraces,* ● *River-bed materials. The mean values and variation limits are shown.*

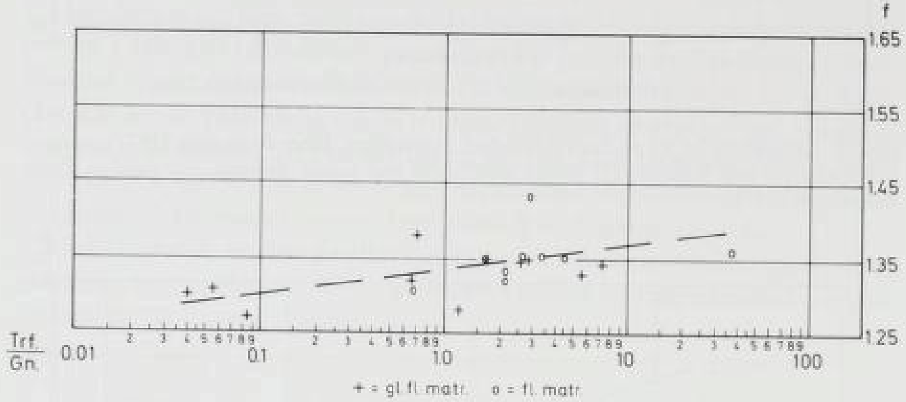


Fig. 14. Forholdet mellom flisighet og petrografi, Surnadalen. Ellers som på fig. 13. Modifisert etter Moseid (1976).
*The relation between flakiness and petrographic composition, Surnadalen valley. (See Fig. 13 for further explanations). Modified from Moseid (1976).*

Fig. 15. Forholdet mellom sprøhet og runding, alle avsetningstyper under ett, Surnadalen. Etter Anundsen 1977).
*The relation between brittleness and roundness, all types of of deposits, Surnadalen. From Anundsen (1977).*

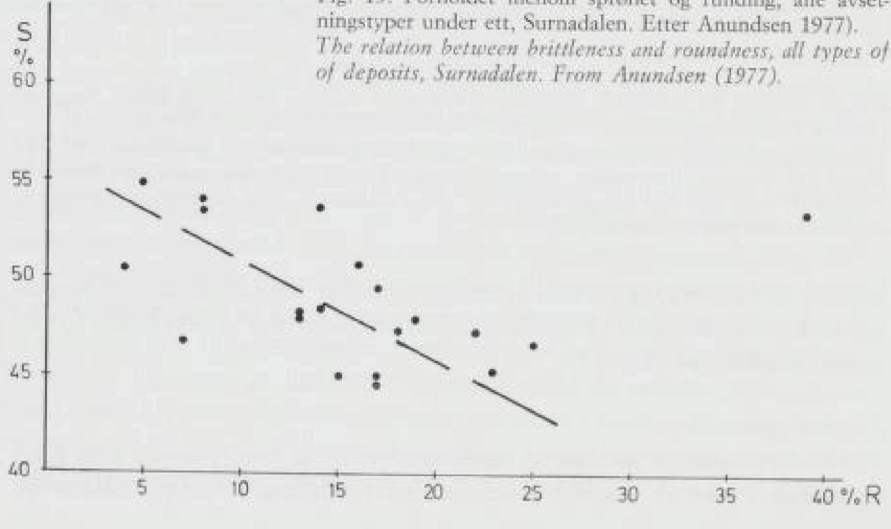

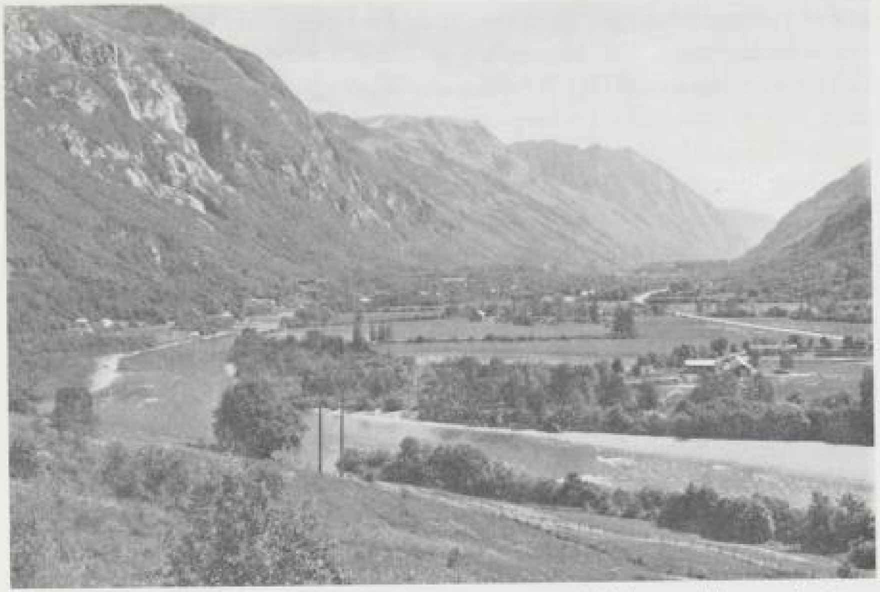

Fig. 16. Sunndalen sett mot øst fra Hoås. I forgrunnen elveleiematerialer og elveslette. Midt på bildet terrasser, og i bakgrunnen glasifluvialt delta (Gikling). Foto: R. Trønnes. *Sunndalen towards the east, from Hoås. In the foreground river-bed materials and the flood plain. In the centre river terraces, and in the background glacifluvial delta (Gikling). Photo: R. Trønnes.*

bergartsammensetninger (Fig. 15). Spredningen er kanskje mindre enn for forholdet petrografi–sprøhet. Det skal allerede her pekes på at den glasifluviale og glasiale behandling må ha vært meget røffere enn den nåtidige fluviale er. En kan derfor tenke seg at den vesentligste anrikningen av sterke korn i fluviale materialer skjedde i en tidligere transportsyklus. En reduksjon i sprøhet med øket runding må derfor i vesentlig grad skyldes selve formen (rundheten) av kornene. Det er antydning til øket flisighet med økende Trf-innhold (Fig. 14).

Der er bare en svak tendens i Surnadalen til at de fluviale jordarter er bedre rundet enn de glasifluviale (Fig. 13). Både p.g.a. dette og den varierende petrografiske sammensetningen, kan man ikke i Surnadalen lage som noen generell regel at elveleiematerialene er de sterkeste materialene.

## SUNNDALEN

### *Geologi*

Også i Sunndalen (Fig. 16) er det meget betydelige kvartære avsetninger. Et typisk tverrprofil av Sunndalens masser er som for Surnadalen (Fig. 7). Ved Hoås og Gikling ligger det randdeltaer (Sollid 1964). Eldre enn disse er eskere og bresjøterrasser ved Jenstad (Nordhagen 1929, 1930). Der er generelt lite bunnmorene i området, unntatt i dalsidene rundt Jenstad og Ottdalen, hvor de tykke avsetningene er utsatt for ras og bekkeerosjon. Særlig i munningen av elven Grøva ligger det derfor store mengder materiale, dels som (rester etter) en høg glasifluvial vifte, men særlig som en betydelig recent vifte. Den petrografiske sammensetningen av viftene er derfor trolig sterkt influert av morenenes sammensetning. Ved Hovhjellen og Linset i Litledalen er det også randdeltaer og terrasselandskap. Randdeltaene er avsatt av breer fra sør, fra bergarter som er forskjellige fra bergartene i hoveddalen.

Fig. 8 viser de berggrunnsgeologiske hovedtrekkene i Sunndalsområdet. Gneisområdet vest for Oppdal består av vekslende bergartsenheter i form av to separate dekkekomplekser over autokton basalgneis med overlagring av sparagmittiske hellegneiser og hornblende – glimmerskifre (Eggen et al. 1979).

Langs Sunndalen vest for Gravem opptrer migmatittiske, hovedsakelig granodiorittiske biotittførende basalgneiser i Frei-gruppen (Råheim 1972). Det undre dekkekomplekset øst for Gjøra domineres av øyegneiser, metagabbro og ultramafiske bergarter. Det øvre dekkekomplekset inneholder bl. a. sparagmittiske hellegneiser, amfibol–glimmerskifre og amfibolitter. Trondheimsfeltets metasedimenter og metavulkanitter med enkelte gabbroide–kvartsdiorittiske intrusjoner overlagrer gneiskomplekset tektonisk. Skyvegrensen for Trondheimsdekket går omtrent N–S forbi Oppdal og følger Drivdalen sørover mot Hjerkinn–Snøhetta-området (Roberts 1978). Grønnskifre, fyllitter, silt- og sandsteiner er dominerende bergartsenheter øst for Oppdal–Drivdalen.

Isskuringsstriper og retningsanalyse av stein i morene (Trønnes 1978) viser at isen i tidlige topografisk uavhengige faser beveget seg først mot V–NV og senere mot SV. Det har vært bevegelse også mot dalen fra høgfjellet på nord- og sørsiden, sannsynligvis ved lokalglasiasjon (Fig. 8). Aldersforholdene mellom de ulike regionale stadiene er ikke kjent.

Som i Surnadal er det derfor meget vanskelig å forutsi hvordan den petrografiske sammensetningen vil være i massene.

*Petrografisk sammensetning av løsmassene*

Med unntak av elveleiematerialer synker innhold av Trondheimsfeltsbergarter mer eller mindre jevnt vestover dalen etter et lokalt minimum i øst. Ved dette minimum er innhold av sparagmittgruppens bergarter tilsvarende høgt (Fig. 17). Gneis øker kraftig umiddelbart nedstrøms tilløpet av elven Otta, særlig i elveleiematerialet. Det er rimelig at dette skyldes ras- og erosjonsaktiviteten i Ottdalens morenemateriale, som helt er dominert av kantet gneismateriale. Derfor må en også vente at materialet i elvebunnen er dårlig rundet umiddelbart nedstrøms Otta. Forøvrig er det meget få trekk som man på forhånd kunne slutte seg til av sammensetninger. Man kan merke seg at elvesletteprøvene viser innbyrdes liten petrografisk spredning, mens glasifluvium og elveleiematerialer viser stor variasjon. Dette er ikke gjeldende i Surnadalen.

Sammensetningen av Litledalens masser er naturlig (se øverst) dominert av gneisbergarter. Imidlertid er det relativt mye sparagmitt og Trondheimsfeltbergarter i den vestlige del av det resente deltaet i Sunndalsøra. Dette tyder på at tilførselen fra Sunndalen er dominerende i forhold til fra Litledalen.

Sammensetningen av morenemateriale og glasifluvialt materiale ved Jenstad er stort sett preget av den lokale berggrunnen. Da isbevegelsen har vært på tvers av den skiftende lithologi, er der derfor flere muligheter for kilder. Dette gjelder også generelt.

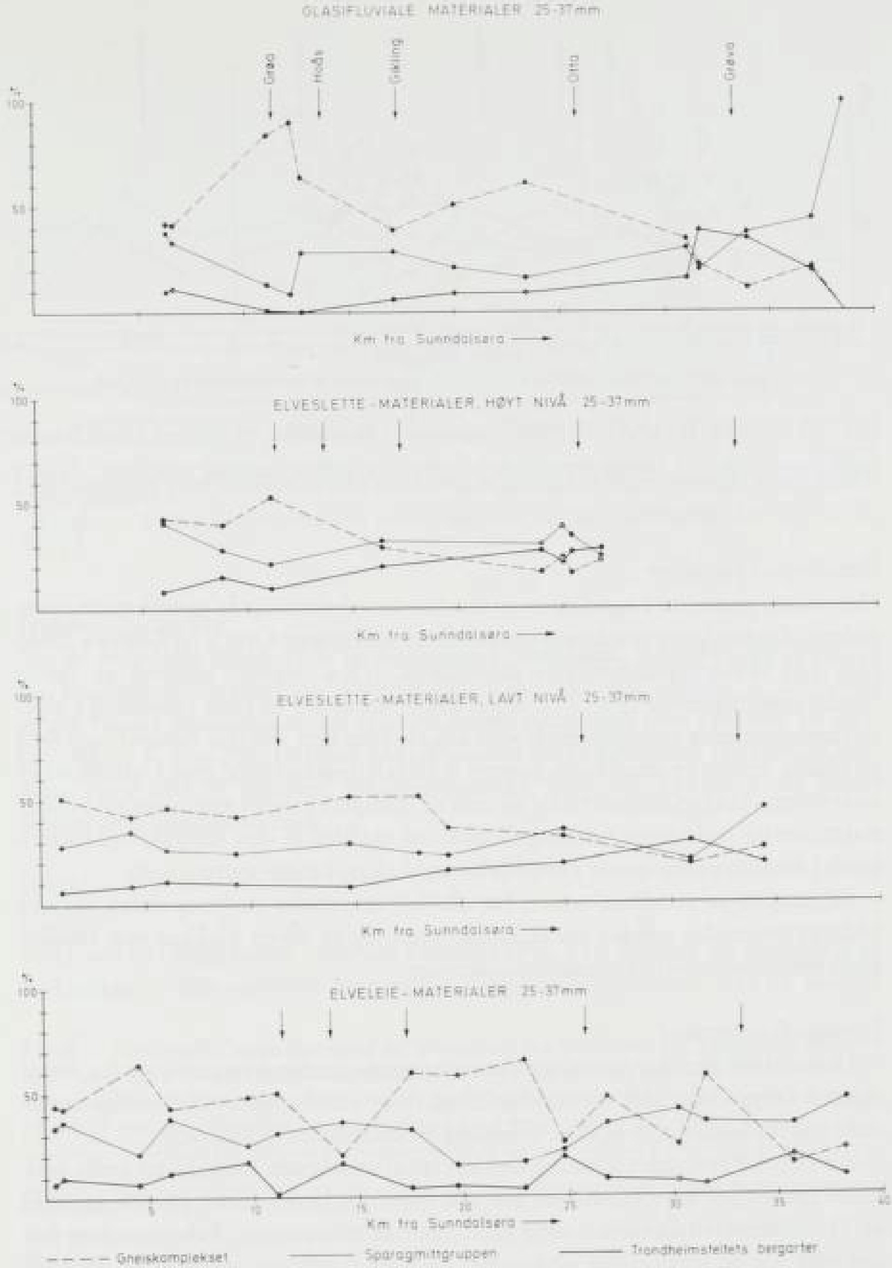


Fig. 17. Petrografisk sammensetning (lengdeprofiler) av ulike avsetningstyper i Sunndalen. En del av gruspartiklene kan ikke med sikkerhet henføres til noen av de tre berggrunnskompleksene. Derfor blir summene (i prosent) mindre enn 100. Modifisert etter Trønnes (1978).

*The petrographical distribution in some types of deposits, Sunndalen valley. Glacifluvial deposits (above), high fluvial terraces, low fluvial terraces and river-bed materials (below). «Trondheimsfeltets bergarter» = metasediments and metavolcanics from the Trondheim region. Parts of the gravel particles cannot be ascribed to any one of the three bedrock complexes (the gneis complex, the sparagmite group or the metasediments and the metavolcanics from the Trondheim region). Thus the percent sums are less than 100. Modified from Trønnes (1978).*

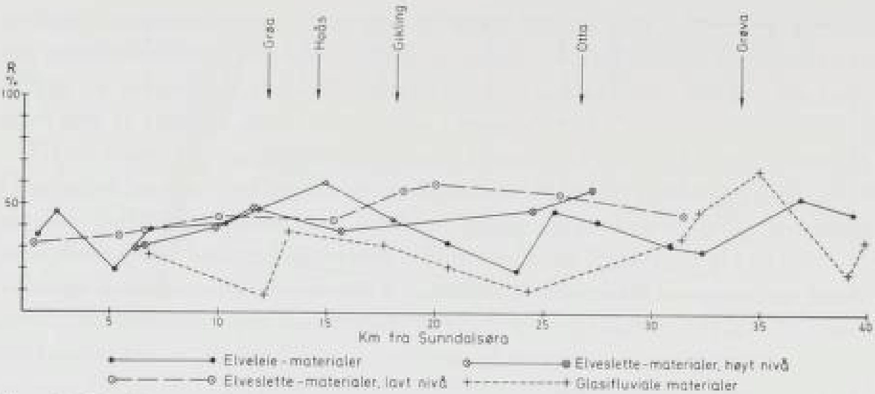


Fig. 18. Runding av forskjellige avsetningstyper i Sunndalen. Modifisert etter Trønnes (1978).
*Roundness of different types of deposits in Sunndalen valley. Modified from Trønnes (1978).*

*Runding av partikler*

Det er stor variasjon i rundingen av elveleiematerialene og de glasifluviale materialene. De markerte minimum umiddelbart nedstrøms Otta's og Grøva's tilløp (Fig. 18) skyldes sannsynligvis glasifluvial, h.h.v. resent, tilførsel av dårlig rundet gneismateriale (Fig. 17). Igjen finner en at der er liten spredning i elveslettematerialenes rundingsgrad, som må skyldes den fluviale behandling. Som en skulle vente, er rundingen høgere i elveslettematerialer enn i glasifluviale materialer. At elveleiematerialer til dels er dårligere rundet enn elveslette-materialer, særlig nedstrøms Otta og Grøva, må skyldes at den utstrakte rasaktiviteten i bunnmorener mater hoveddalen med skarpkantet morenestein.

Stigningen av rundingskurven for elveleie-materialer nedover dalen skyldes både at materialet rundes under transporten, og at elven plukker opp relativt godt rundet elveslette-materialer undervegs.

*Petrografi – runding*

Hovedelven plukker opp skarpkantede gneisbergarter som stammer fra utrast morene langs Otta. Det ser imidlertid ut til at rundingen av det øvrige materiale elven plukker opp også er avhengig av materialets petrografi.

Av Fig. 19 synes det å kunne trekkes ut at et økende innhold av gneis nedsetter rundingen av totalprøven, for alle typer jordarter, mens økende innhold av Trondheimsfeltsbergarter øker rundingen av totalprøven. Relasjonene er her noe ulik for de forskjellige jordartene, da også rundingen generelt er noe forskjellig. Økningen av rundingsgraden er imidlertid sterkere enn den prosentvise økningen av Trondheimsfeltbergarter. Det kunne derfor se ut til at denne gruppen bergarter hadde en gunstig innvirkning på rundingen av grusmaterialer. Det ville imidlertid være underlig om bløte Trondheimsfeltbergarter skulle runde skarpkantede harde partikler. Den rimeligste forklaring på disse to relasjoner synes å være at når det først er lite gneisbergarter, er disse samtidig langtransportert.

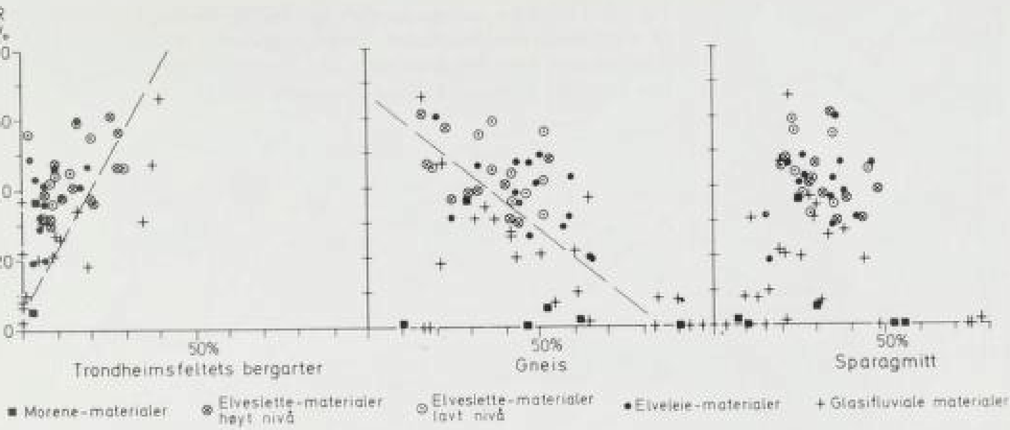


Fig. 19. Forholdet mellom runding og petrografisk sammenestning for ulike avsetningstyper, Sunndalen.
*The relation between roundness and petrograhic composition, Sunndalen. For legend, see Fig. 13.*

### *Sprøhet og runding*

Det er enda bare utført få S- og f-analyser i Sunndalen, som ikke gir grunnlag for lengdeprofil-framstilling. Petrografien i disse er vist i tabell 1. Selv med meget variert petrografi er det først og fremst rundingen som influerer på styrken (tabell 1, Fig. 20). Et klart unntak danner de to prøvene i Litledalen, men dette materialet er kommet fra gneisområdet i sør, og har en totalt annen petrografisk sammensetning.

## SULDAL

### *Geologi*

Stort sett er berggrunnen oppbygd etasjevis (Fig. 21). Nederst er grunnfjell av prekambrisk alder, derover metamorfe suprakrustal-bergarter dels av usikker

*Tabell 1.* Petrografisk sammensetning av grusprøver fra Sunndalen og Litledalen (prøve 8 og 9) som det er utført sprøhets- og flisighetsanalyser på. (Se fig. 20)
*Petrographic composition of gravel samples from Sunndalen and Litledalen (sample 8 and 9) on which analyses of brittleness and flakiness have been carried out. (See Fig. 20)*

| | 1 | 4 | 5 | 7 | 8 | 9 | 11 | 12 | 13 | 17 |
|---|---|---|---|---|---|---|---|---|---|---|
| Grå gneis | 39 | 34 | 29 | 80 | 69 | 72 | 39 | 55 | 34 | 41 |
| Rød gneis | | 3 | | | 20 | 20 | | | | |
| Øyegneis | | 4 | 9 | | | | 12 | 6 | 8 | |
| Sparagmitt/kvartsitt | 27 | 42 | 36 | 13 | 6 | 2 | 24 | 26 | 12 | 15 |
| Amfibolitt/grønnstein | 17 | 6 | 9 | 4 | 1 | 6 | 14 | 6 | 34 | 21 |
| Glimmerskifer/ grønnskifer | 13 | 4 | 12 | 3 | 3 | | 6 | 6 | 2 | 7 |
| Gabbro | | 2 | | | 1 | | | | 1 | 4 |
| Trondhjemitt | | 2 | 3 | | | | | | | 1 |
| Kvartkeratofyr | | | | | | | 4 | | 4 | 2 |
| Ubestemt | 4 | 3 | 2 | | | | 1 | 1 | 5 | 9 |
| | 100 | 100 | 100 | 100 | 100 | 100 | 100 | 100 | 100 | 100 |

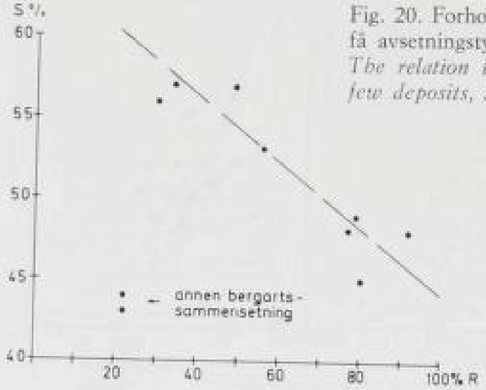


Fig. 20. Forholdet mellom sprøhet og runding for noen få avsetningstyper, Sunndalen. Etter Anundsen (1977). *The relation between brittleness and roundness for a few deposits, Sunndalen. From Anundsen (1977).*

alder og dels av kambro-ordovicisk alder. Derover ligger kaledonsk overskjøvne komplekser av antatt prekambrisk alder.

*Grunnfjellet* består av gneiser, migmatitter, metavulkanitter, sandsteiner og plutonske bergarter (Sigmond 1975). I vest er det foliert, middels- til grovkornet granitt. Ved Suldalsosen er det to brede felt med metavulkanitter (Telemarks suprakrustaler).

*De metamorfe suprakrustalbergarter* består av svart og grå fyllitt, kvartsglimmerskifer, glimmerrik gråvakke, metavulkanitter, meta-sandsteiner (stedvis «blåkvarts»), kataklasitt.

*De kaledonske overskjøvne komplekser* består av gneiser av ulike typer – lyse, båndete, folierte-monzogranittisk øyegneis, spredte lag av kvartsitt og glimmerskifer.

Grensen mellom de to øverste etasjene er stedvis skarp, men kan også være jevn, eller lagene kan opptre i veksellagring. Det er ved petrografisk analyse av grusen ofte meget vanskelig å skille bergarter fra de forskjellige etasjer.

Dalføret (Fig. 22) er dominert av glasifluviale og fluviale masser, som i Surnadalen (Fig. 7). De glasifluviale massene opptrer som terrasserester langs dalsidene. Massene er avsatt som en sandur foran, og i direkte kontakt med, en isbre. Det er store variasjoner i kornfordelingen, som til dels kan tilskrives materialtilførsel fra sideelver. I hovedsak avtar kornstørrelsen fra blokker og usortert materiale ved Suldalsvatnet til silt ved fjorden. Også i Suldal er det en elveslette langs midtpartiet av dalen.

Det er generelt meget sparsomt med morenemateriale i hoveddalen. Bare i dalsiden sør for Mo er det funnet et tynt dekke. Det er ikke spor etter morenemasser i hoveddalen som kan ha vært opphav til øvrige masser i Suldal. Inn over fjellområdene omkring dalen forekommer morenemateriale hyppigere, ikke minst som randmorener (Anundsen 1972).

Isskuringsbildet er komplisert (Fig. 22). En gammel, topografisk uavhengig bevegelse var mot V til NV, en senere mot SV. En enda yngre bevegelse var

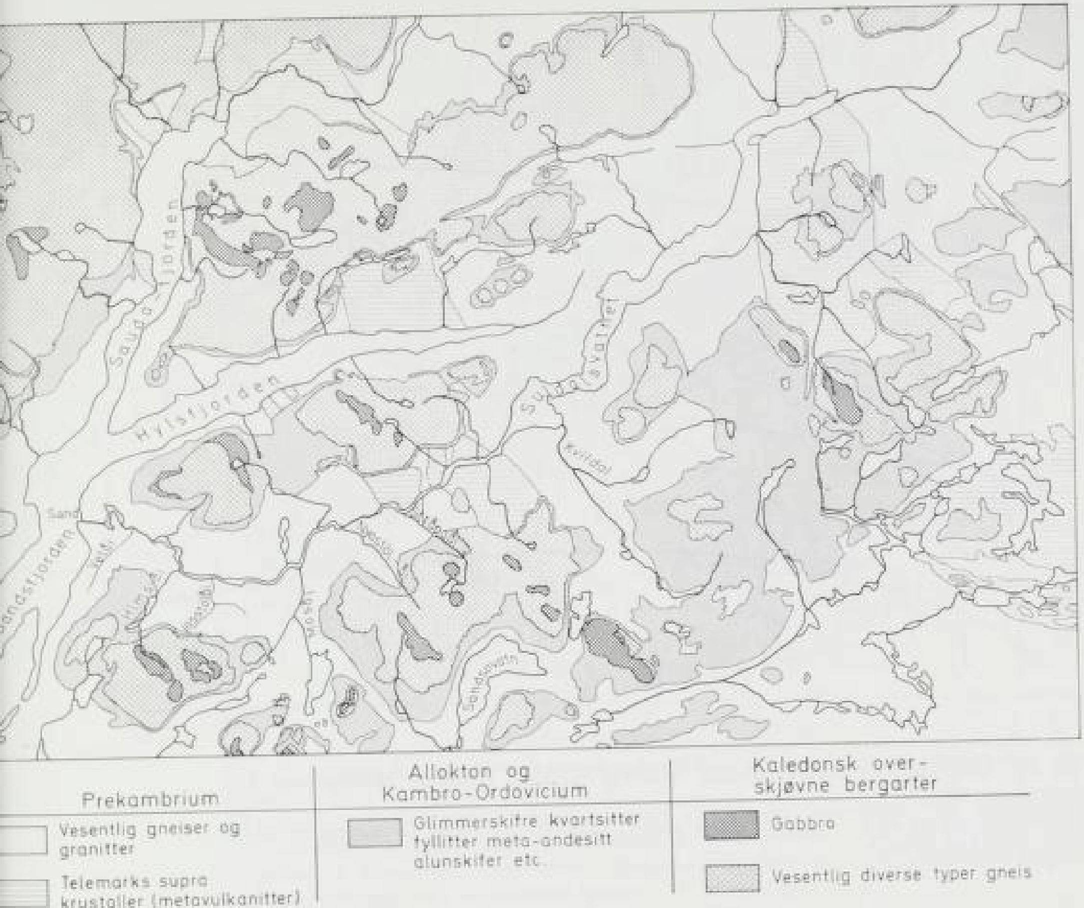


Fig. 21. Berggrunnsgeologisk kart over et område omkring Suldalen, forenklet etter Sigmond (1975).
*Bedrock map from an area around Suldalen valley, simplified after Sigmond (1975).*

mot S, på tvers av fjorder og fjellrygger. Enda senere, i Yngre Dryas, var bevegelsen omtrent mot V i Suldal. Under et breframstøt i Pre-boreal «flommet» øvre deler av en Suldal-bre inn over fjellviddene på N- og S-siden av Suldal. Etter dette har isen i Kvildalsområdet beveget seg til dels mot NV igjen.

Hovedtrekkene av dette blir: 1) den vesentligste matingen til Suldal med breer er fra fjellområdene i Ø og SØ, 2) det er kommet et visst tilskudd av masser med breer fra N.

Som vi skal se har den vesentligste glasifluviale transport foregått langs hoveddalen, mens det etter isavsmeltningen har skjedd og skjer en vesentlig sedimenttransport med sideelver til hoveddalen.

*Petrografisk sammensetning av løsmassene*

De petrografiske analysene er utført av geolog Ruth C. Sørbye, Trondheim. På Fig. 23 er resultatene slått sammen i klasser, dels på grunnlag av antatt styrke,

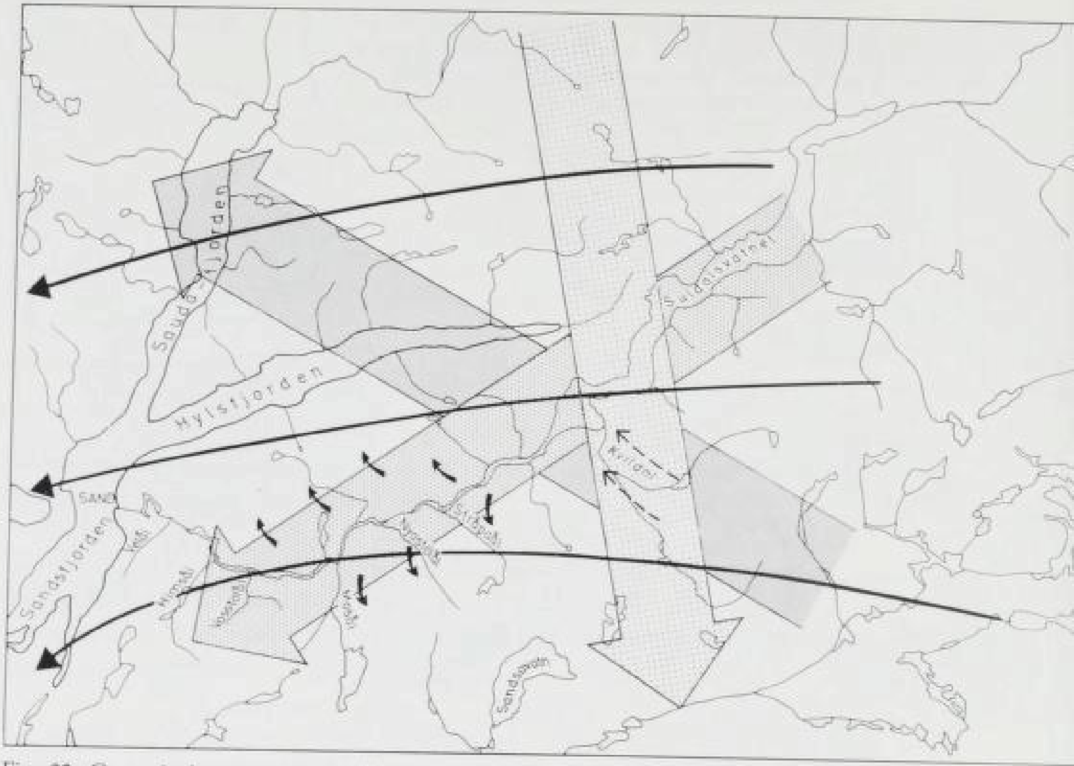


Fig. 22. Grunnriss-kart over et område omkring Suldalen, inntegnet isbevegelsene etter Anundsen (1981).
*Sketch-map of an area around Suldalen valley, with the different ice-movement phases after Anundsen (1981).*

dels på grunnlag av de enkelte bergartsformasjoner (-etasjer), og dels fordi det er meget vanskelig å skille mellom enkelte av bergartene.

Med grunnfjellsbergarter menes på Fig. 23 alle prekambriske bergarter unntatt Telemarks suprakrustaler. Dette er gjort for lettere å kunne spore eventuell transport fra sideelvene.

For enkelte jordarter er det ikke trukket sammenhengende kurver, da dataene er mangelfulle.

Innholdet av Kambro–Ordoviciske + overliggende bergarter (heretter forkortet til (KO+OV) er generelt høyt i de glasifluviale avsetningene, 30–50%. Endringer i sammensetninger generelt skjer ved tilløp av sideelver. Variasjonene er imidlertid meget mindre enn i Surnadalen og Sunndalen. Dette kan skyldes at sideelvene i sistnevnte områder er meget mer betydelig i vannføring og erosjon, i forhold til hovedelven, enn de i Suldal. Innhold av KO+OV har minimum umiddelbart nedstrøms tilløpet av elvene Velåi, Vasstølåi og Mosåi, og muligens også nedstrøms Nyastølåi. Dette kan enten bety noe overraskende at det glasifluviale tilskudd fra sideelvene består av mye grunnfjellsmateriale (unntatt fra Stråpaåi), eller at noen av de overliggende bergarter er tatt for å være prekambriske (idet de ofte er meget like). Imidlertid er det de samme

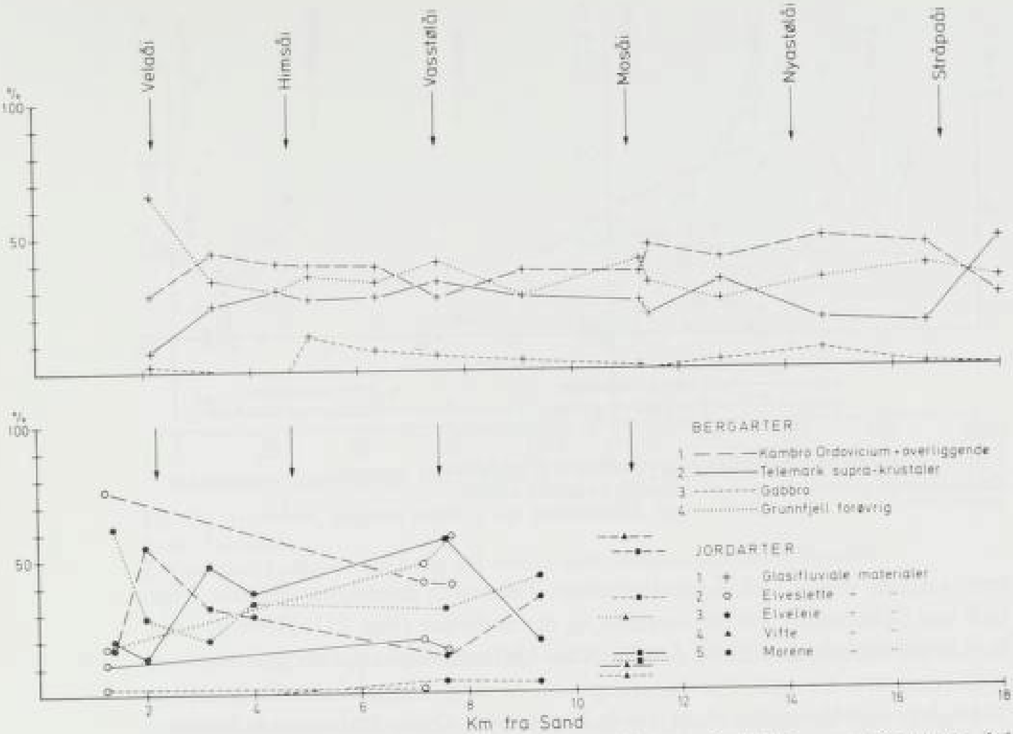


Fig. 23. Petrografisk sammensetning (lengdeprofiler) av forskjellige avsetningstyper, Suldalen.
*The petrographic distribution in some types of deposits. «Bergarter» = Petrography. 1: Cambro-Ordovician + overthrusted rocks, 2: meta-volcanics from the Telemark suite, 3: gabbro, 4: remaining precambrian. «Jordarter» = Deposits. 1: Glacifluvial materials, 2: flood plain materials, 3: river-bed materials, 4: alluvial fans, 5: tills.*

bergarter man finner i de resente og subresente avsetningene, og analyse av disse viser at den fluviale drenering fra sideelvene etter isavsmeltningen har bestått og består av mer KO+OV enn grunnfjellsmateriale (Fig. 23). Dette siste er også noe man skulle vente ut fra berggrunnsgeologien (Fig. 21). Unntak er Velåi, hvor også den nåtidige drenering frakter mye grunnfjellsmateriale. Dette er naturlig, da det i denne elvens nedslagsfelt er et meget begrenset felt med bergarter fra de øverste bergartsformasjoner. Morenematerialet i dalsiden ved Moåi inneholder hele 34% gabbro. Massene har imidlertid meget begrenset volum i dag, og terrengformene tilsier at morenen heller ikke tidligere har hatt betydning som kilde. Det er derfor rimelig at viften ved Moåi's munning bare inneholder 5% gabbro. Gabbroen i de glasifluviale materialene må derfor ha andre kilder. Denne gabbroen har stor likhet med den i fast fjell i Saudatraktene. Da det videre er observert sørgående bevegelse av en innlandsis (Anundsen 1981), er det mulighet for at gabbroen i de glasifluviale materialene virkelig kommer nordfra.

Innholdet av Telemarks suprakrustaler (metavulkanitter) er generelt høgt i de glasifluviale materialene, unntatt mellom elvene Stråpaåi og Nyastølåi,

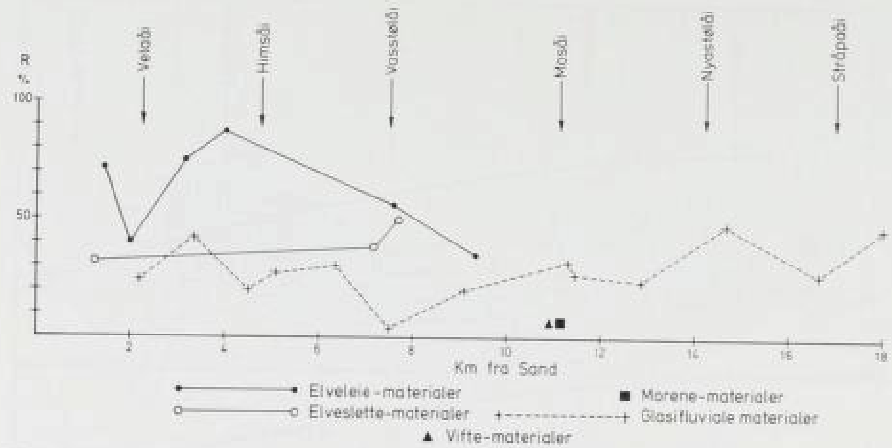


Fig. 24. Runding av forskjellige avsetningstyper i Suldalen.
*Roundness of different types of deposits, Suldalen valley.*

men varierer meget i elveleiematerialene. Telemarks suprakrustaler står i fast fjell ved Suldalsosen, ett felt ovenfor og ett nedenfor (Fig. 21). Det fins imidlertid også metavulkanitter i den Kambro–Ordoviciske bergartsformasjon.

Bortsett fra det naturlige minimum ved Moåi's tilløp, holder innholdet av Telemarks suprakrustaler (heretter forkortet til T-S) seg forbausende konstant på 25% videre nedover dalen, i de glasifluviale materialene. Fra ca. 5 km fra fjorden øker innholdet av alle andre bergartstyper, i glasifluvium. Til tross for spredte analyser er det klart at i de to typer fluviale jordarter, anrikes KO+OV meget sterkt på samme strekning, særlig på bekostning av grunnfjellsmaterialet. Men ved Velåi's munning er grunnfjellsinnholdet høgt, i alle fall i elveleiematerialene. Årsaken til økningen av KO+OV er mest trolig at det skjer et tilskudd av dette fra Himsåi, som drenerer direkte fra et slikt bergartsområde (Fig. 21), og hvor det er en del morenemateriale i sideelvens nedslagsdistrikt.

Fordelingen av T-S i de glasifluviale materialene tyder enten på 1) at det skjer uttallige tilløp fra T-S fra sidene, eller 2) at T-S er meget motstandsdyktig mot fluvial slitasje, eller 3) at det som her er kalt T-S også omfatter metavulkanitter fra de metamorfe suprakrustalbergartene i høgfjellet. T-S har vist seg som en sterk bergart (se senere), men den er vanskelig å skille fra metavulkanittene fra de metamorfe suprakrustalbergartene i etasjen over grunnfjellet. Disse siste ser heller ikke ut til å være av samme styrke som metavulkanittene i grunnfjellet. I tellingene kan det derfor være en mulighet for at disse to grupper av meta-vulkanitter er slått sammen i noen grad.

*Runding av partikler*

Rundingen (Fig. 13) av totalprøve på de glasifluviale materialer varierer lite nedover dalen (Fig. 24), men med et lokalt maksimum ved Nyastølåi's tilløp, og minimum ved Moåi's tilløp.

Tross få analyser av fluviale jordartsprøver er det klart at rundingen av disse

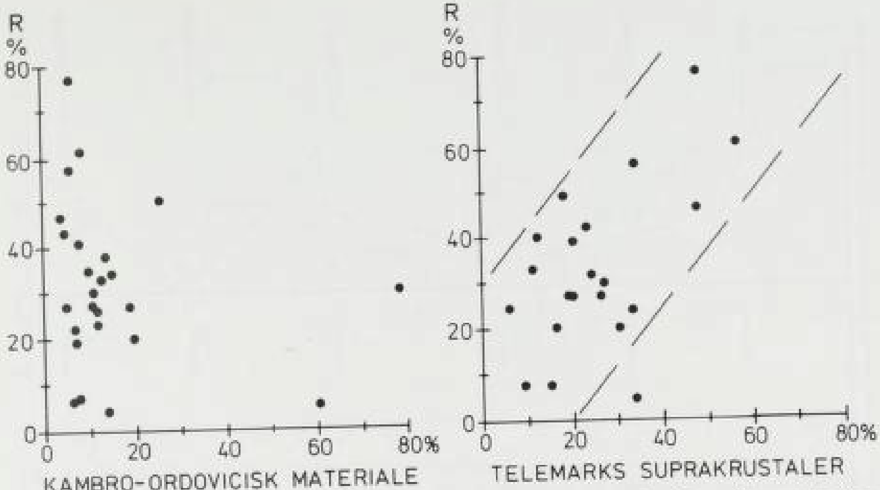


Fig. 25. Forholdet mellom runding og petrografisk sammensetning for ulike avsetningstyper, Suldalen.
*The relation between roundness and petrographic composition, Suldalen valley.*

er meget høgere, men også mye mer variert enn i glasifluvium, det samme som en finner i Surnadalen.

Fordelingen av runding og petrografi tyder på begrenset glasifluvial transport fra sideelvene, men betydelig fluvialt tilskudd.

Det er ingen tydelige tegn på at rundingen av totalprøve øker med økende innhold av Kambro–Ordovicisk materiale (Fig. 25), noe en kan finne i Surnadal. Det er derimot mulig at økende T-S innhold i prøven øker rundingen av denne (Fig. 25). Da økende transportlengde betyr økende runding, kan Fig. 25 indikere at T-S er motstandsdyktig mot fluvial slitasje (knusing).

### *Sprøhet og flisighet*

På Fig. 26 er vist profil langs Suldal av sprøhet og flisighet for de ulike materialtypene.

Variasjonene i sprøhet er meget stor i de glasifluviale og fluviale materialene. Kurvene varierer ikke i takt med hverken petrografi- eller rundingskurvene (Fig. 23 og 24). Det samme gjelder for flisigheten, som imidlertid viser liten variasjon. Det er derfor åpenbart at det er flere faktorer som virker sammen på sprøheten av materialet, ventelig rundingen og de forskjellige bergartstyper. Disse faktorer vil bli analysert nærmere hver for seg i det følgende. Imidlertid kan en spore en viss sammenheng mellom sprøhet og grunnfjellsmateriale, slik at økning av denne bergartsgruppe til dels faller sammen med økning i sprøhet. Dessuten er det en viss tendens til at maksimum eller minimum i sprøhet opptrer ved tilløp av sideelvene. Dette siste kan imidlertid bero på tilfeldigheter, da 1) det ikke er noen slik tendens å spore i Surnadal, og 2) det synes som den glasifluviale matingen fra sideelvene har vært meget beskjeden. Ut fra det siste punktet skulle man heller vente å finne større variasjon i sprøhet i de fluviale

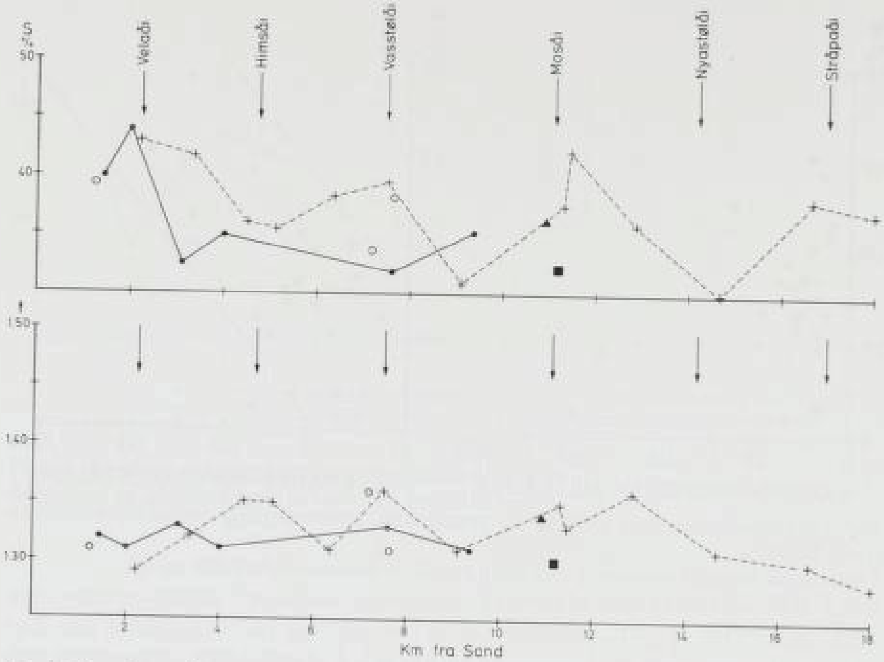


Fig. 26. Lengdeprofiler av sprøhet og flisighet, Suldalen. Tegnforklaring i fig. 24.
*Brittleness (S) and flakiness (f) of different deposits, Suldalen valley. Legend in Fig. 24.*

materialene, hvilket ikke synes å være tilfelle. Her er det forøvrig på sin plass å poengtere at prøvetakingen hele tiden har skjedd i et vilkårlig nivå i glasifluvium, mens det i elveleiematerialene alltid tas prøver bare fra overflaten. Bildet kan vise seg å være enda mer komplisert om man får resultater fra analyser foretatt forskjellige steder vertikalt i en og samme glasifluviale avsetning.

*Sprøhet/flisighet og runding*

Både i Surnadalen (Fig. 15) og i Sunndalen (Fig. 20) er det funnet at økende runding på et materiale gir det lavere sprøhet. Noen tilsvarende sammenheng kan ikke spores for Suldalsmaterialet (Fig. 27). Dette kan skyldes at det i Suldalen er større spredning av bergarter med stor innbyrdes styrkeforskjell (Fig. 27).

Man kan derfor ikke uten videre si at en i Suldal finner det mekanisk sterkeste materialet i elveleiet. Man må enda også se på den petrografiske sammensetningen. Dette er, som tidligere beskrevet, også tilfelle i de øvrige undersøkte områder.

Der er heller ingen påviselig sammenheng mellom runding og flisighet av materialene (Fig. 27), men variasjonen i flisighet er også meget liten.

*Forholdet mellom petrografi og sprøhet/flisighet*

Gabbro er en antatt sterk bergart. Selv om en i Suldal enda ikke har analysert prøver med gabbroinnhold mellom 10% og 30% (Fig. 28), kan man kanskje

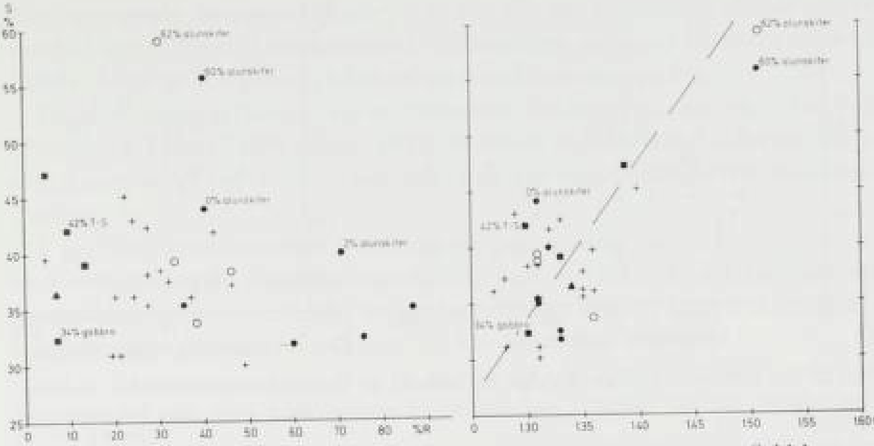

Fig. 27. Forholdet mellom sprøhet/flisighet og runding, alle avsetningstyper, Suldalen.
*The relation between brittleness/flakiness and roundness, all types of deposits, Suldalen.*

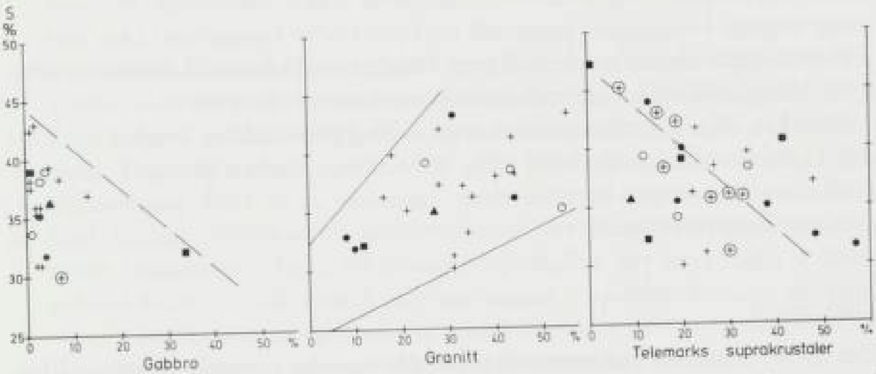


Fig. 28. Forholdet mellom sprøhet og petrografi for de forskjellige avsetningstypene i Suldalen.
*The relation between brittlenes numbers and petrography in the different deposits, Suldalen. Legend in Fig. 24.*

antyde at økende mengde gabbro har en tendens til å redusere sprøheten, alle typer materialer sett under ett. Rundingen er meget varierende, og klart lavest på moreneprøven med 34% gabbro-innhold.

Økende granitt-innhold ser ut til å øke sprøheten, alle materialtyper sett under ett (Fig. 28). En slik sammenheng kunne man allerede antyde ved sammenligning mellom Fig. 23 og Fig. 26.

Innholdet av Telemarks suprakrustaler (T-S) har en viss innflytelse på sprøheten, selv om en ser bort fra rundingen (som varierer mellom 7% og 87%; Fig. 28). Tar man ut de prøver som har samme runding (f. eks. 20–27%) ser relasjonen mellom T-S og sprøhet ut til å være bedre: økende T-S innhold reduserer sprøheten. Noe av spredningen kan skyldes at det er tale om forskjellige typer metavulkanitter, som tidligere nevnt. Samtidig med en tendens til redu-

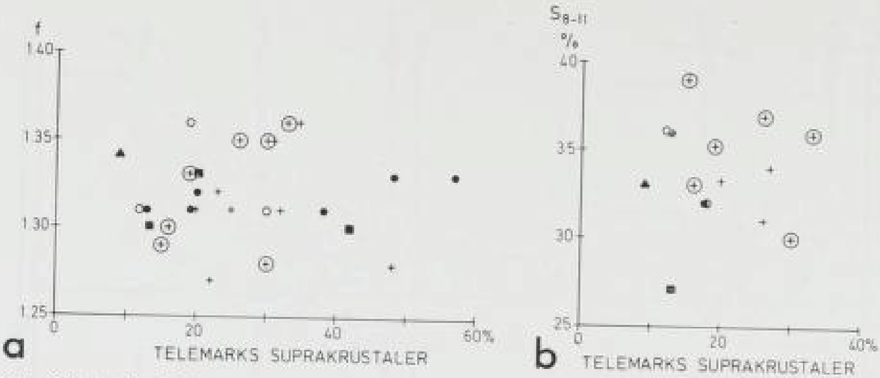


Fig. 29 (a). Forholdet mellom flisighet og innhold av Telemarks suprakrustaler, Suldalen.
*The relation between flakiness and content of metavolcanics from the Telemark-suite, Suldalen.*
29 (b) Forholdet mellom S på 8,0–11,2 mm naturgrus og innhold av Telemarks suprakrustaler, Suldalen.
*The relation between brittleness, on 8.0–11.2 mm natural gravel, and content of metavolcanics, Suldalen.*

sert sprøhet, er det en tendens til øket flisighet med økende T-S innhold (Fig. 29a), i de glasifluviale materialene med ens runding (20–27%).

Man kan ikke spore noen tilsvarende avhengighet mellom sprøhet og T-S i 8,0–11,2 mm naturgrusfraksjon (Fig. 29b). Dette skyldes muligens at petrografien endrer seg med kornstørrelsen. Innholdet av en sterk bergart vil bl. a. avta mot finere fraksjoner.

## Diskusjon

Det ser ut til at man ved materiale utsatt for naturlig rundingsslitasje også har det forhold at «. . . en faktor som partikkelform, vilken till en stor del beror på krossningsteknikken, kan överskugga innverkan av petrografiska faktorer» (Høbeda och Bünzow 1977). Det er i denne sammenheng interessant at sprøhets- og flisighetsanalyser på utborete (32 mm) steinkjerner gir gunstigere sprøhets-resultater enn på utskutte bergartsprøver fra samme lokalitet (Sverdrup & Sørensen 1966, Sørensen & Sverdrup 1974). Man kunne tenke seg at denne forskjellen kunne bero på sjokkeffekt på det skuddpåvirkete materialet. Imidlertid har Jøsang (1967) funnet samme tendens ved en sammenligning mellom sprøhet på biter med glatte boreflater og på borebiter fra det indre av kjernen, uten krumme flater.

Også tidligere undersøkelser tyder på at øket runding av aggregater øker styrken på aggregatet (Woolf 1937, 1948, Macnaughton 1937, Vallerga et al. 1956, Ekse & Morris 1959). Selv om en ikke kan se bort fra at transportslitasjen fort fjerner svake partikler, ser det ut til at det er den runde overflaten av kornene som i stor grad gir styrken, ikke bare mot slagbrudd, men også mot videre abrasjons-slitasje (Augenbach 1963). P.g.a. rundingens betydning er det heller ikke uvesentlig hvilken fraksjon som velges til overgrusfraksjon.

Med avtagende overgrus-størrelse vil det bli en prosentvis økende andel rundete korn(-deler) i testmaterialet. «Finkornig» overgrus i testen må i så tilfelle derfor gi for gunstig bilde av grusforekomstens sprøhet.

En øket transportlengde av et materiale betyr oftest en øket runding (Pittman & Tomas 1968, Goede 1975, Kaitanen & Srøm 1978). Derfor skulle man kunne tenke seg at det materiale som var lengst transportert ville være sterkest.

P.g.a. den store variasjon i runding og petrografisk sammensetning innen hver avsetningstype (oppblandingseffekt), kan en ikke ut fra foreliggende materiale si at det er spesielle avsetnings-enheter som er lengre transportert (sterkere) enn andre.

## Konklusjon

1) Ved sammenstilling av et meget stort antall sprøhetsdata (Høbeda 1977) er det funnet relasjoner mellom det berggrunnsgeologiske bildet, og sprøheten av grusmasser. Disse relasjonene må imidlertid være meget grove, idet det i foreliggende arbeid er påvist like store variasjoner i sprøhet innen ett av Høbeda's «kvalitetsområder», som det er mellom områder med ulik kvalitet. Det synes derfor nødvendig med detaljerte undersøkelser for å få nærmere rede på årsaker til slike store variasjoner innen et begrenset område. Hvis ikke dette gjøres, kan man fort gjøre feilvurderinger av kvaliteter.
2) Ved nitidige undersøkelser av isbevegelser, dreneringsretninger, løsmassetyper, berggrunnsforhold, lokalerosjon og ras, har det vært mulig å finne enkelte årsaker til de store lokale variasjoner i sprøhet. Dermed er det i en viss utstrekning mulig, ved å ta i bruk de lover som er funnet, ved en forutsigelse å komme nærmere den aktuelle sprøhet av massene.
3) Man vil finne igjen de bergartstyper i avsetningene som er representert i fast fjell i området (Matistio 1961). Men mengdeforholdet mellom dem vil variere svært meget (Kaitanen & Strøm 1978), avhengig av isbevegelse, jordartstype (=dreneringslengde?) og av lokale dreneringsforhold.
4) Rundingen av partiklene er meget vesentlig for sprøheten, idet øket runding gir lavere sprøhetstall. Rundingens innvirkning kan muligens være minst like stor som petrografiens innvirkning. Kambro-Silurmateriale (ofte kvartsrike glimmerskifre) rundes fort. Høgt innhold av KS-materiale gir derfor ofte lavere sprøhetstall for materialet, i enkelte områder.
5) Normalt er glasifluviale materialer dårligere rundet enn fluviale materialer. Dette skyldes sikkert at det siste har vært transportert lengst. Elveleiematerialer er derfor ofte de sterkeste materialer i et dalføre dersom de petrografiske forhold er noenlunde ens. Det fins imidlertid mange unntak. Ett viktig unntak får man der sideelver bringer utrast morene ned til hovedelven. Materialet her vil være mer kantet enn umiddelbart oppstrøms, og derfor svakere om det ikke består av spesielt sterke bergarter, som f. eks. gabbro. Det vil ta en viss tid (= en viss distanse nedstrøms tilløpet) før

materialet igjen er blitt like rundet som umiddelbart oppstrøms tilløpet. Et annet unntak får man der én sideelv bringer én type petrografi til hoveddalen, mens den glasifluviale transport brakte en helt annen petrografi til det samme sted i hoveddalen.

6) Både rundingen og den petrografiske sammensetningen i de undersøkte områdene er stort sett mer varierende i elvematerialene enn i de glasifluviale materialene. Tross dette ser sprøheten ut til å være mer varierende i glasifluvium enn i elveleie-materialer. Det er grunn til å anta at dette ikke primært skyldes at vedvarende, sterk fluvial behandling fjerner svake og oppsprukkede partikler, da slike i stor grad må være fjernet allerede ved glasial og glasifluvial behandling. Forholdet må derfor også ha noe med selve kornformen (rundingen) å gjøre.
   Imidlertid må det her pekes på at avrundete partikler har en tendens til å pakkes annerledes i morteren enn kantede partikler. Dette kan gi forskjeller i sprøhet som ikke er reell.
7) De aller fleste naturlige forekomster har en sammensatt petrografi, og variert runding. Det er derfor vanskelig å skille fra hverandre petrografiens og rundingens innflytelse på styrken.

For å forsøke å skille rundingens og petrografiens innflytelse på sprøheten, er det nå ved Geologisk institutt avd. B, Universitetet i Bergen, igangsatt knusing av fjell av ens petrografi. Dette blir rundet i laboratoriet. På denne måten håper en å få kontrollert følgende:

1) hvor fort rundes de enkelte bergartstyper innbyrdes?
2) hvor fort minker de enkelte partikler i størrelse?
3) hva skjer med sprøhet og flisighet til de enkelte bergartstyper under en simulert elvetransport?

Av de tromlede materialene blir det videre foretatt prøvestøping for å søke å klarlegge de samme parametrenes innvirkning på betongstyrken, og eventuelt få en høyere relasjon mellom sprøhetstall, eller en annen styrke-parameter, og betongstyrke.

## Summary

Gravel deposits in five Norwegian valleys (Fig. 1) have been investigated with regard to petrographic composition, roundness, brittleness and flakiness. The aim of the study has been to examine the possibility of deducing the quality of the gravel deposits, in a given region, from these parameters and from the draining directions of glaciers, melwater streams and normal streams. Previous investigations (Høbeda, e.g. 1977) have concluded that the flakiness and brittleness of gravel deposits are related primarly to the bedrock geology.

Normally, the coarse material in a gravel deposit is also utilized. In testing for brittleness and flakiness the procedure has been to use a mixture of 50% natural gravel and 50% crushed stones (19/25–37 mm) in the 11.2–16 mm fraction. The analyses of roundness have been carried out visually (Bergersen 1964).

In the Surnadalen valley (Figs. 6 & 7) glacifluvial deposits are found in terraces up to 140–147 m a.s.l. (marine limit), fluvial deposits in lower terraces and in the flood plain, and glacial till on the valley sides in the eastern part of the valley. The bedrock consists of low-metamorphic volcanics and sediments in a syncline trending along the valley. These rocks tectonically overlie a gneiss complex. Along both sides of the valley there is a narrow zone of sparagmitic quartzitic gneiss (Fig. 8).

Glacial movement was initially from south (from Trollheimen) to north; in later stages it was directed towards the NW and W. During Younger Dryas time local glaciers from Trollheimen seem to have terminated at the outlets of the tributary valleys of Folla and Vindola. The glacifluvial and fluvial transport was from the tributaries and along the main valley. The petrographic composition is therefore very complex (Fig. 9), as is the roundness of the particles (Fig. 10). With a few exceptions the glacifluvial material is less rounded than the fluvial. However, it is difficult to explain the high degree of rounding of all petrographic types in all types of material at the outlet of the river Folla.

The brittleness and flakiness also vary greatly along the valley (Fig. 11). The numbers are more consistent in the fluvial than in the glacifluvial material, even though the petrographic variation of the latter is as least as great as that of the former. The influence of the roundness (of the natural aggregates) on the brittleness seems to be as least as great as that of the petrography (Fig. 15). However, as the roundness of the different types of material varies greatly in the investigated areas (Fig. 13), it is difficult to deduce precisely where the strongest materials can be found.

In the Sunndalen valley (Figs. 7 & 16) as well as in Suldalen (Figs. 7 & 22) there is also a great variation in petrographic composition, brittleness, flakiness and roundness (Figs. 17, 18, 23, 24 & 26), which could hardly been foreseen from analysing the bedrock geology and the transport directions of the materials (Figs. 8 & 21). However, by analysing local features (e.g. avalanches on till-slopes in Ottdalen), it may be possible to tell something more about these parameters. A consistent relationship between roundness and brittleness (Fig. 20) is also a feature of the Sunndalen deposits.

The roundness of the Suldalen materials may be influenced by the petrography (Fig. 25). There does not however seem to be any relationship between brittleness and roundness here (Fig. 27), which may be due to a larger variation in petrographic composition in the Suldalen-materials than in that of the other areas. The two samples with highest brittleness numbers (Fig. 27) contain 50–60% alum shales, and the samples with the lowest brittleness number and low rounding contain up to 34% gabbro.

The influence of roundness on brittleness can hardly be explained only by means of enrichment of the strongest particles by continued fluvial treatment, as the glacial and glacifluvial treatment is presumably stronger than the fluvial. The relationship between brittleness and roundness, also noted by a number of other authors (Woolf 1937, 1948, Macnaughton 1937, Vallerga 1956, Ekse & Morris 1959, Grønhaug 1964, 1967, Sverdrup & Sørensen 1966, Josang

1967, Sørensen & Sverdrup 1974), has therefore most likely something to do with the roundness itself. Because of this relationship the brittleness may be influenced by the small size of the stones (19/25–37 mm) used in the test mixture, as these give a greater percentage of rounded particle-pieces in the mixture than do larger stones. This particular relationship is a subject of current research at the Institute of Geology, University of Bergen.

*Etterord.* – Forfatterne vil takke Norges Teknisk–Naturvitenskapelige Forskningsråd for finansiering av undersøkelsene og av trykking av artikkelen, statsgeolog Peer R. Neeb, statsgeolog Arne J. Reite og vit. ass. Roar Nålsund ved NGU for kritisk gjennomlesning, tegnerstaben ved Geol. inst., Univ. i Bergen, for tegning av illustrasjonene, fru Solveig Helland, Geol. inst., Univ. i Bergen, for maskinskriving, og statsgeolog David Roberts, NGU, for retting av den engelske teksten.

REFERENSER

Anundsen, K. 1972: Glacial Chronology in Parts of Southwestern Norway. *Norges geol. Unders. 280*, 1–24.

Anundsen, K. 1977: Fagrapport til NTNF: Fjellgrunn og gruskvaliteter. I. Foreløpige resultater. *Geol. Inst., Ingeniørgeol. NTH, Trondheim.* 64 sider.

Anundsen, K. 1979: Fagrapport til NTNF: Fjellgrunn og gruskvaliteter. II. Avsluttende rapport om undersøkelser utført ved NTH. *Geol. Inst., Avd. B, Univ. i Bergen.* 51 sider.

Anundsen, K. 1981: Shifting ice-movements in Late Pleistocene in South-west Norway. Unpubl.

Augenbach, N. B. 1963: Degradation of Base Course Aggregates During Compaction. *Purdue University* Thesis (unpubl.).

Bergersen, O. F. 1964: Løsmateriale og isavsmeltning i nedre Gudbrandsdalen og Gausdal. *Norges geol. Unders. 228*, 12–83.

Ekse, M. & Morris, H. C. 1959: A Test for Production of Plastic Fines in the Process of Degradation of Mineral Aggregates. *ASTM, STP nr. 277*, 122–126.

Eggen, et al. 1979: Oppdalsfeltets geologiske historie. Abstract av foredrag. NGT's landsmøte. Trondheim 1979. *Geolognytt nr. 2.*

Goede, A. 1975: Downstream changes in shape in the pebble morphometry of the Tambo river, eastern Victoria. *Journ. of Sed. Petr. 45*, 704–718.

Grønhaug, A. 1964: Steinmaterialers brukbarhet til vegbygging. Prøving og bedømmelse. *Statens Vegvesen, Veglaboratoriet. Medd. nr. 19*, 1–15.

Grønhaug, A. 1967: Evaluation and Influence of Aggregate Particle Shape and Form. *Statens Vegvesen, Veglaboratoriet. Medd. nr. 31*, 1–20.

Holtedahl, O. & Dons, J. A. 1960: Geologisk kart over Norge. *Norges geol. Unders. 208.*

Hugdahl, H. 1976: *Jordartsforholdene i Meråker-området.* Hovedoppgave i Ingeniørgeologi. Geol. Inst., NTH, Trondheim (upubl.).

Höbeda, P. 1966: Erfarenheter av hållfasthets- och kornformsbestämningar för stenmaterial till vägändamål. *Statens Väginstitut, Stockholm. Specialrapport 41.* 91 sider.

Höbeda, P. 1977: Sprödhetstal för naturgrusmaterial. Provningar hovudsakligen utförda vid VTI. *Statens väg- och trafikinstitut (VTI).*

Höbeda, P. & Bünzow, L. 1977: Nedbrytningsbenägenhet hos bärlagergrus – resultat från laboratorieförsök. *Statens väg- och trafikinstitut (VTI). Rapport nr. 140.* 109 sider.

Jøsang, O. 1967: Forsøk med fallprøver på nedknust overstein fra naturgneis og fra nedknuste borkjerner av fast fjell. *Norsk Vegtidsskrift 7*, 97–101.

Kaitanen, V. & Strøm, O. 1978: Shape development of sandstone cobbles associated with the Säkylä–Mellilä esker, southwest Finland. *Fennia 155*, 23–67.

Macnaughton, M. F. 1937: Physical Changes in Aggregates in Bituminous Mixtures under Compaction. *Ass. Asp. Pav. Tech. Proc. V 8.*

Matistio, A. 1961: On the relation between the stones of the eskers and the local bedrock in the area northwest of Tampere, southwestern Finland. *Bull. de la comm. geol. de Finl. 193*, 1–53.

Moavenzadeh, F. & Goetz, W. H. 1963: Aggregate degradation in bituminous mixtures. *Highway Research Record 24.*

Moseid, T. 1976: *Løsmassenes fordeling, dannelse og kvalitet i relasjon til de geologiske forhold i Surnadal, Møre og Romsdal.* Hovedoppgave i Ingeniørgeologi. Geol. Inst., NTH, Trondheim. (Upubl.).

Nordhagen, R. 1929: Bredemte sjøer i Sunndalsfjellene. *Norsk Geogr. Tidsskr. 2.*

Nordhagen, R. 1930: Nye iakttagelser over de bredemte sjøer i Sunndalsfjellene. *Norsk Geogr. Tidsskr. 3.*

Norges Standardiseringsforbund, 1962: NS 427 A. Betongarbeider. Del 2. Prøvningsregler.

Pittman, E. D. & Tomas, A. O. 1968: Pebble morphology in the Merced River (California). *Sedimentary Geology 2*, 125–140.

Rake, A. 1976: *Sand- og grusressurser i Hjelmeland kommune, Rogaland.* Hovedoppgave i Ingeniørgeologi. Geol. Inst., NTH, Trondheim. (Upubl.).

Roberts, D. 1978: Caledonides of south central Norway. Caledonian–Appalachain orogen of the north Atlantic region. *Geological Survey of Canada paper, 78 – 13*, 31–37. Ottawa.

Råheim, A. 1972: Petrology of high grade metamorphic rocks of the Kristiansund area. *Norges geol. Unders. 279*, 75 pp.

Råheim, A. 1977: A Rb–Sr study of the rocks of the Surnadal syncline. *Norsk geol. Tidsskr. 57*, 193–204.

Råheim, A. 1979: Structural and metamorphic break between the Trondheim basin and the Surnadal Synform. *Norsk geol. Tidsskr. 59*, 195–198.

Sigmond, E. M. 1975: Geologisk kart over Norge, berggrunnskart SAUDA, 1:250 000. *Norges geol. Unders.*

Sollid, J. L. 1964: Isavsmeltningsforløpet langs hovedvasskillet mellom Hjerkinn og Kvikneskogen. *Norsk Geogr. Tidsskr. 19*, 51–76.

Statens Vegvesen 1966: Analyseforskrifter. Vegdirektoratet, Veglaboratoriet, Oslo.

Stokke, J. 1976: *Løsmassenes dannelse, oppbygning og kvalitet i Skjomdalen, Nordland.* Hovedoppgave i Ingeniørgeologi. Geol. Inst., NTH, Trondheim. (Upubl.).

Sverdrup, T. L. & Sørensen, E. 1966: Orienterende undersøkelser vedrørende sprøhet og flisighet av bergarter. *Norges geol. Unders. 247*, 39–43.

Sørensen, E. & Sverdrup, T. L. 1977: Sammenligning av sprøhet og flisighet for borkjernemateriale og utskutte bergartsprøver. *Norges geol. Unders. 304*, 61–77.

Trønnes, R. 1978: *Den petrografiske og mineralogiske sammensetningen av løsmassene i Sunndalsområdet.* Hovedoppgave i Malmgeologi. Geol. Inst., NTH, Trondheim. (Upubl.).

Vallerga, B. A. et al. 1956: Effect of Shape, Size and Surface Roughness of Aggregate Particles on the Strength of Granular Materials. *ASTM, STP 212*, 63–74.

Woolf, D. O. 1937: The relation between Los Angeles abrasion test results and the service records of coarse aggregates. *Proc. Highway Res. Rec. 17.*

Woolf, D. O. 1948: Needed Research, Symposium on Mineral Aggregates. *ASTM, STP 83*, 221–233.

# RECENT MAPS PUBLISHED BY NGU

(A list of earlier maps appears on the inside back cover of all Bulletins and Skrifter from and including Bulletin 20, NGU nr. 300)

MAPS PRINTED IN COLOUR (On sale from Universitetsforlaget, Nkr. 30,—)

| | | |
|---|---|---|
| 1:250 000 | Enontekio | Bedrock geology |
| | Skien | —»— |
| | Svolvær | —»— |
| 1:100 000 | I 19 Bindal | Bedrock geology |
| | H 19 Helgelandsflesa | —»— |
| | H 18 Vega | —»— |
| 1: 50 000 | 2028 II Bjøllådal | Bedrock geology |
| | 1413 IV Botsvatn | —»— |
| | 1716 I Bruflat | —»— |
| | 1719 II Elgå | —»— |
| | 2018 III Elvdal | —»— |
| | 1917 I Evenstad | —»— |
| | 1819 III Grøthogna | —»— |
| | 1719 III Holøydal | —»— |
| | 1415 III Hårteigen | —»— |
| | 1817 II Lillehammer | —»— |
| | 1522 II Rissa | —»— |
| 1:50 000 | 1314 I Røldal | Bedrock geology |
| | 1918 II Storsjøen | —»— |
| | 1721 II Stugusjø | —»— |
| | 1414 II Sæsvatn | —»— |
| | 2028 II Bjøllådal | Quaternary geology |
| | 2035 I Børselv | —»— |
| | 1816 IV Dokka | —»— |
| | 1816 II Eina | —»— |
| | 1717 III Fullsenn | —»— |
| | 2128 II Graddis | —»— |
| | 1916 IV Hamar | —»— |
| | 1815 III Hønefoss | —»— |
| | 1917 IV Møklebysjøen | —»— |
| | 1915 III Nannestad | —»— |
| | 1734 III Reisadalen | —»— |
| | 1814 II Drøbak | Hydrogeology |
| 1: 20 000 | Brumunddal, COP O67068–20 | Quaternary geology |
| | Brøttum, CMN 071072–20 | —»— |
| | Elverum, CUV 067068–20 | —»— |
| | Jakobsnes, HUV 273274–20 | —»— |
| | Nordseter, SMN 073074–20 | —»— |
| | Sandnes, HUT 271272–20 | —»— |
| | Steinsgård, CQR 053054–20 | —»— |
| | Vingrom, CKL 071072–20 | —»— |

MAPS IN BLACK AND WHITE (On sale direct from NGU either as paper-copies (Nkr. 12,—) or as transparent-copies (Nkr. 60,—))

| | | | |
|---|---|---|---|
| 1:250 000 | Kristiansund | Bedrock geology | (preliminary) |
| | Mo i Rana | —»— | —»— |
| | Saltdal | —»— | —»— |
| | Stavanger | —»— | —»— |
| 1:100 000 | I 16 Dønna | Bedrock geology | (preliminary) |
| | J 14 Meløy | —»— | —»— |
| | A 42 Oppdal | —»— | —»— |
| | Y 4 Polmak | —»— | —»— |
| | H 16 Skibotnsvær | —»— | —»— |
| 1: 50 000 | 1818 IV Atnsjøen | Bedrock geology | (preliminary) |
| | 1416 IV Aurland | —»— | —»— |
| | 2028 I Beiardalen | —»— | —»— |
| | 1313 I Blåfjell | —»— | —»— |
| | 1414 III Breive | —»— | —»— |
| | 1720 II Brekken | —»— | —»— |
| | 1814 II Drøbak | —»— | —»— |
| | 1415 IV Eidsfjord | —»— | —»— |
| | 1916 IV Hamar | —»— | —»— |
| | 2017 III Julussa | —»— | —»— |
| | 1417 III Kaupanger | —»— | —»— |
| | 1317 II Leikanger | —»— | —»— |
| | 1417 I Lustrafjorden | —»— | —»— |
| | 1916 I Løten | —»— | —»— |
| | 1713 IV Nordagutu | —»— | —»— |
| | 1214 IV Onarheim | —»— | —»— |
| | 1833 III Raisjavrre | —»— | —»— |
| | 1520 I Rennebu | —»— | —»— |
| | 1720 III Røros | —»— | —»— |
| | 1918 III Stor-Elvdal | —»— | —»— |
| | 2017 II Søre-Osen | —»— | —»— |
| | 1433 III Tranøy | —»— | —»— |
| | 1312 III Ørsdalsvatnet | —»— | —»— |
| | 2128 IV Junkerdal | Quaternary geology | (preliminary) |

Because of lack of space, aeromagnetic and water-resource maps are not included in this list.

Nr. 363

NGU
Norges geo[logiske]
undersøkelse

CONTENTS





ISBN 82-00-31432-4
ISSN 0377-8894

Printed in Norway by Sentrum Trykkeri, Trondheim